HEEGAARD-FLOER HOMOLOGY AND STRING LINKS

LAWRENCE P. ROBERTS

1. Introduction

In [15] P. Ozsváth and Z. Szabó use the technology of Heegaard-Floer homology to refine the Alexander-Conway polynomial of a marked knot in S^3. In particular, they define Knot-Floer homology groups for relative $Spin^c$ structures, invariant up to isotopy of K, that correspond to the terms in the polynomial: the Euler characteristic of the homology with rational coefficients corresponding to i gives the coefficient of t^i. They have since shown that the non-vanishing of these groups characterizes the genus of the knot, [18]. In [12] they employ Kauffman's state summation approach to the Alexander-Conway polynomial to give a concrete realization of the generators of the chain complex for each i and their gradings (though not, unfortunately, for the differential). Furthermore, the techniques extend to *null-homologous* knots in an arbitrary three manifold, Y, where the knot may also be interpreted as giving a filtration of the Heegaard-Floer chain groups for Y that is also an invariant of the isotopy class of the knot. They also refine the one variable Alexander-Conway polynomial of an m-component link in S^3 by converting the link, in a way preserving isotopy classes, to a null-homologous knot in a $\overset{m-1}{\#} S^1 \times S^2$.

In this paper we simultaneously generalize the preceding picture in two ways: first, by removing the restriction on the homology class of the embedding, and second, by defining chain complexes corresponding to a *multi-variable* Alexander polynomial, with a variable for each component of a "string link", corresponding to the universal Abelian $\mathbb{Z}^k$-covering space of the complement of the "string link".

The string link restriction corresponds to basing a link in Y in a particular way: we require an oriented disc D embedded in Y so that the link components intersect the disc once, positively. This configuration is known as a d-basing, following the work of N. Habegger and X.S. Lin, [4]. There are many d-basings of the same link, and our invariant will be sensitive to these.

In S^3 there is a more perspicuous description of string links:

Definition 1.1. *Choose k points $p_1, \ldots, p_k$ in D^2. A k-stranded "string link" in $D^2 \times I$ is a proper embedding, $\coprod_{i=1}^k f_i$ of $\coprod_{i=1}^k I_i$ into $D^2 \times I$, where $f_i : I_i \to D^2 \times I$, such that $f_i(0) = p_j \times 0$ and $f_i(1) = p_s \times 1$. Following the literature, we call the string link "pure" if $j = s$ for each interval.*

A neighborhood of a d-base, D, is a copy of $D^2 \times I$, and its complement in S^3 is also a copy of $D^2 \times I$. In this $D^2 \times I$, the d-based link appears as k copies of I extending from one end to the other. For more general three manifolds, we will present our string link as a string link in $D^2 \times I$ with the data of a framed link diagram where all the surgeries occur in $D^2 \times I$

We consider a d-based link $\mathbb{L} \cup D$ embedded in a general three manifold Y. We measure the homology of the components of the embedding by a lattice, Λ, in $\mathbb{Z}^k$ spanned by the all vectors of the form $([h] \cap L_1, \ldots, [h] \cap L_k)$, where $[h] \in H_2(Y;\mathbb{Z})$ and the L_i are the components of the associated link. We will prove:

Theorem 1. *Let $\mathbb{L} \cup D$ be a d-based link in Y. Then, for each Spin^c structure, $\mathfrak{s}$, on Y, there is a relatively $\mathbb{Z}^k/\Lambda$-indexed abelian group $\oplus_\lambda \widehat{HF}(Y, \Gamma; \mathfrak{s}, \lambda)$ where each of the factors is an isotopy invariant of the based link.*

When $\Lambda \equiv 0$, most of the results for knots transfer straightforwardly. In particular, the presence of the d-based link imposes a filtration upon the Heegaard-Floer chain complexes of the ambient manifold that is filtered chain homotopy invariant up to isotopy of based link. The case where $\Lambda \not\equiv 0$ occurs naturally when trying to define chain maps from cobordisms of knots in cobordisms of three manifolds.

Note: In [**?**] the Knot-Floer homology is denoted by $\widehat{HFK}(Y, K; \cdot)$. We will assume that the presence of a $\Gamma = \mathbb{L} \cup D$ or K implies the use of the data determined by that object. Thus, we will use $\widehat{HF}(Y, K; \cdot)$ for the knot-Floer homology. When we wish to refer to the Heegaard-Floer homology of the ambient three manifold (ignoring the information provided by K) we will simply omit reference to the knot or bouquet. However, these are not relative homology groups, though they are homology groups for pairs and do not solely depend upon the complement of the knot or link.

When $\mathbb{L} \cup D \subset S^3$, we may re-state the theorem in terms of the associated string link, S:

Corollary 1. *For each $\overline{v} \in \mathbb{Z}^k$ there is an isotopy invariant $\widehat{HF}(S; \overline{v})$ of the string link S.*

In section 8, we realize the generators of the chain complex for a string link S in $D^2 \times I$ from a projection of S. They are identified with a sub-set of maximal forests – satisfying specific constraints imposed by the meridians – in a planar graph constructed from the projection of S. This description generalizes the description of generators, their indices, and their gradings given by P. Ozsváth an Z. Szabó in [12].

Lemma 1. *There are vector weights assigned to crossings so that for each tree, adding the weights calculates in which index, $\overline{v}$, the corresponding generator occurs. Furthermore, there are weights assigned to crossings which likewise calculate the grading of the generator.*

For the specific weights see Figure 10. This lemma requires a generalization of L. Kauffman's "Clock Lemma" to maximal forests that describes the connectivity of the set of maximal forests in a planar graph under two natural operations.

The weights and gradings are enough to form the Euler characteristic of the homology groups with rational coefficients, which is related to the Alexander-Conway polynomials of the link components in section 8.7. However, the Euler characteristic can also be interpreted as a polynomial arising from the first homology of a covering space.

We let $X = D^2 \times I - \text{int}(N(S))$ and $E = \partial X - D^2 \times \{0\}$. Consider the $\mathbb{Z}^k$-covering space, $\widetilde{X}$, determined by the Hurewicz map $\pi_1(X) \to H_1(X;\mathbb{Z}) \cong \mathbb{Z}^k$ taking meridians

to generators. Let $\widetilde{E}$ be the pre-image of E under the covering map. Then there is a presentation, [11], $\mathbb{Z}^k \to \mathbb{Z}^k \to H_1(\widetilde{X}, \widetilde{E}; \mathbb{Z}) \to 0$ of $\mathbb{Z}[t_1^{\pm 1}, \ldots, t_k^{\pm 1}]$-modules whose 0^{th} elementary ideal is generated by a $\det M$, a polynomial called the *torsion* of the string link.

Theorem 2. *Let S be a string link. The Euler characteristic of $\widehat{HF}(S; \overline{v}; \mathbb{Q})$ is the coefficient of $t_1^{v_1} \cdots t_k^{v_k}$ in a polynomial $p(t_1, \cdots, t_k)$ describing the torsion of the string link, $\tau(S)$,* [8].

R. Litherland appears to have originated the study of the module $H_1(\widetilde{X}, \widetilde{E}; \mathbb{Z})$ as a source of Alexander polynomials, [11]. He used it to study generalized θ-graphs, which, once we pick a preferred edge, correspond to the string links above.

Many results follow from trying to replicate known properties of the torsion. Braids are a special sub-class of string links, for which it is known that the torsion is always trivial. Likewise, it follows easily that

Lemma 2. *If the string link S is isotopic to a braid, then $\widehat{HF}(S) \cong \mathbb{Z}_{(0)}$ where $\widehat{HF}(S) \cong \oplus_{\overline{v}} \widehat{HF}(S; \overline{v})$*

The subscript in $\mathbb{Z}_{(0)}$ designates the grading.

This result should be likened to the analogous result for 1-stranded string links, i.e. marked knots, that are also braids: the unknot has trivial knot Floer homology. While string links are usually considered up to isotopy fixing their endpoints on $D^2 \times \{0, 1\}$, this result has the implication that our invariant will be unchanged if we move the ends of the strings on $D^2 \times \{0, 1\}$ (but not between ends). There is a composition for string links similar to that for braids, and our invariant is a map on the semi-group quotient **Strings/Braids**.

Furthermore, as in [12],

Lemma 3. *Alternating string links have trivial differential in each index, $\overline{v}$, for the Heegaard decomposition arising from an alternating projection.*

The proof may be found in section 8.6.2

As P. Ozsváth and Z. Szabó can extend the knot Floer homology to links, we may extend the constructions for string links to a sub-class of colored tangles in $D^2 \times I$. For a tangle, T, we allow closed components, in addition to open components requiring that the open components independently form a string link. To each open or closed component we assign a color $\{1, \ldots, k\}$ which corresponds to the variable t_i used for that component. We require that each color be applied to one and only one open component. We may then use the colors to construct a string link, $S(T)$ in a second manifold, $\overset{n}{\#} S^1 \times S^2$, where n is the number of closed components in T. The isotopy class of $S(T)$ is determined by that of T in $D^2 \times I$, allowing us to consider $\widehat{HF}(Y, S(T); \mathfrak{s}_0, i)$ as an isotopy invariant of T. With this definition, we may extend the skein exact sequence of [15] to crossings where each strand has the same color, see section 8

Finally, we analyze how the homology changes for three types of string link compositions. Each has the form of connect sum in its Heegaard diagram, and the proofs roughly follow the approach for connect sums taken by P. Ozsváth and Z. Szabó . We picture our three manifolds as given by surgery on framed links in $D^2 \times I$ with an additional string link, S, with k components. Given such diagrams for S_1 in Y_1 and S_2 in Y_2 we may 1) place them

side by side to create a string link, $S_1 + S_2$ with $k_1 + k_2$ components, 2) when $k_1 = k_2$ we may stack one diagram on top of the other (as with composition of braids) to obtain the string link $S_1 \cdot S_2$, and 3) we may replace a tubular neighborhood, i.e. a copy of $D^2 \times I$, of the i^{th} strand in S_1 with the entire picture for S_2 to obtain a string satellite, $S_1(i, S_2)$. The analysis of the second type proceeds differently than in [15]: we consider it as a closure of $S_1 + S_2$ found by joining the ends of S_1 on $D^2 \times \{1\}$ with the ends of S_2 on $D^2 \times \{0\}$ in a particular way. We prove the following formulas for the homologies, where $\mathfrak{s} = \mathfrak{s}_0 \# \mathfrak{s}_1$:

$$\widehat{HF}(Y, S_1 + S_2; \mathfrak{s}, [\overline{j}_0] \oplus [\overline{j}_1]) \cong H_*(\widehat{CF}(Y_0, S_0; \mathfrak{s}_0, [\overline{j}_0]) \otimes \widehat{CF}(Y_1, S_1; \mathfrak{s}_1, [\overline{j}_2]))$$

$$\widehat{HF}(Y, S_1 \cdot S_2; \mathfrak{s}, [\overline{k}]) = \bigoplus_{[\overline{k}_1]+[\overline{k}_2]=[\overline{k}] \, \mathrm{mod}\Lambda} H_*(\widehat{CF}(Y_1, S_1; \mathfrak{s}_1, [\overline{k}_1]) \otimes \widehat{CF}(Y_2, S_2; \mathfrak{s}_2, [\overline{k}_2]))$$

$$\widehat{HF}(Y, S_1(i, S_2); \mathfrak{s}, [(l_1, \ldots, l_{k_1+k_2-1})] \cong$$

$$\bigoplus_{[\overline{v}']+[\overline{w}']=[\overline{l}] \mathrm{mod}\ \Lambda'} H_*(\widehat{CF}(Y_0, S_0; \mathfrak{s}_0, [\overline{v}]) \otimes \widehat{CF}(Y_1, S_1; \mathfrak{s}_1, [\overline{w}]))$$

where $\overline{v}' = (v_1, \ldots, v_{i-1}, v_i, \ldots, v_i, v_{i+1}, \ldots, v_{k_1})$, repeating v_i a total of k_2-times, and $\overline{w}' = (0, \ldots, 0, w_1, \ldots, w_{k_2}, 0, \ldots, 0)$ with zero entries except for places $i, \ldots, i + k_2 - 1$. and $\Lambda' = \Lambda + \overline{0} \oplus \Lambda_1 \oplus \overline{0}$.

Summary by section:

In section 2 we describe Heegaard decompositions for string links. In particular, we analyze the Heegaard equivalences preserving the structure of a d-based link and relate them to the types of diagrams – multi-point Heegaard diagrams – used to define the chain complexes. Section 3 describes the indices that replace the exponents of the Alexander polynomials in the general setting and defines the chain complexes we will use. We define the homology theory and record its basic properties. In section 5 we provide a summary of invariance slanted towards dealing with the effects of an ambient manifold with non-zero second Betti number. Section 4 develops the necessary theory for chain maps and is here largely for completeness. Section 4.6 illustrates the first substantive examination of the effect of Λ. Section 6.4 records the proofs of the results cited for combining string links. In section 7 we review the study of Alexander invariants related to string links in $D^2 \times I$. In 8 we describe the state summation approach to the Euler characteristic and its relationship with the generators of the chain complex. We also describe the results for braids and alternating string links; the relationship with the Alexander-Conway polynomial of the link components; and the skein exact sequence.

Note: We do not address issues of orientation of moduli spaces in the paper. However, nothing we say will alter the existence of the coherent orientations. It is merely convenient to suppress this information. As usual we may work with $\mathbb{Z}/2\mathbb{Z}$-coefficients to avoid these issues.

Contents

2. String Links and Heegaard Diagrams

2.1. **String Links in $D^2\times I$.** In this section, the topological input for our invariant will be laid out. To start we consider the situation in S^3:

Definition 2.1. *Choose k points $p_1,\dots,p_k$ in D^2. A k-stranded "string link" in $D^2\times I$ is a proper embedding, $\coprod_{i=1}^k f_i$ of $\coprod_{i=1}^k I_i$ into $D^2\times I$, where $f_i: I_i\to D^2\times I$, such that $f_i(0)=p_j\times 0$ and $f_i(1)=p_s\times 1$. The string link is pure if $j=s$ for each interval. We orient the strands "down" from 1 to 0.*

We consider these up to isotopy, preserving the ends $D^2\times\{i\}$ for $i=0,1$. Then braids form a sub-set of string links. However, the invariant we define will allow us to move the ends of the string link on their end of the cylinder, but not between ends. With this additional freedom we can always undo any braid.

We consider $D^2\times I$ embedded inside S^3. A projection of the string link onto a plane provides the data for a Heegaard decomposition of S^3. For a string link whose strands are oriented downwards, we may draw a Heegaard diagram as in Figure 1.

We take a small tubular neighborhood of each strand in $D^2\times I$ and glue it to the three ball that is $S^3-i(\,D^2\times I\,)$. This is a handlebody to which we attach 1 handles at each of the crossings. These handles occur along the axis of the projection, between the two strands; when we compress the handle to obtain the tubular neighborhood of an "X", the attaching circles appear as in Figure 1, one for each type of crossing, cf. [12]. The attaching circles for the handles from the strands are placed in $D^2\times\{0\}$ as meridians for each strand.

The complement of this in S^3 is also a handlebody. It can be described by taking two 0-handles in $D^2\times I$, above and below the plane we projected onto (thought of as cutting $D^2\times I$ through the middle). We then attach handles through the faces of image of the projection: a copy of the D^2 factor in the handle should be the face. We use 1-handle for the face on the leftmost side of the diagram, called U, to cancel one of the 0-handles. As these two handlebodies have the same boundary, they must have the same number of handles, and the decomposition is a Heegaard decomposition.

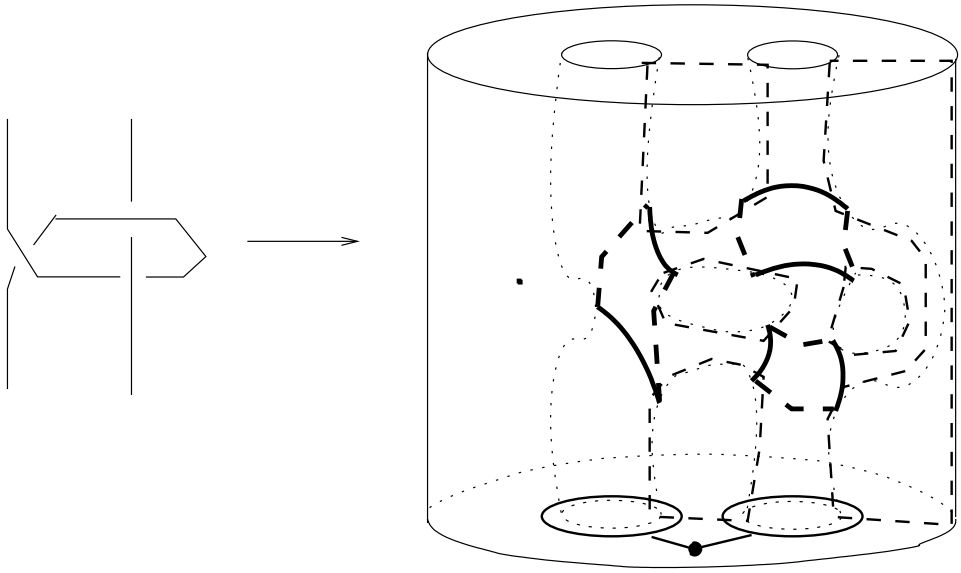

FIGURE 1. The Heegaard Diagram for a String Link. We place the meridians at the bottom of the diagram and α curves at each of the crossings, reflecting the type of crossing.

To each strand of a string link, we may associate a knot: ignore the other strands and join the two ends of our strand with an unknotted arc in the complement of $D^2 \times I$. Likewise we may associate a link to a pure string link by using k unknotted, unlinked arcs as for the closure of a braid. Furthermore, by retaining $D^2 \times \{0\}$, oriented as the boundary of $D^2 \times I$, we have an embedded disc which intersects the strands of the link in one point with $L_i \cap D = +1$. This is a d-base in the language of Habbegger and Lin, [4].

2.2. **String Links in Y.** For general three manifolds, Y, we define a string link to be a d-based link:

Definition 2.2. *A d-base for an oriented link $\mathbb{L}$ is an oriented disc, D, embedded in Y whose interior intersects each component of $\mathbb{L}$ exactly once, positively.*

By thickening the disc, D, we obtain an embedded ball with the structure of a cylinder, $D^2 \times I$. $\mathbb{L}$ in the complement of this ball comports more with our intuition for a string link. We consider these complexes up to isotopy of the complex $D \cup \mathbb{L}$, preserving the orientations on the parts. However, the invariant will allow the strands of $\mathbb{L}$ not to return to the same point, and these ends to move independently on, but not between, the two sides of D.

Example: For knots in S^3 a d-basing amounts to picking a point on the knot, the intersection point with D. This is a marked knot as used in [15]. The string link associated to a knot comes from dividing the knot at that point and pulling the ends apart.

We will use Heegaard diagrams for Y where the α-handlebody extends the handlebody that is a neighborhood of $D \cup \mathbb{L}$. If we think of this neighborhood up to isotopy we would

have great freedom in moving around the handles corresponding to the strands. When we transfer to the Heegaard picture the additional freedom allows us to braid the ends of the strands through isotopies of the Heegaard surface without altering the disc. We may even disjoin the link componenets: if the endpoints of a strand correspond, we have a d-based link, but we may braid the ends on one side of the disc independently of the other. However, the data from D prevents the ends from moving between the different sides D.

Example: To draw the Heegaard diagram for a string link in Y, we think of $D \cup \mathbb{L}$ embedded in a framed link diagram for Y in S^3. We may then draw a Heegaard diagram from a projection of the whole configuration, attaching the framed components by paths to $D \cup \mathbb{L}$. The α curves on the new components are no longer the meridians, but instead are chosen to be framing curves for the surgery, oriented opposite the longitudes from S^3. All of this can be done away from the disc $D^2 \times \{0\}$ containing the meridians. By inverting a neighborhood of the disc, we can present the string link in Y by a string link in a framed link diagram in $D^2 \times I$ with $D^2 \times \{0\}$ as preferred disc.

2.3. **Heegaard Diagrams and Based Links.** We describe the general approach to Heegaard diagrams subordinate to a string link, $D \cup \mathbb{L}$. Above we gave specific examples of such diagrams; we would now like to characterize all such diagrams and describe the Heegaard equivalences between them. In particular, we will be concerned with retaining the data provided by D.

First we establish some conventions. Let Y be a three manifold. Assume, as given, a Heegaard decomposition, $Y = H_\alpha \cup_{\Sigma^g} H_\beta$, where $\partial H_\alpha = \Sigma = -\partial H_\beta$ and the gradient flow corresponds to the outward-pointing normal to H_α. We denote this decomposition by $(\Sigma, \{\alpha_i\}_{i=1}^g, \{\beta_i\}_{i=1}^g)$ with $\{\alpha_i\}_{i=1}^g$ being the co-cores of the one handles in H_α and likewise for $\{\beta_i\}_{i=1}^g$.

To make our diagram reflect a string link $\mathbb{L} \cup D$, we additionally require that our Heegaard decomposition satisfies:

(1) The three manifold $(\Sigma, \{\alpha_i\}_{i=k+1}^g, \{\beta_i\}_{i=1}^g)$ is $Y^3 - N(\mathbb{L} \cup D)$. The complement of $(\Sigma, \{\alpha_i\}_{i \neq j}, \{\beta_i\}_{i=1}^g)$ for $j \leq k$, should be homeomorphic to a tubular neighborhood of L_j in Y. We require α_j to be an oriented meridian for this tubular neighborhood.
(2) There is a disc D' in $\Sigma - \{\alpha_i\}_{i=1}^g - \{\beta_i\}_{i=1}^g$ whose boundary contains one connected segment from each of $\alpha_1, \ldots, \alpha_k$. The string link formed from D' glued to the attaching discs for $\alpha_1, \ldots, \alpha_k$ and the components of $\mathbb{L}$ from (1) is isotopic to $\mathbb{L} \cup D$.

The first condition requires that the diagram be subordinate to the string link. The second requires that there be a disc in the Heegaard data that produces a d-basing for $\mathbb{L}$ and that induces a string link isotopic to the original one. Such diagrams are said to be *subordinate* to $\mathbb{L} \cup D$. Furthermore, a diagram with such a choice of α's and a disc D' determines a string link as in item (2). Note that D' must be oriented opposite to Σ.

We may relate diagrams subordinate to a configuration $\mathbb{L} \cup D$, embedded inside a three manifold, Y, by the following lemma:

Lemma 4. *[cf. Lemma 4.5 [16]] Let Y be a closed, oriented three-manifold. Let $\mathbb{L} \cup D \subset Y$ be an embedded d-base. Then there is a Heegaard diagram subordinate to $\mathbb{L} \cup D$ and any two such subordinate diagrams may be connected by a sequence of the following moves:*

1. *Handleslides and isotopies among the elements of $\{\alpha_i\}_{i=k+1}^{g}$*
2. *Handleslides and isotopies of $\{\beta_i\}_{i=1}^{g}$.*
3. *Stabilization introducing α_{g+1}, β_{g+1} intersecting in a single point.*
4. *Isotopies of $\{\alpha_i\}_{i=1}^{k}$ and handleslides of them over elements of $\{\alpha_i\}_{i=k+1}^{g}$.*

where we disallow isotopies and handleslides of any attaching circles resulting in a curve intersecting the disc D'.

Proof: Let $\Gamma = \mathbb{L} \cup D$. $N(\Gamma)$ is a handlebody which we may extend to a Heegaard decomposition for Y. The disc D corresponds to a disc D' in $\partial N(\Gamma)$ at one end of the thickening of D, determined by the orientation requirements. The meridians are chosen to occur in the disc, and thus abut D' in accordance with requirements. The additional α's and β's may be chosen to avoid D' as D' is contractible in Σ. Thus, such a diagram does exist. It is shown in [13], Prop. 7.1, that any isotopy across a contractible region in Σ may be obtained by handleslides and isotopies not crossing that contractible region; any β isotopy which crosses the entire star may be accomplished by handleslides not intersecting the star. This assures us that the choice made in pushing the β's away from D' does not affect the outcome.

Given the diagrams for two isotopic embeddings of Γ, we must see that they can be related by the moves described above. These moves preserve the region D in the original diagram. This region and a small neighborhood of it in Y act as the disk for the d-base. On the other hand, the isotopy carries a neighborhood of the disc into a neighborhood of the new disc; these neighborhoods are all homeomorphic and may be used as a 3-handle for each of the Heegaard diagrams. That the isotopy preserves $\mathbb{L}$ outside this ball allows us to fix the meridians and consider the additional handles, describing $Y - N(\Gamma)$.

If we consider $\partial N(\Gamma)$ as $\partial_+(Y - N(\Gamma))$ then the existence of the Heegaard diagram follows from the existence of a relative Morse function that is equal to 1 on the boundary and that the isotopy class of $\{\alpha_i\}_{i=1}^{k}$ is determined by their being meridians of the knots determined by the strands of $\mathbb{L}$. As usual, we may cancel 1-handles with 0-handles until there is only one 0-handle. Similarly we may cancel off 3-handles until there are none. The relative version of Cerf's theorem states that any two such diagrams can be linked through the first three moves and the introduction of new index 0/1 cancelling pairs or new index 2/3 cancelling pairs.

However, we would like to ensure that the path can be chosen through diagrams with only one index 0 handle and no index 3 handles. As we introduce a new 3-handle, we also introduce a cancelling 2-handle. The new 2-handle will have one end of its co-core on $\partial N(\Gamma)$, since there are no other 3-handles. In the diagram for Y, the one with the prescribed meridians, this 2-handle has a core that is a homological linear combination of the α's. If we cut Σ along $\{\alpha_{k+1}, \ldots, \alpha_g\}$, and cap the new boundaries with discs, the image of the core will be null-homotopic: it will be homotopic to the boundary of the B^2 at the end of the co-core lying on $\partial N(\Gamma)$. Since it is null-homotopic, the core cannot have a non-zero coefficient for a meridian for its homology class. Thus, it is linear combination of $\{\alpha_{k+1}, \ldots, \alpha_g\}$. According to lemma 2.3 of [13], the core curve can be obtained as the image

of a $\{\alpha_{k+1}, \ldots, \alpha_g\}$ under handleslides. Thus, any diagram obtained from the diagram after a 2/3 pair is added, could be obtained from the old diagram as handleslides over the new core can be given by handleslides over α's, not using any meridians. We may bypass 2/3-handle pairs. The same argument applies for 0-handles, as there are fewer restrictions on the β's.

Allowing the meridians to move, the last equivalence follows from considering the bouquet after surgering out $\{\alpha_i\}_{i=k+1}^{g}$. The meridians are determined up to isotopy, and as those isotopies cross surgery discs there are corresponding handleslides. Likewise, two curves for the same meridian, abutting the same disc D' at a specified point, will be isotopic. Thus, any choice of meridians may be moved to the one chosen above. This takes care of all our choices, so any two diagrams subordinate to the same isotopy class of string link can be related with the moves in the lemma. **Q.E.D.**

Without disallowing equivalences that intersect D', the moves above preserve the handlebody neighborhood of $\mathbb{L} \cup D$. This is weaker than preserving the isotopy class of $\mathbb{L} \cup D$. However, with the additional data provided by D', any isotopy will pull the disc along, preventing the ends of strands from twisting at the intersection point with D.

Example: We return to our method for drawing a Heegaard diagram for a string link in Y. Using the reduced Heegaard equivalences, we argue that the construction does not depend upon how the framed components are joined to $N(\mathbb{L} \cup D)$. The argument comes from [16], for the same result for a bouquet, with minor alteration.

Consider two distinct arcs, s_1 and s_2, joining a framed component to Γ, and form a regular neighborhood of the graph provided by $\Gamma \cup s_1 \cup s_2$. We extend this to a diagram for S^3 (by adding handles for crossings, etc). We draw a subordinate diagram using s_1 to attach the framed component by placing α_{k+1} as a meridian to s_2. To obtain a diagram subordinate to the second choice of paths we erase α_{k+1} and replace it with α'_{k+1}, a meridian to s_1. We surger out all the α_i for $i > k+1$ to obtain a genus $k+1$ surface. We wish to see that α_{k+1} and α'_{k+1} are isotopic; if they are we may move the correponding curves in the original diagram through isotopies and handleslides one into the other. The two curves, along with some non-meridional α's, bound a punctured torus coming from the framed component. After surgering, the other boundaries are filled, and surgering the framing attaching circle transforms the torus into a cylinder. Therefore, the α_{k+1} and α'_{k+1} now bound a cylinder which does not involve the disc D'. Each time the isotopy of curves determined by the cylinder crosses a disc coming from the surgered handles, there is a corresponding handleslide in the original picture. This provides a sequence of Heegaard equivalences that are allowed under the reduced equivalences of d-based links.

Sliding a strand in the string link over a framed curve produces a new string link which, along with the framed components, produces a second Heegaard diagram for Y equivalent to that from before handlesliding (a simple process, but lengthy, and not provided here). Handleslides of framed components over each other can be effected by a bouquet with a path joining the two components, which we have seen is available, and then using the same argument as above. Likewise, adding ± 1 framed unlinked, unknots (blowing up/down) can be effected using the reduced Heegaard equivalences. Hence, using two different framed link descriptions for Y will not change the equivalence of the Heegard diagram.

2.4. **Marked Diagrams.** It is cumbersome to retain the disc, D', in our Heegaard diagrams. Furthermore, since the restricted Heegaard equivalences eliminate handleslides over the meridians they often impede the simplification of the Heegaard diagram. We give another interpretation of the topology making our diagrams more tractable.

Using the embedded star, D', we may introduce marked points into Σ. We choose w to be in the interior of D' and z_i to be on the other side of α_i in the region of $\Sigma - \{\alpha_i\}_{i=1}^g - \{\beta_i\}_{i=1}^g$ abutting the same segment as D'. From a subordinate diagram for the d-based link we have realized a *multi-pointed diagram*. The equivalences for multi-pointed diagrams are the standard Heegaard equivalences – with no restriction on handleslides – but with the caveat that no isotopy of an attaching circle or marked point may allow one to cross the other.

Conversely, for any Heegaard diagram with a choice of marked points $w, z_1, \ldots, z_k$ in $\Sigma - \{\alpha_i\}_{i=1}^g - \{\beta_i\}_{i=1}^g$ we can construct a Heegaard diagram subordinate to a string link. First, choose paths from each z_i to w crossing only α's. Then take neighborhoods of the gradient flow lines, in H_β, joining the index 0 critical point and the marked points Σ, remove these neighborhoods from H_β and add them to H_α. The complement in H_β is still a handlebody, since we have removed the neighborhood of $k+1$ segments. Adding the neighborhoods to H_α creates a new handlebody $H_{\alpha'}$. The new α's are meridians of the gradient flow lines, and the new β's are loops following the flow line from w to the critical point, then to z_i and back along the path we chose in Σ, crossing only α's. It is straightforward to find the region D': it is a disc in the portion of $\partial H_{\alpha'}$ coming from the exchange. Thus, a multi-point diagram gives us a diagram subordinate to a string link through the preferred disc D. Furthermore, if we use the preferred disc, D, to produce a multi-point diagram, after some handleslides of the α's over the new meridians, we can de-stabilize the new α's and β's to obtain the original multi-point diagram.

The relationship between the equivalences for multi-point diagrams and those subordinate to string links comes from by noticing that when going from a multi-point diagram to a string link diagram, performing an illicit isotopy over a marked point z_i corresponds to an illicit handleslide over a meridian, according to the construction above. In fact, were we to surger out the meridians, the point z_i would correspond to one of the two discs used to replace that meridian (the other would be close to w inside the region D). Isotoping across it would be the same as a handleslide across a meridian.

This construction may depend upon the choice of the new β-paths. If we surger all the β attaching circles in the multi-point diagram, the chosen paths become a star in S^2 joining z_i to w for all i. If two such stars are isotopic in the complement of the marked points, the resulting diagrams for the θ_{k+1} graph are equivalent. Each time the isotopy of a segment crosses a disc introduced by the surgery, we should think of our new β being slid over an old β. Braiding of the marked points in S^2, carrying along the star, will not, in general, produce a diagram isotopic to the one with the star before braiding. However, these produce equivalent diagrams as they are both stabilizations of the same diagram. This discrepancy, once again, reflects the inability to detect braiding once we switch to considering Heegaard diagrams.

Note: We may perform handleslides to ensure that in our Heegaard diagrams the meridians each intersect only one β-curve. When the meridian intersects only one β, the boundary of such a region must include multiples of the full meridian When there is more than one

β intersecting the meridian, we will instead count the intersections with the the embedded θ_{k+1}-graph found from the gradient flow lines through the marked points.

2.5. **Admissibility and d-Based Links.**
In Heegaard-Floer homology, when $H_2(Y;\mathbb{Z}) \ncong 0$, we must use diagrams submitting to certain admissibility requirements, [13]. We argue here that presenting a d-based link as a string link in $D^2 \times I$, with an additional framed link defining Y, can be made admissible without disrupting the disc D or the structure of $D^2 \times I$.

We make use of the lemmas in section 5 of [13].

Lemma 5. *Let $\mathbb{L} \cup D \subset Y$ be a d-based link. Let $\mathfrak{s}$ be a Spin^c structure on Y. Then there is a strongly/weakly admissible diagram for $(Y, \mathfrak{s}, \mathbb{L} \cup D)$ presented as a framed link on the complement of a string link in $D^2 \times I$.*

Proof: Suppose Y is presented as surgery on a link in S^3, and Γ is $\mathbb{L} \cup D$ in this diagram. We adjust this, as above, to be a framed link diagram in $D^2 \times I$ with a string link. Recall that we must join the framed components to $\mathbb{L} \cup D$ by paths which we assume do not touch $D^2 \times \{0\}$. With the framing curves as α-curves, this provides a diagram for Y. However, it need not be admissible; we may need to wind the attaching circles to make it so. We must ensure that the winding paths do not affect the discs $D^2 \times \{0\}$ or $D^2 \times \{1\}$. We make two observations.

(1) First, any doubly periodic domain must have at least one boundary containing multiples of a framing curve. Otherwise, by replacing framing curves with the meridians of the link components, we would obtain a periodic domain in a diagram for S^3. Furthermore, two periodic domains may not produce the same linear combination of framing curves in their boundaries.
(2) Second, a meridian of a framed component may be chosen to intersect the framing curve which replaces it, once and only once, and intersect no other α's. Each will, however, intersect at least one β curve in the projection. By Proposition 5.3.11 of [3], these meridians generate all of $H_1(Y;\mathbb{Z})$. By winding along them we may obtain intersection points representing any *Spin*^{c} structure; we have an intersection point which employs the framing curves intersecting the same β's as the meridian.

These are the conditions necessary to draw the conclusion of lemmas 5.2, 5.4, and 5.6 of [13]. These lemmas guarantee the results in the proposition. **Q.E.D.**

When we present a d-based link in Y as a string link in a framed surgery diagram

Remark: There are other embedded objects lurking in the background of our Heegaard diagrams. The first:

Definition 2.3. [16] *An oriented bouquet, Γ, is a one-complex embedded in Y which is the union of a oriented link $\mathbb{L} = \cup_{i=1}^{k} L_i$ with a collection of k embedded segments, γ_i, each connecting a point on L_i to a fixed reference point in Y, and otherwise disjoint from $\mathbb{L}$ and each other.*

We will consider such objects up to isotopy in Y, preserving the graph structure. They are also known as clover links, [9]. Such embedded graphs underly the construction of maps in Heegaard-Floer homology from four-dimensional cobordisms formed by 2-handle additions.

Given a d-based link, we may form such an object by choosing our reference point in D and joining it to the intersections with $\mathbb{L}$ by a tree. There are many such trees, found, for instance, by braiding in D, and these are not necessarily isotopic. However, our invariant does not distinguish them. Furthermore, two different string links can give the same isotopy class of bouquet corresponding to twisting the bouquet along the reference paths (or moving the ends of the string link back and forth between the ends of the cylinder). We can record this twisting by adorning a bouquet with a d-base formed from a disc neighborhood of its reference paths.

Additionally, in an associated multi-pointed diagram, the critical points corresponding to the 3-cell and the 0-cell for a Morse function compatible with the Heegaard decomposition along with the gradient flow lines though the marked points gives an embedded copy of a θ_{k+1}-graph with a preferred edge arising from w: a graph with two vertices and $k+1$ edges oriented from one vertex to the other. By taking a tubular neighborhood of the preferred edge we have a copy of $D^2 \times I$; in its complement is a string link determined by the other edges. The region around v_- together with discs bounded by the meridians of the non-preferred edges forms the d-base. The θ_{k+1} graph may be obtained from a diagram subordinate to a string link by stretching Σ along the boundary of $D' \cup_{i \leq k} D(\alpha_i)$ where $D(\alpha_i)$ is the attaching disc for α_i. The result is a diagram for a tubular neighborhood of the θ_{k+1}-graph with one edge linked by the embedded circle. The region bounded by the meridians and the new curve, containing D', corresponds to v_-, the vertex into which the edges point. Isotopies of d-based links correspond to isotopies of the associated θ_{k+1}-graphs.

3. Multi-point Heegaard-Floer Homology

3.1. **Background and Notation.** Let $H_\alpha \cup_{\Sigma^g} H_\beta$ and a choice of $w \in \Sigma$ be a pointed strongly/weakly admissible Heegaard decomposition of Y, [13]. Let $\{\alpha_i\}_{i=1}^g$ be a set of g disjoint, simple, closed curves in Σ whose images are linearly independent in $H_1(\Sigma;\mathbb{Z})$ and which bound compression discs in H_α. Define $\{\beta_i\}_{i=1}^g$ similarly for H_β.

These sets give rise to g-dimensional tori embedded in $Sym^g(\Sigma)$ and found by taking the image of

$$\alpha_1 \times \cdots \times \alpha_g \qquad \beta_1 \times \cdots \times \beta_g$$

under the quotient map $\Sigma^{\times g} \to Sym^g(\Sigma)$. A choice of orientation on each element of $\{\alpha_i\}_{i=1}^g$ induces an orientation on orientation on the image, $\mathbb{T}_\alpha$.

An intersection point, $\mathbf{x}$ between the tori $\mathbb{T}_\alpha$ and $\mathbb{T}_\beta$ corresponds to a set, $\{x_1, \ldots, x_g\}$, of points in Σ where $x_i \in \alpha_i \cap \beta_{\sigma(i)}$ for $i = 1, \ldots, g$ and some permutation $\sigma \in S_g$. We will denote the point in Σ defining $\mathbf{x}$ and lying on α_i by $\mathbf{x}(\alpha_i)$, and likewise for the β curves.

We consider homotopy classes of continuous maps, $u : \mathbb{D} \to Sym^g(\Sigma)$ taking i to $\mathbf{y}$, $-i$ to $\mathbf{x}$ and the remainder of the boundary into $\mathbb{T}_\alpha$ if $\mathfrak{Re} > 0$ or $\mathbb{T}_\beta$ if $\mathfrak{Re} < 0$. The set of such classes is denoted by $\pi_2(\mathbf{x}, \mathbf{y})$. When we have classes $\phi_1 \in \pi_2(\mathbf{x}, \mathbf{y})$ and $\phi_2 \in \pi_2(\mathbf{y}, \mathbf{z})$ there is a well-defined class $\phi_1 * \phi_2 \in \pi_2(\mathbf{x}, \mathbf{y})$

The intersection points divide into equivalence classes according to whether $\pi_2(\mathbf{x}, \mathbf{y})$ is the empty set or not. The set of all equivalence classes will be denoted $\mathcal{S}_{\alpha\beta}$ and a specific equivalence class will be denoted $\mathfrak{s}$. The set of intersection points representing $\mathfrak{s}$ will be

denoted by $\mathcal{I}(\mathfrak{s})$. Once we add the point w to the diagram, the equivalence classes can be interpretted as $Spin^c$ structures for Y (see [13]).

Let $z \in \Sigma - \{\alpha_i\}_{i=1}^g - \{\beta_i\}_{i=1}^g$ and denote by $n_z(\phi)$ the intersection number of a generic representative of ϕ with the image $z \times \Sigma^{g-1}$ under the quotient onto $Sym^g(\Sigma)$. If we consider $\Sigma - (\{\alpha_i\}_{i=1}^g \cup \{\beta_i\}_{i=1}^g) = \coprod D_i$ be the disjoint union of domains, D_i, we may calculate a multiplicity for each domain by assigning $n_{\mathcal{D}_i}(\psi) = n_z(\psi)$ for some $z \in int(\mathcal{D}_i)$.

Definition 3.1. *The domain of a class $\phi \in \pi_2(\mathbf{x}, \mathbf{y})$ is defined to be the formal linear combination*

$$\mathcal{D}(\phi) = \sum_{i=1}^{s} n_{\mathcal{D}_i}(\phi)\mathcal{D}_i$$

P. Ozsváth and Z. Szabó describe the structure of $\pi_2(\mathbf{x}, \mathbf{y})$ when $g > 1$.

$$\pi_2(\mathbf{x}, \mathbf{y}) \cong \begin{cases} \emptyset & when\ \epsilon(\mathbf{x}, \mathbf{y}) \neq 0 \\ \mathbb{Z} \oplus H_2(Y, \mathbb{Z}) & when\ \epsilon(\mathbf{x}, \mathbf{y}) = 0 \end{cases}$$

The value in $\mathbb{Z}$ arises from evaluating $n_w(\phi)$. It can be altered by adding or subtracting the generator of $\pi_2(Sym^g(\Sigma)) \cong \mathbb{Z}$ to the homotopy classes of discs:

$$\pi_2(Sym^g(\Sigma)) * \pi_2(\mathbf{x}, \mathbf{y}) \to \pi_2(\mathbf{x}, \mathbf{y})$$

This, in turn, corresponds to adding or subtracting $\mathcal{D}(\Sigma)$ to or from $\mathcal{D}(\psi)$ and will be referred to as adding or subtracting $[S]$.

The $H_2(Y, \mathbb{Z})$ term arises from the doubly periodic domains:

Definition 3.2. *A doubly periodic region is a two chain $\mathcal{P} = \sum a_i \mathcal{D}_i$ whose boundary is a sum of curves contained in $\{\alpha_i\}_{i=1}^g \cup \{\beta_i\}_{i=1}^g$. Let $\mathcal{D}_i$ be the domain containing w. A doubly periodic domain is a periodic region with $a_i = 0$.*

To each periodic region, $\mathcal{P}$, there is an associated homology class, $H(\mathcal{P})$, in $H_2(Y; \mathbb{Z})$ found by gluing copies of the attaching discs associated to the boundary curves of $\mathcal{P}$. Furthermore, every homology class in $H_2(Y; \mathbb{Z})$ defines a periodic domain. These may be thought of as classes in $\pi_2(\mathbf{x}, \mathbf{x})$ and have the property that

$$\mathcal{D}(\phi + \mathcal{P}) = \mathcal{D}(\phi) + \mathcal{D}(\mathcal{P})$$

3.2. **Pseudo-Holomorphic discs in $Sym^g(\Sigma)$.** For a given $\phi \in \pi_2(\mathbf{x}, \mathbf{y})$ we consider the moduli space of pseudo-holomorphic representatives:

$$\mathcal{M}_{J_s}(\phi) = \left\{ u \in \phi \;\middle|\; \begin{array}{c} u(1 + t\,i) \subset \mathbb{T}_\alpha \\ u(0 + t\,i) \subset \mathbb{T}_\beta \\ \lim_{t \to +\infty} u(z) = \mathbf{y} \\ \lim_{t \to -\infty} u(z) = \mathbf{x} \\ \frac{\partial u}{\partial s} + J(s)\frac{\partial u}{\partial t} = 0 \end{array} \right\}$$

Translating in the t direction provides a natural $\mathbb{R}$ action on $\mathcal{M}_{J_s}(\phi)$. We will usually take the quotient

$$\widehat{\mathcal{M}}_{J_s}(\phi) = \mathcal{M}_{J_s}(\phi)/\mathbb{R}$$

The reader should consult [13] for further details.

The formal dimension of the moduli space, found from the index of a certain Fredholm operator, called the Maslov index of ϕ and denoted $\mu(\phi)$. The index has the property that $\mu(\phi + k[S]) = \mu(\phi) + 2k$ for any ϕ and is additive under splicing.

For $\mu \leq 2$ these spaces are orientable and have Gromov compatifications, [13]. Hence, generically, there will be no elements of a moduli space with $\mu = 0$. When $\mu = 1$, $\widehat{\mathcal{M}}_{J_s}(\phi)$ is a compact, zero-dimensional manifold. When $\mu(\phi) = 2$ and ϕ possesses holomorphic representatives, the ends of the corresponding moduli spaces can occur either through bubbling off spheres, boundary degenerations, or through limiting to holomorphic representatives of ϕ_1 and ϕ_2 where $\phi = \phi_1 * \phi_2$, [13].

3.3. **The Chain Complex for a Multi-point Diagram.** We start with a multi- pointed Heegaard diagram $(\Sigma, \{\alpha_i\}_{i=1}^g, \{\beta_i\}_{i=1}^g)$ where the curves in $\{\alpha_i\}_{i=1}^g$ and $\{\beta_i\}_{i=1}^g$ are in general position. We choose a path of generic nearly symmetric almost-complex structures, J_s, on $Sym^g(\Sigma)$, in accordance with the restrictions in [13]. Furthermore, we choose an equivalence class of intersection points, $\mathfrak{s}$, for Y and a coherent system of orientations for the equivalence class, [13][1]. We also assume that marked points $w, z_1, \ldots, z_k$ have been prescribed. We denote the additional marked point data by Γ.

Take the set $\mathbf{x} \in \mathcal{I}(\mathfrak{s})$ and define $CF^\infty_\Gamma(Y;\mathfrak{s})$ as the $\mathbb{Z}$-module

$$Span_{\mathbb{Z}}\{[\mathbf{x}, i, \overline{v}] | \mathbf{x} \in \mathcal{I}(\mathfrak{s}),\ i \in \mathbb{Z},\ \overline{v} \in \mathbb{Z}^k\}$$

There is a natural map on CF^∞_Γ:

$$U([\mathbf{x}, i, \overline{v}]) = [\mathbf{x}, i-1, v_1 - 1, \ldots, v_k - 1]$$

which makes CF^∞_Γ into a module over $\mathbb{Z}[U]$.

As in [13], we may define other groups by taking $CF^-_\Gamma(Y;\mathfrak{s})$ to be the sub-group of CF^∞_Γ where $i < 0$; by taking $CF^+_\Gamma(Y;\mathfrak{s})$ to be the resulting quotient group (with $i \geq 0$); and by taking $\widehat{CF}_\Gamma(Y, \mathfrak{s})$ to be that sub-group spanned by those generators with $i = 0$.

We may define a relative grading by the formula

$$gr_w([\mathbf{x}, i, \overline{v}_1], [\mathbf{y}, j, \overline{v}_2]) = \mu(\phi) - 2\, n_w(\phi) + 2(i - j)$$

where we may use any $\phi \in \pi_2(\mathbf{x}, \mathbf{y})$. However, when $c_1(\mathfrak{s}_w(\mathbf{x}))$ is not torsion the right side is only well-defined in $\mathbb{Z}/\delta(\mathfrak{s})\mathbb{Z}$ where

$$\delta(\mathfrak{s}) = \gcd_{\xi \in H_2(Y;\mathbb{Z})} < c_1(\mathfrak{s}), \xi >$$

since

$$\mu(\mathcal{P}_\mathbf{x}) =< c_1(\mathfrak{s}_w(\mathbf{x})), [\mathcal{P}] >$$

[1]Those willing to work with $\mathbb{Z}/2\mathbb{Z}$-coefficients may ignore this requirement

The map U reduces this grading by 2, [13].

If $\mathfrak{s}$ has torsion first Chern class, the relative grading lies in $\mathbb{Z}$. In addition, for a torsion $Spin^c$ structure, P. Ozsváth and Z. Szabó in [16] show that there exists a absolute $\mathbb{Q}$-grading, $gr_{\mathbb{Q}}$, lifting the relative grading. The absolute $\mathbb{Q}$ grading in [16] depends only upon the i component, so the multi-point complex inherits it. Alternately, we may present Y as surgery on a link which includes the components of $\mathbb{L}$, which receive an ∞-framing. Then we can assign the absolute grading to the generators using the formula in [16].

3.4. **Filtration Indices.** The additional marked points $z_1, \ldots, z_k$ provide indices for the generators related to the grading.

3.4.1. *Complete Sets of Paths.*

For the equivalence class $\mathfrak{s}$, we choose a complete set of paths for $\mathfrak{s}$ as in Definition 3.12 of [13]:

(1) An enumeration $\mathcal{S} = \{\mathbf{x_0}, \mathbf{x_1}, \ldots, \mathbf{x_m}\}$ of the intersection points in $\mathcal{I}(\mathfrak{s})$.
(2) A collection of homotopy classes $\phi_i \in \pi_2(\mathbf{x_0}, \mathbf{x_i})$ with $n_w(\phi_i) = 0$
(3) Periodic domains $\Xi_1, \ldots, \Xi_{b_2} \in \pi_2(\mathbf{x_0}, \mathbf{x_0})$ representing a basis for $H_2(Y; \mathbb{Z})$.

Any path in $\pi_2(\mathbf{x_i}, \mathbf{x_j})$ can then be written uniquely as splicings of the Ξ_i and the paths ϕ_i, and any periodic domain in $\pi_2(\mathbf{x}, \mathbf{x})$ can be identified with one in $\pi_2(\mathbf{x_0}, \mathbf{x_0})$.

As in [14], given a complete set of paths we may find a map

$$\mathcal{A} : \pi_2(\mathbf{x}, \mathbf{y}) \to H_2(Y; \mathbb{Z})$$

by taking $\phi_y^{-1} * \phi * \phi_x \in \pi_2(\mathbf{x_0}, \mathbf{x_0}) \cong \mathbb{Z} \oplus H_2(Y; \mathbb{Z})$, and projecting to the second factor. This map has the property that $\mathcal{A}(\phi_1 * \phi_2) = \mathcal{A}(\phi_1) + \mathcal{A}(\phi_2)$. The procedure provides an identification of $\pi_2(\mathbf{x}, \mathbf{x})$ with $\pi_2(\mathbf{x_0}, \mathbf{x_0})$, and the action of $\mathcal{P} \in \pi_2(\mathbf{x}, \mathbf{x})$ on $\phi \in \pi_2(\mathbf{x}, \mathbf{y})$ produces ϕ' with $\mathcal{A}(\phi') = \mathcal{A}(\phi) + \mathcal{A}(\mathcal{P})$.

Furthermore, a choice of basepoint $\mathbf{x_0}$, a basis for $H_2(Y, \mathbb{Z})$, and a choice of an additive $\mathcal{A}$ which maps $\pi_2(\mathbf{x_0}, \mathbf{x_0})$ surjectively onto $H_2(Y; \mathbb{Z})$ and is invariant under the action of $[S]$, gives a complete set of paths. For a doubly periodic domain $\mathcal{P} \in \pi_2(\mathbf{x_0}, \mathbf{x_0})$, $\mathcal{A}$ assigns it a value in $H_2(Y; \mathbb{Z})$. For $\phi \in \pi_2(\mathbf{x_0}, \mathbf{y})$ we have two quantities $\mathcal{A}(\phi)$ and $n_w(\phi)$. By subtracting the periodic domain $\mathcal{P}$ with the same value under $\mathcal{A}$ as ϕ and subtracting the right number of $[S]$'s, we find a ϕ' where both quantities are zero. This ϕ' is unique since $\mathcal{A}$ is surjective, so we choose it as our element, ϕ_y, in a complete set of paths.

3.4.2. *Definition of Filtration Indices.* We may define a filtration index for the complete set of paths as a map $\overline{\mathcal{F}} : \mathcal{I}(\mathfrak{s}) \to \mathbb{Z}^k$ satisfying the basic relation

$$\overline{\mathcal{F}}(\mathbf{y}) - \overline{\mathcal{F}}(\mathbf{x}) = (n_w - n_{\overline{z}})(\phi) + n_{\overline{z}}(\mathcal{A}(\phi))$$

where $n_{\overline{z}}(\phi) = (n_{z_1}(\phi), \ldots, n_{z_k}(\phi))$ and $n_w(\phi) = (n_w(\phi), \ldots, n_w(\phi))$. These compare the information found at the preferred point, w, to that at any other marked point z_k.

When we add a periodic domain $\mathcal{P}$ to ϕ the right hand side of the filtration relation changes by $-n_{\overline{z}}(\mathcal{P}) + n_{\overline{z}}(\mathcal{P}) = 0$. Thus, with the complete set of paths, the relation

determines the value of $\overline{\mathcal{F}}$ on every intersection point, independent of ϕ, up to a vector: any other filtration index for $\mathbf{x_0}$ and $\mathcal{A}$ has the form $\overline{\mathcal{F}} + v$ for some vector $v \in \mathbb{Z}^k$.

The last term on the right can be re-written in the i^{th} coordinate as $L_i \cap \mathcal{A}(\phi)$. The orientation on the meridians is the one induced from the attaching disk oriented to intersect L_i positively: $L_i \cap D_i = +1$. If we choose $\mathcal{P}$ a periodic region representing the homology class $h \in H_2$ then $\partial\mathcal{P}$ may contain multiples of the meridians. By drawing the diagrams we find that with this orientation convention $(n_w - n_{z_i})(\mathcal{P}) = -L_i \cap h$. The quantity $n_w - n_{z_i}$ measures[2] the number of times the i^{th} meridian occurs in $\partial\mathcal{P}$.

Adding or subtracting elements of $\pi_2(\mathbf{x}, \mathbf{x})$ thus alters the last term by vectors in the lattice, $\Lambda \subset \mathbb{Z}^k$, spanned by:

$$\begin{gathered}(n_{z_1}(\Xi_1), \ldots, n_{z_k}(\Xi_1)) \\ \vdots \\ (n_{z_1}(\Xi_k), \ldots, n_{z_k}(\Xi_k))\end{gathered}$$

since we assume $n_w(\Xi_j) = 0$.

Differences in the filtration index can be calculated directly if we know explicitly the homotopy classes in the complete set of paths. The difference between $\mathbf{x}$ and $\mathbf{y}$ is given by $n_{\overline{z}}(\phi_y * \phi_x^{-1})$. For this composite disc $\mathcal{A} = 0$ and $n_w = 0$. For rational homology spheres the choice of $\phi \in \pi_2(\mathbf{x}, \mathbf{y})$ varies only by multiples of $[S]$. Thus, $\phi_y * -\phi_x = \phi + r[S]$. In this case, or in any case where $\Lambda \equiv 0$, the filtration index takes values in $\mathbb{Z}^k$, and we recover the formulas used for knots in [15].

Once we have fixed the value of $\mathbf{x_0}$, the choice of $\mathcal{A}$ prescribes a value in $\mathbb{Z}^k$ for each $\mathbf{y}$. Different choices of complete sets of paths prescribe different values for $\mathbf{y}$; however, all these values map to the same element of $\mathbb{Z}^k/\Lambda$. For example, consider $\mathbf{x}$ and $\mathbf{y}$ joined by a path ϕ with $n_w(\phi) = 0$. If we change to $\mathcal{A}'$ then $-n_z(\phi - \mathcal{A}'(\phi)) = -n_z(\phi'_{\mathbf{y}}) + n_z(\phi'_{\mathbf{x}})$ $= -n_z(\phi_{\mathbf{y}} * -\phi_{\mathbf{x}} * \mathcal{P}) = -n_z(\phi - \mathcal{A}(\phi)) + \lambda$. Changing $\mathcal{A}$ to $\mathcal{A}'$ changes the relation by an element of Λ for each pair of intersection points.

Thus, we may remove the dependence upon $\mathcal{A}$ by considering filtraion indices with values in the quotient $\mathbb{Z}^k/\Lambda$. The intersection points are then relatively $\mathbb{Z}^k/\Lambda$-indexed. The $\mathbb{Z}^k$ indices are "lifts" of these indices, which we use when needing to facilitate comparisons as Λ changes.

Remark 3.3. *From now on, we assume, as chosen, a point $\mathbf{x_0} \in \mathcal{I}(\mathfrak{s})$ and a complete set of paths for $\mathfrak{s}$ and $\mathbf{x_0}$. Furthermore, we require that if z_i and z_j are in the same component of $\Sigma - \{\alpha_i\}_{i=1}^g - \{\beta_i\}_{i=1}^g$ then $\mathcal{F}_i$ and $\mathcal{F}_j$ must be equal. If z_i is in the same component as w then $\mathcal{F}_i \equiv C_i$, a constant, which we require to be 0, unless otherwise noted.*

3.4.3. *A Special Case.*
For null-homologous knots and torsion $\mathfrak{s}$ there is a canonical choice of filtration index found from the first Chern class, [15]. Suppose all the knots in Y found by closing strands in S are null-homologous, and that we have a Heegaard diagram where the intersection point

[2]When α_i intersects more than one β, and with the gradient flowing with the outward normal of H_α, $n_w - n_{z_i}$ is minus the intersection number with the edge corresponding to L_i in the graph, $\Theta(\Gamma)$.

on the each meridian is fixed. Let λ_i be a longitude for the closure of the i^{th} strand, L_i. This curve can be realized in the Heegaard diagram for the string link as a curve crossing only one α-curve, the i^{th} meridian. Interchanging the meridian with this longitude gives a Heegaard diagram for the manifold found by performing 0-framed surgery on L_i. To each intersection point in $\mathbf{x} \in \mathbb{T}_\alpha \cap \mathbb{T}_\beta$ we can associate an intersection point, $\mathbf{x}'$, for the new Heegaard diagram, cf. [15]. The Seifert surface for the closure of the i^{th} strand becomes a doubly periodic domain, $\mathcal{P}_i$, in the new diagram. Following the argument in [15] shows that we may choose

$$\mathcal{F}_i(\mathbf{x}) = \frac{1}{2} < c_1(\mathfrak{s}_w(\mathbf{x}'), [\mathcal{P}_i] >$$

for our filtration index. This provides a canonical choice over different $Spin^c$ structures on Y, which the axiomatic description lacks.

3.5. **The Relationship Between Gradings and Filtration Indices.** There is another interpretation of the filtration indices, which we describe for a knot. If we choose $\phi \in \pi_2(\mathbf{x}, \mathbf{y})$ we can lift the relative $\mathbb{Z}/\delta(\mathfrak{s})\mathbb{Z}$-grading using the procedure for filtrations:

$$gr_w([\mathbf{x}, i], [\mathbf{y}, j]) = \mu(\phi) - 2\, n_w(\phi) + 2(i - j) - < c_1(\mathfrak{s}_w), \mathcal{A}(\phi) >$$

where $\mathfrak{s}_w$ is the $Spin^c$ structure represented by $(w, \mathbf{x})$. When we use z as the basepoint for Heegaard-Floer homology, we have

$$gr_z([\mathbf{x}, i], [\mathbf{y}, j]) = \mu(\phi) - 2\, n_z(\phi) + 2(i - j) - < c_1(\mathfrak{s}_z), \mathcal{A}(\phi) >$$

calculating $\mathcal{A}(\phi)$ using the complete set of paths for w. If we add a periodic domain for z, the term with n_z does not change. However, $\mathcal{P}_z = \mathcal{P}_w + r\,[S]$, so $\mathcal{A}(\mathcal{P}_z) = \mathcal{A}(\mathcal{P}_w)$ and this expression is independent of ϕ. The difference

$$gr_z([\mathbf{x}, i], [\mathbf{y}, j]) - gr_w([\mathbf{x}, i], [\mathbf{y}, j]) = 2(n_w - n_z)(\phi) - < c_1(\mathfrak{s}_w), \mathcal{A}(\phi) > + < c_1(\mathfrak{s}_z), \mathcal{A}(\phi) >$$

is equal to $2(\mathcal{F}(\mathbf{y}) - \mathcal{F}(\mathbf{x}))$ since $\mathfrak{s}_z - \mathfrak{s}_w = [K]$ and $n_z(\mathcal{A}(\phi)) = [K] \cap \mathcal{A}(\phi)$. We can adapt this discussion to string links by considering each coordinate separately. In effect, the filtration indices are measuring the difference in relative gradings for $Spin^c$ structures induced by the same intersection point but with different basepoints.

3.6. **The Differential and the Γ-Sub-Complex.** As in [13] there is a differential, ∂° on $CF^\circ_\Gamma(Y; \mathfrak{s})$ for $\circ$ equal to ∞, $+$, $-$, or $\widehat{\cdot}$, defined by the linear extension of

$$\partial[\mathbf{x}, i, \overline{v}] = \sum_{\mathbf{y} \in \mathcal{I}(\mathfrak{s})} \sum_{\substack{\phi \in \pi_2(\mathbf{x}, \mathbf{y}) \\ \mu(\phi) = 1}} \#\widehat{\mathcal{M}}(\phi)[\mathbf{y}, i - n_w(\phi), \overline{v} - n_{\overline{z}}(\phi) + n_{\overline{z}}(\mathcal{A}(\phi))]$$

where the signed count is made with respect to a choice of a coherent system of orientations. We verify that this is a differential below. The differential is a $\mathbb{Z}[U]$-module map when $\circ$ is $\pm$ or ∞. Since $i - n_w(\phi) \leq i$ when ϕ admits holomorphic representatives, we see that the sub-group CF^-_Γ is a sub-complex. The differential on CF^+_Γ makes it into a quotient complex. For $\widehat{CF}_\Gamma$ we restrict to those generators with $i = 0$ and those ϕ with $n_w(\phi) = 0$.

When the lattice $\Lambda_{(Y,\Gamma)} \equiv 0$ this complex is $\mathbb{Z}^{k+1}$ filtered by the relation

$$(i, j_1, \dots, j_k) < (i', j_1', \dots, j_k')$$

when $i < i'$ and $j_l < j_l'$ for all l. We have $\partial[\mathbf{x}, i, \overline{v}] \leq [\mathbf{x}, i, \overline{v}]$ since $n_w(\phi), n_{z_i}(\phi) \geq 0$ on classes represented by a holomorphic disc. (The partial ordering on non-zero linear combinations of generators, $\sum \mathbf{y}_i \leq \sum \mathbf{x}_j$, occurs when every generator $\mathbf{y}_i \leq \mathbf{x}_j$ for each j). When $\Lambda \not\equiv 0$ the additional terms in the differential can disrupt the monotonicity of the indices, precluding similar filtrations. For $\widehat{CF}_\Gamma$ and $\Lambda \equiv 0$ there is a $\mathbb{Z}^k$ filtration defined analogously for the indices from the vector, $\overline{v}$.

We choose a complete set of paths and a multi-point filtration index $\overline{\mathcal{F}}$. Consider the sub-group of $CF^\infty_\Gamma(Y; \mathfrak{s})$ generated by those $[\mathbf{x}, i, \overline{v}]$ with

$$(v_1, v_2, \dots, v_k) - (i, i, \dots, i) = \mathcal{F}(\mathbf{x})$$

For a choice of $\mathcal{A}$, there is a unique k-tuple $(v_1, \dots, v_k)$ associated with $[\mathbf{x}, i]$ giving an element of this sub-group. When $\Lambda \equiv 0$ this k-tuple induces a $\mathbb{Z}^k$ filtration on the chain complexes for the Heegaard-Floer homology, $CF^\circ(Y, \mathfrak{s})$ in [13]. We define the filtration by $(v_1, \dots, v_k) \leq (c_1, \dots, c_k)$ for each fixed k-tuple $(c_1, \dots, c_k)$.

The filtration index relation ensures that this sub-group is a sub-complex. In particular, if $\mathbf{y}$ is in the boundary of $\mathbf{x}$, i.e. $< \partial\mathbf{x}, \mathbf{y} > \neq 0$, then

$$\overline{\mathcal{F}}(\mathbf{y}) = \overline{\mathcal{F}}(\mathbf{x}) + (n_{\overline{w}} - n_{\overline{z}})(\phi) + n_{\overline{z}}(\mathcal{A}(\phi))$$

$$= (v_1, \dots, v_k) - (i, \dots, i) + ((n_w - n_{z_1})(\phi), \dots, (n_w - n_{z_1})(\phi)) + n_{\overline{z}}(\mathcal{A}(\phi))$$

$$= ((v_1 - n_{z_1}(\phi)) - (i - n_w(\phi)) + n_{z_1}(\mathcal{A}(\phi)), \dots, (v_k - n_{z_k}(\phi)) - (i - n_w(\phi)) + n_{z_k}(\mathcal{A}(\phi))$$

$$= \big(\overline{v} - n_{\overline{z}}(\phi) + n_{\overline{z}}(\mathcal{A}(\phi))\big) - \big(i - n_{\overline{w}}(\phi)\big)$$

Thus $[\mathbf{y}, i - n_w(\phi), \overline{v} - n_{\overline{z}}(\phi) + n_{\overline{z}}(\mathcal{A}(\phi))]$ still satisfies the sub-complex condition. Furthermore, the action of U preserves the sub-complex, affording it the structure of a $\mathbb{Z}[U]$-module. We call this sub-complex $CF^\infty(Y, \Gamma; \mathfrak{s})$.

Lemma 6. *The map $\partial : CF^\infty(Y, \Gamma; \mathfrak{s}) \to CF^\infty(Y, \Gamma; \mathfrak{s})$ is a differential.*

Proof: This follows from [13] with almost no alteration. We consider $\psi \in \pi_2(\mathbf{x_0}, \mathbf{x_2})$ with a moduli space of holomorphic representatives of dimension $\mu(\psi) = 2$. We already know that the components of the boundary of $\mathcal{M}(\psi)$ which contribute to ∂^2 are of the form $\mathcal{M}(\phi_1) \times \mathcal{M}(\phi_2)$ for classes $\phi_1 \in \pi_2(\mathbf{x_0}, \mathbf{x_1})$ and $\phi_2 \in \pi_2(\mathbf{x_1}, \mathbf{x_2})$. The other possible ends are eliminated as in [13]. We choose our almost complex structures to exclude the bubbling of spheres at the intersection points. The introduction of marked points in the diagram does not alter this. On the other hand, we know that boundary bubbles will cancel in the summation of coefficients. This occurs for counts in specified degenerate homotopy classes, and all representatives of the homotopy class will induce the same change in the indices: $i, v_1, \dots, v_k$. All other degenerations are excluded for dimension reasons.

Since every homotopy class of discs satisfies the filtration index relation so will each of the classes ψ, ϕ_1 and ϕ_2. In particular, every boundary component of $\mathcal{M}(\psi)$ of the form $\phi_1 * \phi_2$ contributes to ∂^2. We know that

$$n_w(\psi) = n_w(\phi_1) + n_w(\phi_2)$$

$$n_{z_i}(\psi) = n_{z_i}(\phi_1) + n_{z_i}(\phi_2)$$

$$\mathcal{A}(\psi) = \mathcal{A}(\phi_1) + \mathcal{A}(\phi_2)$$

As a result, different ends of the compactification of $\widehat{\mathcal{M}}(\psi)$ are taken to the same element $[\mathbf{y}, i, \overline{v}]$ in ∂^2 and still cancel after a choice of a coherent orientations for the moduli spaces. So $\partial^2 = 0$ and defines a differential on both our complex and sub-complex.
Q.E.D.

The action of $H_1(Y, \mathbb{Z})/\mathrm{T}ors$ on the Heegaard-Floer homology, [13], extends to an action on the homology of the sub-complex. Let $\gamma \subset \Sigma$ be a simple, closed curve representing the non-torsion class $h \in H_1$ and missing every intersection point between an α and a β. Let $a(\gamma, \phi)$ be the intersection number in $\mathbb{T}_\alpha$ of $\gamma \times Sym^{g-1}(\Sigma) \cap \mathbb{T}_\alpha$ and $u(1+it)$ where u represents ϕ. This induces a map $\zeta \in Z^1(\Omega(\mathbb{T}_\alpha, \mathbb{T}_\beta), \mathbb{Z})$. The action of such a co-cycle is defined by the formula:

$$A_\zeta([\mathbf{x}, i, \overline{v}]) = \sum_{\mathbf{y}} \sum_{\{\phi : \mu(\phi)=1\}} \zeta(\phi) \cdot \left(\#\widehat{\mathcal{M}}(\phi)\right)[\mathbf{y}, i - n_w(\phi), \overline{v} - n_{\overline{z}}(\phi - \mathcal{A}(\phi))]$$

If Λ_Y is trivial then the map A_ζ is a filtered chain morphism. In addition, A_ζ preserves the sub-complex $CF^\infty(Y, \Gamma; \mathfrak{s})$, as ∂ does.

Following the argument presented above that $\partial^2 = 0$, we can verify that this is a chain map. We have the analog of Proposition 4.17 of [13]:

Theorem 3. *There is a natural action of the exterior algebra, $\Lambda^*(H_1(Y, \mathbb{Z})/\mathrm{T}ors)$ on the homology $HF^\infty(Y, \Gamma; \mathfrak{s})$, where $\zeta \in H_1(Y, \mathbb{Z})/\mathrm{T}ors$ lowers degree by 1 and induces a filtered morphism of the chain complex when $\Lambda_Y \equiv 0$.*

Proof: To see that this is a chain map note that the formula in lemma 4.17 of [13] for the coefficients of $\partial A_\zeta \pm A_\zeta \partial$ still applies as it only depends upon the ϕ's and not upon the additional indices. As for the differential, any ϕ used in $\pi_2(\mathbf{x}, \mathbf{z})$ with $\mu(\phi) = 2$ will give the same set of indices for $\mathbf{z}$. The same observation applies to lemmas 4.18 and 4.19 of [13].

Various other chain complexes may be defined from the above construction. When $\Lambda \equiv 0$ we may require any sub-set of the indices to be less than zero to get a sub-complex. Or we may take the quotient by this sub-complex. We can require that $i = 0$ and look at holomorphic discs with $n_w = 0$, or also disallow discs that cross some of the z_i. When we require $n_{z_i}(\phi) = 0$ for some or all of the marked points, we denote the resulting complex by $\widehat{CF}$. We then examine the sub-complexes generated by the intersection points inducing a given filtration index for the z_i we have disallowed. If we allow the disc to intersect the marked points associated with the components in a sub-link $\mathbb{L}_2$, but not all marked points, then the filtration indices from $\mathbb{L}_2$ define a $\mathbb{Z}^{|\mathbb{L}_2|}$- filtration on each complex $\widehat{CF}(Y, \Gamma - \mathbb{L}_2; \overline{v}_1)$, where $\overline{v}_1$ records the fixed filtration indices for the complementary sub-complex. When $\Lambda \not\equiv 0$ the only obvious sub-complexes are those that depend upon the i index, as in Heegaard-Floer homology. However, it is still meaningful to look at the sub-complex where $i = 0$ and the differential includes only those ϕ with $n_w(\phi) = 0$ and $n_{z_i}(\phi) = 0$ for all of the z_i. The differential in this complex is

$$\widehat{\partial}[\mathbf{x},\overline{j}] = \sum_{y}\sum_{\phi} \#\widehat{\mathcal{M}}(\phi)[\mathbf{y},\overline{v}+n_{\overline{z}}(\mathcal{A}(\phi))]$$

The $\overline{v}$ index may change, but only by an element of Λ. Thus the sub-complex differential preserves the summands:

$$\bigoplus_{\overline{v}\equiv\overline{v}' \bmod \Lambda} CF(Y,\Gamma;\mathfrak{s},\overline{v})$$

For null-homologous links, this definition reduces to the complex $\widehat{CF}(Y,\Gamma;\mathfrak{s},\overline{v})$. The equivalent when $\Lambda \not\equiv 0$ should be a complex $\widehat{CF}(Y,\Gamma;[\overline{v}])$ where the last entry is a coset of $\mathbb{Z}^k/\Lambda$. The specific filtration index prescribes a specific coset; however, only the relative difference between cosets will be invariant.

Convention: For the rest of the paper, $\widehat{CF}(Y,\Gamma;\mathfrak{s},[\overline{v}])$ is the complex with differential counting ϕ's with $n_w(\phi)=0$ and $n_{z_i}(\phi)=0$ for all of the z_i. When $\Lambda\equiv 0$, it is the E^1 term in the spectral sequence defined by the $\mathbb{Z}^k$ filtration on $\widehat{CF}_\Gamma(Y;\mathfrak{s})$.

Altogether we will have the following theorem, an extension of the theorem in [15] which provided the statement for null-homologous knots. The union $\Gamma_1\cup\Gamma_2=\Gamma$ requires that Γ_j be found from Γ by ignoring a set of link components, sets that are disjoint for $j=1,2$.

Theorem 4. *For $\Gamma\subset Y$ coming from a d-based link, the homology $\widehat{HF}(Y,\Gamma;\mathfrak{s})$ is a relatively $\mathbb{Z}^k/\Lambda$ indexed invariant of $\mathbb{L}\cup D$ up to isotopy which is a direct sum $\oplus_{[\lambda]}\widehat{HF}(Y,\Gamma;\mathfrak{s},[\lambda])$ of invariant sub-groups. There is a natural action of $H_1(Y;\mathbb{Z})/\mathrm{Tors}$ on each of the factors. When $\Gamma_1\cup\Gamma_2=\Gamma$, and $\Lambda_{\Gamma_2}\equiv 0$, the filtration indices for Γ_2 may be defined using the first Chern class. In this case, the $\mathbb{Z}^{|\Gamma_2|}$ filtered chain homotopy type of $CF^{\Gamma_2}(Y,\Gamma_1;\mathfrak{s},[\overline{j}])$ is an invariant of Γ for each coset, $[\overline{j}]$, of $\mathbb{Z}^{|\Gamma_1|}/\Lambda_{\Gamma_1}$.*

Comments:

(1) Although it seems plausible, when $\Lambda\not\equiv 0$, to consider those ϕ with $n_{\overline{z}}(\phi)\in\Lambda$, this does not prescribe a differential. That $\phi=\phi_1*\phi_2$ does not imply that $n_{\overline{z}}(\phi_j)\in\Lambda$. Hence the terms in ∂^2 may give rise to complementary boundaries one of which does not arise from the definition of the differential.

(2) The complexes for Γ are superficially similar to the twisted coefficients of [14]. Indeed, the proof of invariance parallels that for the twisted coefficients. However, twisted coefficients are used to distiguish homotopy classes that are otherwise indistiguishable; we cancel distinctions which would otherwise appear.

(3) The action of $H_1(Y;\mathbb{Z})$ may be extended to the various sub-complexes discussed. The definition mimics that for the differential. In particular, we may limit ourselves to ϕ with $n_w(\phi)=0$ and $n_{z_i}(\phi)=0$. When $\Lambda\equiv 0$, this action will be natural as filtered morphisms of chain complexes.

4. Maps of Multi-Pointed Homologies

We may extend the theory of maps on HF° induced by cobordisms of three manifolds.

4.1. **More about Complete Sets of Paths.** Let X be a Heegaard triple $\Sigma_{\alpha\beta\gamma}$. We wish to choose an assignment $\mathcal{A}$ from triangles representing certain $Spin^c$ structures to $H_2(X,\mathbb{Z})$ that is

I. Additive under splicing and addition of periodic domains.
II. Restricts to each boundary of the triple as a specified additive assignment from a complete set of paths for that component.

Let $\mathfrak{u}$ be a $Spin^c$ structure for X. We show how to define an additive assigment for the homotopy classes representing an orbit of $\mathfrak{u}$ under the action of $H_2(X;\mathbb{Z})$. The endpoints of these triangles represent the same $Spin^c$ structures on the boundary. The homology classes of doubly periodic domains do not change the $Spin^c$ structure on X; while the other $Spin^c$ structures in the orbit occur through $Im\,(\,H_2(X) \to H_2(X,\partial X)\,)$.

Given a single triangle $\psi_0 \in \pi_2(\mathbf{x_0},\mathbf{y_0},\mathbf{z_0})$ with $n_w(\psi_0)=0$, representing $\mathfrak{u}$, and complete sets of paths $\mathcal{A}_{\alpha\beta}$, $\mathcal{A}_{\gamma\alpha}$, and $\mathcal{A}_{\gamma\beta}$ for the $Spin^c$ structures it restricts to at the boundary, we may define a triply periodic domain for any triangle $\psi \in \pi_2(\mathbf{x},\mathbf{y},\mathbf{z})$ which restricts to the boundaries as the same $Spin^c$ structures as ψ_0. Take $\phi_{\mathbf{x}}$, $\phi_{\mathbf{y}}$, and $\phi_{\mathbf{z}}$ in their respective complete set of paths and consider the triply periodic domain such that

$$\phi_{\mathbf{z}} * \psi_0 + \mathcal{T} = \psi * (\phi_{\mathbf{x}} \otimes \phi_{\mathbf{y}}) + r[S]$$

Then $\mathcal{A}_{\alpha\beta\gamma}(\psi) = [\mathcal{T}]$ in $H_2(X;\mathbb{Z})$.

If we change ϕ_x, ϕ_y, and ϕ_z by $\mathcal{P}_{\alpha\beta}$, $\mathcal{P}_{\gamma\alpha}$, and $\mathcal{P}_{\gamma\beta}$, respectively, then we obtain a new additive assignment, related to the old by:

$$\mathcal{A}'(\psi) = \mathcal{A}(\psi) - \mathcal{P}_{\gamma\beta} + \mathcal{P}_{\gamma\alpha} + \mathcal{P}_{\alpha\beta}$$

Thus, if in $H_2(X,\mathbb{Z})$, we have $[\mathcal{P}_{\gamma\beta}] = [\mathcal{P}_{\alpha\beta}] + [\mathcal{P}_{\gamma\alpha}]$, and we get the same assignment of classes of triangles to $H_2(X;\mathbb{Z})$. Furthermore, for any triple of intersection points representing the correct $Spin^c$ structures, the map, $\mathcal{A}$, chooses a base-triangle for $\pi_2(\mathbf{x},\mathbf{y},\mathbf{z})$, the one for which $[\mathcal{T}]=0$ in $H_2(X;\mathbb{Z})$: $\phi_{\mathbf{z}} * \psi_0 * (\phi_{\mathbf{x}}^{-1} \otimes \phi_{\mathbf{y}}^{-1})$.

Alteration of ψ by a class ϕ in one of the boundaries induces the relation:

$$\mathcal{A}_{\alpha\beta\gamma}(\psi * \phi) = \mathcal{A}_{\alpha\beta\gamma}(\psi) + \mathcal{A}_{\circ}(\phi)$$

where $\circ$ should be replaced with the pair of subscripts designating that boundary. Applying the definitions, $\mathcal{A}(\psi * \phi)$ is the class $[\mathcal{T}]$ where

$$\phi * \psi * (\phi_{\mathbf{x}} \otimes \phi_{\mathbf{y}}) = \phi_{\mathbf{z}'} * \psi_0 + \mathcal{T} + r[S]$$

but $\psi * (\phi_{\mathbf{x}} \otimes \phi_{\mathbf{y}}) = \phi_{\mathbf{z}} * \psi_0 + \mathcal{A}(\psi)$ so $\phi * \psi * (\phi_{\mathbf{x}} \otimes \phi_{\mathbf{y}}) = (\phi * \phi_{\mathbf{z}}) * \psi_0 + \mathcal{A}(\psi)$. However, $\phi * \phi_{\mathbf{z}} = \phi_{\mathbf{z}'} + \mathcal{A}_{\circ}(\phi)$.

For the particular case that $\psi = \phi_{\gamma\beta} * \psi_0 * (\phi_{\alpha\beta} \otimes \phi_{\gamma\alpha})$ where $\phi_{\alpha\beta} \in \pi_2(\mathbf{x},\mathbf{x_0})$, $\phi_{\gamma\alpha} \in \pi_2(\mathbf{y},\mathbf{y_0})$, $\phi_{\gamma\beta} \in \pi_2(\mathbf{z_0},\mathbf{z})$, we have:

$$\mathcal{A}_{\alpha\beta\gamma}(\psi) = \mathcal{A}_{\gamma\beta}(\phi_{\gamma\beta}) + \mathcal{A}_{\alpha\beta}(\phi_{\alpha\beta}) + \mathcal{A}_{\beta\gamma}(\phi_{\gamma\alpha})$$

Finally, alteration of ψ_0 without changing the basepoints on the boundary components changes the identification with homology classes by adding the class of a triply periodic domain.

4.2. **Push-Forward Filtration Indices.** In analogy to the three dimensional case, let $\Lambda_{\alpha\beta\gamma}$ be the lattice in $\mathbb{Z}^k$ of vectors $(n_{z_1}(\mathcal{T}),\dots,n_{z_k}(\mathcal{T}))$ where $\mathcal{T}$ is any triply periodic domain. With additive identifications on the boundaries compatible with that on the homotopy classes of triangles, we can push forward the filtration indices from $Y_{\alpha\beta}$ and $Y_{\gamma\alpha}$. We define

$$\overline{\mathcal{G}}(\mathbf{z}) = \overline{\mathcal{F}}_{\alpha\beta}(\mathbf{x}) + \overline{\mathcal{F}}_{\gamma\alpha}(\mathbf{y}) + (n_w - n_{\overline{z}})(\psi) + n_{\overline{z}}(\mathcal{A}(\psi))$$

where $\psi \in \pi_2(\mathbf{x},\mathbf{y},\mathbf{z})$. The expression on the right does not change under the addition of any triply periodic domains or the class $[S]$. Thus it does not depend upon the specific homotopy class of triangles joining three given intersection points. Nor indeed does it change if we use a triangle abutting $\mathbf{z}$ but with different intial intersection points. Since

$$\overline{\mathcal{F}}_{\alpha\beta}(\mathbf{x}) - \overline{\mathcal{F}}_{\alpha\beta}(\mathbf{x}') = (n_w - n_{\overline{z}})(\phi_1) + n_{\overline{z}}(\mathcal{A}_{\alpha\beta}(\phi_1))$$
$$\overline{\mathcal{F}}_{\gamma\alpha}(\mathbf{y}) - \overline{\mathcal{F}}_{\gamma\alpha}(\mathbf{y}') = (n_w - n_{\overline{z}})(\phi_2) + n_{\overline{z}}(\mathcal{A}_{\gamma\alpha}(\phi_2))$$

when $\psi' = \psi * \phi_1 * \phi_2$, we find

$$\overline{\mathcal{G}}(\mathbf{z}) = \overline{\mathcal{F}}_{\alpha\beta}(\mathbf{x}') + \overline{\mathcal{F}}_{\gamma\alpha}(\mathbf{y}') + (n_w - n_{\overline{z}})(\psi') + n_{\overline{z}}(\mathcal{A}(\psi'))$$

since

$$\mathcal{A}_{\alpha\beta\gamma}(\psi) + \mathcal{A}_{\alpha\beta}(\phi_1) + \mathcal{A}_{\gamma\alpha}(\phi_2) = \mathcal{A}_{\alpha\beta\gamma}(\psi')$$

We may then check that $\overline{\mathcal{G}}$ is a filtration index for the $Spin^c$ structure on the $\gamma\beta$ boundary. Let $\phi \in \pi_2(\mathbf{z},\mathbf{z}')$ and $\psi \in \pi_2(\mathbf{x_0},\mathbf{y_0},\mathbf{z})$, then

$$\overline{\mathcal{G}}(\mathbf{z}') - \overline{\mathcal{G}}(\mathbf{z}) = (n_w - n_{\overline{z}})(\phi) + n_{\overline{z}}(\mathcal{A}_{\alpha\beta\gamma}(\psi')) - n_{\overline{z}}(\mathcal{A}_{\alpha\beta\gamma}(\psi))$$

where $\psi' = \phi * \psi$. But $\mathcal{A}_{\alpha\beta\gamma}(\psi') = \mathcal{A}_{\alpha\beta\gamma}(\psi) + \mathcal{A}_{\gamma\alpha}(\phi)$, and we are done.

Note: If we require the filtration index to be 0 on the basepoints, $\mathbf{x_0}$ and $\mathbf{y_0}$, we may use ψ_0 to calculate the value of $\overline{\mathcal{G}}(\mathbf{z_0}) = -n_{\overline{z}}(\psi_0)$. We will assume, unless otherwise stated, that $n_{\overline{z}}(\psi_0) = \overline{0}$.

We will often consider only those triangles which include $\mathbf{y}_0$ in $\Sigma_{\gamma\alpha}$. A similar argument allows us to pull back filtration indices from $\Sigma_{\gamma\beta}$ to $\Sigma_{\alpha\beta}$, written for this case:

$$\overline{\mathcal{G}}'(\mathbf{x}) = \overline{\mathcal{F}}_{\gamma\beta}(\mathbf{z}) - (n_w - n_{\overline{z}})(\psi) - n_{\overline{z}}(\mathcal{A}_{\alpha\beta\gamma})(\psi)$$

4.3. **Constructing Additive Assignments.** Suppose we have a four manifold $X_{\alpha\beta\gamma}$ defined by a Heegaard triple. We can consider the long exact sequence

$$\cdots \to H_3(X, Y_{\gamma\beta}) \to H_2(Y_{\gamma\beta}) \to H_2(X) \to H_2(X, Y_{\gamma\beta}) \to \cdots$$

$H_2(Y_{\gamma\beta})$ injects into $H_2(X)$ for a Heegaard triple because each doubly periodic domain is also a triply periodic domain. Furthermore, the image of $H_2(X)$ inside $H_2(X, Y_{\gamma\beta})$ is a free group as it consists of those triply periodic domains with non-trivial α-boundary; it is finitely generated and torsion free, since no multiple except 0 can eliminate that boundary. We may choose a splitting $H_2(X) \cong H_2(Y_{\gamma\beta}) \oplus C$, which we hope will reflect our Heegaard diagram.

Suppose we have additive assignments $\mathcal{A}_{\alpha\beta}$, $\mathcal{A}_{\gamma\alpha}$, and a specified basepoint $\mathbf{z_0}$ in $\mathbb{T}_\gamma \cap \mathbb{T}_\beta$. Suppose further that we have chosen a single triangle $\psi_0 \in \pi_2(\mathbf{x_0}, \mathbf{y_0}, \mathbf{z_0})$ and for each $\mathbf{z} \in \mathbb{T}_\gamma \cap \mathbb{T}_\beta$, there is a preferred triangle, $\psi_\mathbf{z} \in \pi_2(\mathbf{x}, \mathbf{y}, \mathbf{z})$, abutting $\mathbf{z}$ and representing a $Spin^c$ structure whose restrictions to the three boundary components are the same as those of ψ_0. We will assume that all these triangles have $n_w(\psi_\mathbf{z}) = 0$. We wish to see that this induces a complete set of paths on $\Sigma_{\gamma\beta}$ for the $Spin^c$ structure represented by $\mathbf{z_0}$.

For each $\mathbf{z}$ and $\phi \in \pi_2(\mathbf{z_0}, \mathbf{z})$, $n_w(\phi) = 0$, there is a triply periodic domain satisfying $\psi_\mathbf{z} * (\phi_\mathbf{x} \otimes \phi_\mathbf{y}) = \phi * \psi_0 + \mathcal{T}$. Using the splitting we may divide $[\mathcal{T}] = [\mathcal{P}] \oplus [\mathcal{T}']$. If we subtract $\mathcal{T}'$ from $\psi_\mathbf{z} * (\phi_\mathbf{x} \otimes \phi_\mathbf{y})$, we have a triangle which differs from $\phi * \psi_0$ by a doubly periodic domain in $Y_{\gamma\beta}$. We add this periodic domain to ϕ to get $\phi_\mathbf{z}$. Different choices of ϕ produce the same choice for $\phi_\mathbf{z}$ relative to the splitting. Suppose $\phi' = \phi + \mathcal{P}_{\gamma\beta} + r[S]$. We can ignore the term involvong $[S]$. Then $\mathcal{T}_{\phi'} = \mathcal{T}_\phi - \mathcal{P}$. Projecting to $H_2(Y_{\gamma\beta})$, we have $\mathcal{P}_{\phi'} = \mathcal{P}_\phi - \mathcal{P}$. Adding this to ϕ' shows that $\phi' + \mathcal{P}_{\phi'} = \phi + \mathcal{P}_\phi$.

4.4. **Chain Maps.** As in [13] and [16], we start with a Heegaard triple defining a four manifold $X_{\alpha\beta\gamma}$. We assume that we have complete sets of paths on the boundaries for the restriction of a $Spin^c$ structure, $\mathfrak{u}$, and that there is a compatible map $\mathcal{A}$ for $\Sigma_{\alpha\beta\gamma}$. We may define a multi-point chain map for the $Spin^c$ structure:

$$F_\mathfrak{s}([\mathbf{x}, i_1, \overline{j}_1], [\mathbf{y}, i_2, \overline{j}_2]) = \sum_\mathbf{z} \sum_\psi \#\mathcal{M}(\psi)[\mathbf{z}, i_1 + i_2 - n_w(\psi), \overline{j}_1 + \overline{j}_2 - n_{\overline{z}}(\psi) + n_{\overline{z}}(\mathcal{A}_{\alpha\beta\gamma}(\psi))]$$

where ψ is class representing $\mathfrak{s}$ with $\mu(\psi) = 0$.

That this is a chain map follows from the usual arguments by examining ends of moduli spaces with $\mu(\psi') = 1$. The identities for compatibility of additive assignments imply that for an end modelled upon

$$\mathcal{M}(\psi_{\alpha\beta\gamma}) \times \mathcal{M}(\phi_{\gamma\alpha})$$

we have

$$\mathcal{A}_{\alpha\beta\gamma}(\psi') = \mathcal{A}_{\alpha\beta\gamma}(\psi) + \mathcal{A}_{\gamma\alpha}(\phi_{\gamma\alpha})$$

Thus, the additional indices appear in the composition of the map and the differential in each boundary according to the triangles that arise in the splicing. Different ends from moduli spaces joining the same three intersection points will have the same value in the last entry, allowing us to conclude that the various cancellations necessary for this to be a chain map still occur.

Furthermore, the map is U invariant as the moduli spaces do not depend upon the particular i or j_l. Finally, the map preserves the sub-complexes defined from the filtration relations, where the filtration on the $\gamma\beta$-boundary is the push-forward of those on the $\alpha\beta$ and $\gamma\alpha$-boundaries for a choice of a complete set of paths. This follows from the formula for the push-forward index.

Note: The next section outlines the invariance of the homology groups under the reduced Heegaard equivalences. We should additionally check the invariance of the cobordism maps on homology under the various alterations: invariance of the almost complex structure, isotopies of attaching circles, handleslides, and stabilizations. Using the observations of the next section, these proofs follow directly. The compatibility of the maps, $\mathcal{A}$, ensure that the new indices do not disrupt the chain homotopy identities found in [13]. The following

sub-section relates the associativity properties of these maps. Once that is done, we can recover the arguments in the first sections of [16] by slight modifications. The naturality of the strong equivalence maps follows from these considerations. Specifically, under our restricted set of Heegaard equivalences, the chain maps for two presentations of (Y,Γ) commute with the maps induced by strong equivalences on homology.

4.5. **Associativity with Multi-point Filtrations.**
We consider two triples $(\Sigma,\{\alpha_i\}_{i=1}^g,\{\beta_i\}_{i=1}^g,\{\gamma_i\}_{i=1}^g;w)$ and $(\Sigma,\{\gamma_i\}_{i=1}^g,\{\beta_i\}_{i=1}^g,\{\delta_i\}_{i=1}^g;w)$ where we have equipped Σ with marked points $z_1,\dots,z_k$. We assume a choice of $Spin^c$ structures, $\mathfrak{s}_1$ and $\mathfrak{s}_2$, for the respective triples and a complete sets of paths for $\Sigma_{\alpha\beta}$, $\Sigma_{\gamma\beta}$, $\Sigma_{\delta\beta}$, $\Sigma_{\gamma\alpha}$, and $\Sigma_{\gamma\delta}$, as well as $\psi_{\alpha\beta\gamma}\in\pi_2(\mathbf{x_0},\mathbf{y_0},\mathbf{u_0})$ and $\psi_{\gamma\beta\delta}\in\pi_2(\mathbf{u_0},\mathbf{z_0},\mathbf{w_0})$ representing the $Spin^c$ structures. Let $\mathfrak{s}$ be the $Spin^c$ structure, $\mathfrak{s}_1\#\mathfrak{s}_2$ on the quadruple, $X_{\alpha\beta\delta\gamma}$.

In this paper we consider chain maps resulting from diagrams which represent surgeries, handleslides, or the other Heegaard equivalences. For these diagrams, each of the three manifolds described by $\Sigma_{\gamma\alpha}$, $\Sigma_{\delta\gamma}$, and $\Sigma_{\delta\alpha}$ will be homeomorphic to a connected sum of S^3's and $S^1\times S^2$'s, although the additional basepoints may prevent the reduced Heegaard equivalences from converting the diagram into the standard picture. The only triply periodic domains for this triple will be sums of doubly periodic domains from $\Sigma_{\gamma\alpha}$ and $\Sigma_{\gamma\delta}$. Furthermore, every doubly periodic domain, $\mathcal{P}_{\alpha\delta}\subset\Sigma_{\alpha\delta}$, will be a linear combination of doubly periodic domains from $\Sigma_{\gamma\alpha}$ and $\Sigma_{\gamma\delta}$.

Each diagram will possess only one torsion $Spin^c$ structure which will admit a special, closed generator for its chain group: Θ^+. All our homotopy classes of triangles and quadrilaterals will be required to use those special generators when available. For example, in the class $\psi_{\alpha\beta\gamma}$ we will require that $\mathbf{y}_0=\Theta^+_{\gamma\alpha}$), and our chain map will be $F_{\mathfrak{s}_1}(\mathbf{x}\otimes\Theta^+_{\gamma\alpha})$ These generators will always have filtration index equal to $\overline{0}$ and be basepoints for their respective complete set of paths. We denote by $\mathfrak{s}_0$ the unique $Spin^c$ structure represented by classes in $\pi_2(\Theta^+_{\alpha\delta},\Theta^+_{\delta\gamma},\Theta^+_{\gamma\alpha})$. The geometry of the Heegaard diagram will often provide a splitting $H_2(Y_{\gamma\alpha})\oplus H_2(Y_{\gamma\delta})$ as $H_2(Y_{\alpha\delta})\oplus\mathbb{Z}^m$ and a homotopy class of triangles, ψ_Θ abutting the special intersection points in $X_{\alpha\delta\gamma}$. We will use this data in the construction of a complete set of paths for the $Spin^c$ structure represented by $\Theta^+_{\delta\alpha}$.

Adding $\mathcal{P}_{\alpha\delta}$ to $\psi_1*\psi_2$ will not alter the $Spin^c$ structure on the quadruple, since in homology it is homlogous to a boundary class. However, adding a doubly periodic domain from $\Sigma_{\beta\gamma}$ may alter that $Spin^c$ structure (although not on the original triples). Given $\mathfrak{s}$ let $\mathfrak{G}$ be its orbit under the action of $i_*\big(H_2(Y_{\beta\gamma};\mathbb{Z})\big)$. We may then extend the coherent systems of orientations for the triples to one for quadruple $X_{\alpha\beta\delta\gamma}$ and this orbit, see [13]. We also assume that the quadruple is strongly/weakly admissible, as necessary.

The choices made above define maps, $\mathcal{A}$, on the boundaries of the quadruple and on the two original triples. As before, we may define such a map on the quadruple: $\mathcal{A}_{\alpha\beta\gamma\delta}(\psi)$ as the homology class of the sum of doubly periodic domains from pairs of $\{\alpha,\beta,\gamma,\delta\}$ which must be added to $\phi_{\mathbf{w}}*\psi_0$ to get $\psi*\big(\phi_{\mathbf{x}}\otimes\phi_{\mathbf{y}}\otimes\phi_{\mathbf{z}}\big)+r[S]$. The map

$$H_{\mathfrak{G}}([\mathbf{x},i_1,\overline{j}_1]\otimes[\mathbf{y},i_2,\overline{j}_2]\otimes[\mathbf{z},i_3,\overline{j}_3])=$$

$$\sum_{\mathbf{w}}\sum_{\{\psi|\mu(\psi)=0\}}\#\mathcal{M}(\psi)[\mathbf{w},i_1+i_2+i_3-n_w(\psi),\overline{j}_1+\overline{j}_2+\overline{j}_3-n_{\overline{z}}(\psi)+n_{\overline{z}}(\mathcal{A}_{\alpha\beta\gamma\delta}(\psi))]$$

where ψ represents a $Spin^c$ structure from $\mathfrak{G}$. This map induces a chain homotopy

$$F_{\mathfrak{s}_1} \circ F_{\mathfrak{s}_2} - \sum_{\{\mathfrak{u}\in\mathfrak{G}\}} F_{\mathfrak{u}|X_{\alpha\beta\delta}} \circ F_{\mathfrak{s}_0} = \partial_{\delta\beta} \circ H \pm H \circ \partial_{\alpha\beta\otimes\gamma\alpha\otimes\delta\gamma}$$

in the standard way, [13], thereby establishing associativity for our cobordism maps if we can find compatible additive assignments. (In the above formula, $F_{\mathfrak{s}_0} = F(\Theta^+_{\alpha\delta} \otimes \Theta^+_{\gamma\alpha})$ which, under our assumptions, if almost always $\pm\Theta^+_{\gamma\delta}$; however, with the additional marked points, this will need to be verified.)

Suppose that $\psi = \psi_1 * \psi_2$ represents an element of $\mathfrak{G}$ with ψ_1 occuring on $\Sigma_{\alpha\beta\gamma}$ and ψ_2 occuring on $\Sigma_{\gamma\beta\delta}$ and that they restricts to the boundary of the quadruple as does $\psi_0 = \psi_{\alpha\beta\gamma} * \psi_{\gamma\beta\delta}$. By the construction of $\mathcal{A}_{\alpha\beta\delta\gamma}$ we have $\mathcal{A}_{\alpha\beta\delta\gamma}(\psi) = \mathcal{A}_{\alpha\beta\gamma}(\psi_1) + \mathcal{A}_{\gamma\beta\delta}(\psi_2)$ and the additive assignments for the decomposition as quadrilateral and disc add correctly. We must examine the other decomposition into Heegaard triples: $X_{\alpha\beta\delta} \cup X_{\alpha\delta\gamma}$. to find compatible choices for $\mathcal{A}_{\alpha\beta\delta}$ and $\mathcal{A}_{\alpha\delta\gamma}$.

Since $X_{\alpha\beta\delta\gamma}$ is homotopy equivalent to four three-dimensional handlebodies glued along their boundary, any three of the boundary components form a basis for $H_3(X)$. We have the Meyer-Vietoris sequence for the decomposition along $Y_{\alpha\delta}$:

$$0 \to H_2(Y_{\alpha\delta}) \to H_2(X_{\alpha\delta\gamma}) \oplus H_2(X_{\alpha\beta\delta}) \to H_2(X) \to \mathrm{Tors}\, H_1(Y_{\alpha\delta})$$

since the transverse intersection of an element of $H_2(X;\mathbb{Z})$ cannot non-trivially intersect a class in $H_2(Y_{\alpha\delta})$, as these come from ∂X. However, Tors $H_1(Y_{\alpha\delta}) = 0$.

Each element of $\mathfrak{G}$ therfore restricts to $Y_{\alpha\delta}$ as the torsion $Spin^c$ structure. By assumption, it must restrict to the other boundary components of $X_{\alpha\delta\gamma}$ as their torsion $Spin^c$ structure, and thus be in the same equivalence class as ψ_Θ. We may use this triangle, and the assumptions on this triple to construct an additive assignment on $\Sigma_{\alpha\delta}$. Then for each element in $\mathfrak{G}$ there is a triangle $\psi_\mathfrak{u}$ such that $\psi_\mathfrak{u} * \psi_\Theta = \psi_{\alpha\beta\gamma} * \psi_{\gamma\beta\delta}$. By the long exact sequence above, the only variation in these choices arise from periodic domains in the $Y_{\alpha\delta}$, i.e. from the boundary of the quadruple diagram. These choices determine maps $\mathcal{A}_{\alpha\beta\delta}$ and $\mathcal{A}_{\alpha\delta\gamma}$, which will be compatible with the choices on the other decomposition.

Finally, if we push forward filtrations from $Y_{\alpha\beta}$ to $Y_{\gamma\beta}$ and then to $Y_{\delta\beta}$, using the basepoints for the complete sets of paths in the other boundaries, we find that for the homotopy classes ψ representing a $Spin^c$ structure on $\alpha\beta\delta$, the relationship is:

$$\overline{\mathcal{F}}_{\delta\beta}(\mathbf{w}) = \overline{\mathcal{F}}_{\alpha\beta}(\mathbf{x}) - n_{\overline{z}}(\psi_\Theta) + (n_w - n_{\overline{z}})(\psi) + n_{\overline{z}}(\mathcal{A}_{\alpha\beta\delta}(\psi))$$

Implicit here is the calculation of $-n_{\overline{z}}(\psi' - \mathcal{A}(\psi')) = -n_{\overline{z}}(\psi_\Theta)$ since ψ' abuts the three basepoints. When $n_{\overline{z}}(\psi_\Theta) = 0$ we recover the push forward from the $\alpha\beta\delta$-diagram, so the filtraion indices are also correct.

4.6. **Filtration Changes under Chain Maps in Various Settings.**

Suppose $(\Sigma, \{\alpha_i\}_{i=1}^g, \{\beta_i\}_{i=1}^g, \{\gamma_i\}_{i=1}^g)$ defines a cobordism from Y_0 to Y_1 presented as surgery on a framed link in Y_0. We will think of this as a diagram in Y_0 with the components of $\mathbb{L}$ receiving $+\infty$ framing. We now elucidate the effect of chain maps on the Λ-lattices and the filtration indices in the common situations in which they arise. We will assume that any initial triangle, ψ_0, for building $\mathcal{A}$ has $n_w(\psi_0) = 0$ and $n_{z_i}(\psi_0) = 0$ for every i. This

condition ensures that the push-forward filtration is 0 on the basepoint abutting ψ_0.

I. When considering the complexes $\widehat{CF}(Y_0,\Gamma;\mathfrak{s}_0)$ and $\widehat{CF}(Y_1,\Gamma;\mathfrak{s}_1)$ we restrict to homotopy classes of triangles, ψ, with $n_w(\psi)=n_{\overline{z}}(\psi)=0$. The chain complexes are relatively $\mathbb{Z}^k/\Lambda_{\alpha\beta}$ and $\mathbb{Z}^k/\Lambda_{\gamma\beta}$ -indexed, respectively, and the homology group for each filtration index is an invariant. Let F be the chain map defined as before for a $Spin^c$ structure restricting to $\mathfrak{s}_0$ and $\mathfrak{s}_1$. Both $\Lambda_{\alpha\beta}$ and $\Lambda_{\gamma\beta}$ inject into $\Lambda_{\alpha\beta\gamma}$. We may consider, by taking direct sums of the homologies at each end, that $\widehat{CF}(Y_i,\Gamma;\mathfrak{s}_i)$ is $\mathbb{Z}^k/\Lambda_{\alpha\beta\gamma}$- indexed. The direct sums occur over the pre-images of the maps $\mathbb{Z}^k/\Lambda_{\alpha\beta}$, $\mathbb{Z}^k/\Lambda_{\gamma\beta}\to\mathbb{Z}^k/\Lambda_{\alpha\beta\gamma}$. The chain map preserves the relative $\mathbb{Z}^k/\Lambda_{\alpha\beta\gamma}$ structure as the filtrations now satisfy

$$\overline{\mathcal{G}}(\mathbf{x})=\overline{\mathcal{F}}(\mathbf{x})+n_{\overline{z}}(\mathcal{A}_{\alpha\beta\gamma}(\psi))$$

II. $\Lambda_{\alpha\beta\gamma}\equiv 0$: For example, when we have a string link in S^3 and the cobordism is generated by surgeries on curves which are algebraically split from S. In this case, the push-forward filtration satisfies

$$\overline{\mathcal{G}}(\mathbf{y})=\overline{\mathcal{F}}(\mathbf{x})+(n_w-n_{\overline{z}})(\psi)$$

for every ψ representing a $Spin^c$ structure on the cobordism restricting in a specified way to the ends, and for any choice of a complete set of paths. The filtrations on the ends are $\mathbb{Z}^k$ filtrations and the chain map is a filtered map for the $\mathbb{Z}^{k+1}$-filtration. This situation occurs in the long exact skein sequence of [15]. In S^3, a filtration index on each component can be calculated using the first Chern class of a $Spin^c$ structure on the manifold obtained by performing 0 surgery on the knot. In [15], P. Ozsváth and Z. Szabó show that, in the case under consideration, the push forward of this filtration is the one determine by the first Chern class calculation on Y_1 and the formula above corresponds to their identity for c_1.

III. We will assume that no periodic domain from $\Sigma_{\gamma\alpha}$ has $n_{z_i}(\mathcal{P})\neq 0$. The diagrams encoding legitimate handleslides of attaching circles satisfies this assumption. Additionally, surgery on components of a bouquet, but not on any of the components of Γ, produces such a diagram. These periodic domains arise from the $S^1\times S^2$ connected sum components in $\Sigma_{\gamma\alpha}$. Then the filtration on $\Sigma_{\gamma\alpha}$ for the torsion $Spin^c$ structure is equivalent to 0. We require our ψ's to restrict to this $Spin^c$ structure. The filtration index will now satisfy

$$\overline{\mathcal{F}}_{\gamma\beta}(\mathbf{z})=\overline{\mathcal{F}}_{\alpha\beta}(\mathbf{x})+(n_w-n_{\overline{z}})(\psi)+n_{\overline{z}}(\mathcal{A}_{\alpha\beta\gamma}(\psi))$$

The last term may be improved when we are considering only ψ's representing a given $Spin^c$ structure. For then, $\mathcal{A}_{\alpha\beta\gamma}$ takes values in those triply periodic domains formed by summing doubly periodic domains from the boundary components. The value of $n_{\overline{z}}(\mathcal{A}_{\alpha\beta\gamma}(\psi))$ is $n_{\overline{z}}([\mathcal{P}_{\alpha\beta}])+n_{\overline{z}}([\mathcal{P}_{\gamma\beta}])$. Upon taking the quotient by $\Lambda_{\alpha\beta}+\Lambda_{\gamma\beta}\subset\mathbb{Z}^k$ we have the same relationship as in case I. In the proof of invariance in the next section we will give example of the general push-forward filtration index and the construction of complete sets of paths for a triple.

5. Invariance

To see that homology of these complexes are truly an invariant of the triple $(Y, \Gamma; \mathfrak{s})$, we need to show that performing any of the following moves will produce a chain homotopy equivalent complex:

- Handleslides and isotopies of $\{\beta_i\}_{i=1}^{g}$.
- Handleslides and isotopies of $\{\alpha_i\}_{i=k+1}^{g}$.
- Stabilization.
- Istopies of $\{\alpha_i\}_{i=1}^{k}$ and handleslides of them over element of $\{\alpha_i\}_{i=k+1}^{g}$.

Furthermore, we are not allowed to isotope or slide over any portion of the disc D'. We can, however, arrange for a β curve to isotope past the entire disc. The resulting diagram can be achieved by allowable handleslides in $\{\beta_i\}_{i=1}^{g}$ because the disc is contractible, [13].

We develop the proof of invariance through the multi-pointed diagrams; it precisely mimics the proof for Heegaard-Floer homology, [13], and uses the same technical results.

5.1. **Invariance Under Alteration of the Complete Set of Paths.** It does not matter which additive identification one uses. Let $\mathbf{x}_0$ be the basepoint for both $\mathcal{A}$ and $\mathcal{A}'$. This data determines the filtration index using the defining relation after choosing a value for $\overline{\mathcal{F}}(\mathbf{x}_0)$, which we also take to be $\overline{\mathcal{F}}'(\mathbf{x}_0)$. We define a map between the two complexes by $[\mathbf{x}, i, \overline{v}] \to [\mathbf{x}, i, \overline{v} + n_{\overline{z}}(\mathcal{A}'(\phi_x))]$ where ϕ_x is the special path found from $\mathcal{A}$. This is an isomorphism on the generators and is a chain map. Furthermore, the map takes the subcomplex defined by $\mathcal{A}$ to that defined by $\mathcal{A}'$. Thus it is an isomorphism on the homology groups determined by the different sets of data. Note that altering $\mathcal{A}$ changes the filtration index for an intersection point by an element of Λ. The identification with cosets remains unalterred by this isomorphism.

For changing $\mathbf{x}_0$ to $\mathbf{y}_0$, we may use $\phi_{y_0}^{-1}$ for ϕ'_{x_0} and $\phi_z * \phi_{y_0}^{-1}$ as ϕ'_z to define a complete set of paths and associated identification $\mathcal{A}'$. This does not alter $n_{\overline{z}}(\mathcal{A}(\phi))$ and changes $\overline{\mathcal{F}}$ by $\overline{\mathcal{F}}(\mathbf{y}_0)$. The map $[\mathbf{x}, i, \overline{v}] \to [\mathbf{x}, i, \overline{v} + n_{\overline{z}}(\phi_{y_0})]$ will induce a chain isomorphism from the homologies defined by one complete set of paths to that defined by the other, although shifting in the assignment to cosets of $\mathbb{Z}^k/\Lambda$ will occur.

Likewise, changing the value of $\overline{\mathcal{F}}(\mathbf{x}_0)$ shifts the values of the filtration index, and the assigment to a coset, but does not change any of the homology groups or their relation to each other in the relatively indexed groups.

5.2. **Results on Admissibility.** Strong/Weak admissibility can be achieved for all our diagrams without disrupting the assumptions coming from Γ. We have seen the existence of such diagrams already. In section 5 of [13] P. Ozsváth and Z. Szabó show how to ensure that isotopies, handlelsides and stabilizations can be realized through such diagrams. In each case this is achieved by finding a set $\{\gamma_i\}_{i=1}^{g} \subset \Sigma$ of disjoint, simple closed curves with the property that $\#(\beta_i \cap \gamma_j) = \delta_{i,j}$ and that $\mathbb{T}_\alpha \cap \mathbb{T}_\gamma \neq \emptyset$ (or the same but with the roles of α and β switched).

We convert, through stabilization, our multi-point diagram into a diagram with an embedded disc. We only need require that w and the entire disc do not intersect the winding region. However, we may always choose our γ's to lie in the disc's complement. If we wish to wind α's we can do the same, requiring only that each γ_i that intersects a meridian does

so away from the segment in $\partial D'$. With this arrangement of $\{\gamma_i\}_{i=1}^g$ the proofs of lemmas 5.4, 5.6, and 5.7 of [13] carry through.

5.3. **Invariance of Complex Structure and Isotopy Invariance.** In these cases, we re-write the chain maps defined in [13] to incorporate the new indices. For example, P. Ozsváth and Z. Szabó define a chain map for a homotopy of paths of almost complex structures which we adjust to be, cf. [13]:

$$\Phi^{\infty}_{J_{s,t}}[\mathbf{x}, i\,\overline{j}] = \sum_{\mathbf{y}} \sum_{\phi} \#\mathcal{M}_{J_{s,t}}(\phi)[\mathbf{y}, i - n_w(\phi), \overline{j} - n_{\overline{z}}(\phi - \mathcal{A}(\phi))]$$

where the sum is over all ϕ with $\mu(\phi) = 0$ and the moduli space consists of sutiable holomorphic representatives of ϕ.

Note that in this case, $\mathcal{A}$ requires no adjustment, as alteration of the almost complex structure does not change the homotopy classes of discs. That the filtration relation holds for all homotopy classes of discs ensures this is still a chain map and that the map preserves the Γ-sub-complex. When $\Lambda_{(Y,\Gamma)} \equiv 0$ the above map is a filtered chain morphism by the positivity of n_{z_i} and the absence of the $\mathcal{A}$ term.

Similar alterations ensure that the map does induce an isomorphism on homology (we need to adjust the chain homotopy in [13] which shows that the map has an inverse on homology). We need only that the trivial homotopy class of discs from $\mathbf{x}$ to $\mathbf{x}$ has $\mathcal{A}(\phi) = 0$ since $-\phi_x * \phi_x \sim 0$ in $\pi_2(\mathbf{x}_0, \mathbf{x}_0)$. The invariance of the action of $H_1(Y, \mathbb{Z})/\text{Tors}$ follows as in [13] adjusting the maps as above and using our previous observations.

For the isotopy invariance, the same argument applies (as the proofs are roughly parallel). We write the chain map coming from the introduction/removal of a pair of intersection points as:

$$\Gamma^{\Psi}[\mathbf{x}, i, \overline{j}] = \sum_{y} \sum_{\phi \in \pi_2^{\Psi}(\mathbf{x}, \mathbf{y}} \#\mathcal{M}^{\Psi}(\phi)[\mathbf{y}, i - n_w(\phi), \overline{j} - n_{\overline{z}}(\phi - \overline{\mathcal{A}}(\phi))]$$

where we count holomorphic representatives with moving boundary, [13]. Making these adjustments as necessary, we mimic the proof in [13].

Two new features occur: first, the isotopy may remove $\mathbf{x}_0$, and second, new intersection points need to be included in the complete set of paths. If we must change the basepoint for the complete set of paths, the homologies will be unalterred. However, the identification with the cosets of $\mathbb{Z}^k/\Lambda$ will alter as the filtration index changes by the constant vector $\overline{\mathcal{F}}(\mathbf{x}_0')$. This explains why we have only a relatively indexed homology group.

When we have a pair creation, with a fixed basepoint, we get new intersection points in pairs $\mathbf{q}_+$ and $\mathbf{q}_-$ with an obvious holomorphic disc in $\pi_2(\mathbf{q}_+, \mathbf{q}_-)$. The homotopy classes of discs joining intersection points from the original diagram do not change in this process. Thus we may extend $\mathcal{A}$ by choosing $\phi_{\mathbf{q}_+}$ for each $\mathbf{q}_+$ and amalgamating with the newly created disc to get $\phi_{\mathbf{q}_-}$. We use the extended $\mathcal{A}$ in our definition of Γ^{Ψ} as $\pi_2^{\Psi} \cong \pi_2'$. This restricts to the original identification on the homotopy classes for the original intersection points. For a pair annihilation we do not necessarily have the arrangement of preferred

paths as we have just described, but we may change the complete set of paths without changing the homologies to obtain it. This merely changes $\mathcal{F}(\mathbf{q}_-)$ by an element of Λ.

5.4. **Invariance under Handleslides.** The standard proof for handleslide invariance applies in this context, using the chain maps induced by a Heegaard triple as in the previous section. We show below that the element corresponding to Θ^+ is still closed and explain which additive assignment for homotopy classes of triangles will work.

We will describe this solely for the α's. Away from the curves involved in the handleslide, the resulting boundary $\Sigma_{\gamma\alpha}$ is the connected sum of genus 1 diagrams for $S^1 \times S^2$. Because we have not moved a curve across a marked point, the corresponding multi-point diagram has all the basepoints, w and z_i, in the same domain D of $\Sigma - \{\alpha_i\}_{i=1}^g - \{\gamma_i\}_{i=1}^g$.

If we calculate the multi-point filtration indices for $\Sigma_{\gamma\alpha}$ we see that 1) $\Lambda \equiv 0$ and 2)all 2^g representatives of the torsion $Spin^c$ structure have filtration index 0. None of the holomorphic discs cross any marked points, so the homology is the standard homology for the connected sum of $S^1 \times S^2$'s but with generators of the form $[\Theta^+, i, i, \dots, i]$. As usual, we will use the canonical generator Θ^+, the maximally graded generator with $i = 0$. We will use strongly admissible diagrams for the $Spin^c$ structures on the ends of the cobordism. The cobordism, $X_{\alpha\beta\gamma}$, is $Y \times I$ so each triangle will represent $\mathfrak{s} \times I$.

As in the proof of handleslide invariance in Heegaard-Floer homology, [13], our diagrams may be drawn so that each intersection point in $\mathbb{T}_\alpha \cap \mathbb{T}_\beta$ can be joined to an intersection point $\mathbf{x}' \in T_\gamma \cap T_\beta$ by a unique holomorphic triangle $\psi_{\mathbf{x}} \in \pi_2(\mathbf{x}, \Theta^+, \mathbf{x}')$ with domain contained in the sum of the periodic domains from $\Sigma_{\gamma\alpha}$.

We choose additive assignments $\mathcal{A}_1$ and $\mathcal{A}_2$ and their corresponding complete set of paths on both $\Sigma_{\alpha\beta}$ and $\Sigma_{\gamma\beta}$, respectively. We require that $\mathbf{x}'_{\mathbf{0}}$ on $\Sigma_{\gamma\beta}$ be the intersection point abutting $\psi_{\mathbf{x}_0}$. Because the handleslide does not cross a meridian we have that $n_w(\psi_{\mathbf{x_0}}) = n_{z_i}(\psi_{\mathbf{x_0}}) = 0$. If we identify $\pi_2(\mathbf{x}_0, \mathbf{x}_0)$ with $\pi_2(\mathbf{x}'_{\mathbf{0}}, \mathbf{x}'_{\mathbf{0}})$ using $\psi_{\mathbf{x}_0}$ then we implicitly have an identification $H_2(Y_0) \cong H_2(Y \times I) \cong H_2(Y_1)$. Any other triangle representing the same $Spin^c$ structure can be found from this triangle by splicing discs in the boundaries $\Sigma_{\alpha\beta}$ and $\Sigma_{\gamma\beta}$, by splicing doubly periodic domains from $\Sigma_{\gamma\alpha}$ (we always require our triangles include Θ^+), and by adding copies of Σ. If we think of $\psi = \phi' * \psi_{\mathbf{x}_0} * \phi^{-1} + \mathcal{P}_{\gamma\alpha} + k[S]$ then, using the formulas from section 4.1,

$$\mathcal{A}_{Y\times I}(\psi) = \mathcal{A}_2(\phi') - \mathcal{A}_1(\phi) + H(\mathcal{P}_{\gamma\alpha})$$

To the handleslide cobordism we associate the multi-point chain map determined by this additive assignment on $\Sigma_{\alpha\beta\gamma}$. The last term $H(\mathcal{P})$ plays no role in the chain map as the doubly periodic domains from that boundary contain no marked points in their support. With these observations the usual proof applies directly.

5.5. **Stabilization Invariance.** Stabilization changes the surface Σ to $\Sigma' = \Sigma \# \mathbb{T}^2$ and adds an additional α and an additional β curve, intersecting in a single point c. Stabilization does not alter H_2 nor does it affect the structures of $\pi_2(\mathbf{x}, \mathbf{y})$. Given an additive identification $\mathcal{A}$, we may extend $\mathcal{A}$ to the stabilization. Since any intersection point must involve the additional point c, we need only that $\mathcal{A}(\phi') = \mathcal{A}(\phi)$ and the choice $\mathbf{x}'_{\mathbf{0}} = \mathbf{x}_0 \times c$. We make the necessary alterations for the gluing result, Theorem 10.4 in [13], to hold.

This theorem provides the invariance under stabilization in the standard case. Our extension of the additive identification ensures that the Γ-sub-complex is preserved. Thus, we have an isomorphism from the homology for $(\Sigma, \{\alpha_i\}_{i=1}^g, \{\beta_i\}_{i=1}^g, \mathbf{x}_0, \mathcal{A})$ to that for $(\Sigma', \{\alpha_i\}_{i=1}^g \cup \alpha_{g+1}, \{\beta_i\}_{i=1}^g \cup \beta_{g+1}, \mathbf{x}_0 \times c, \mathcal{A}')$. In addition, in [13], P. Ozsváth and Z. Szabó show that the action of $H_1(Y, \mathbb{Z})/\text{Tors}$ is invariant under stabilization. That this also applies to multi-point diagrams follows analgously to the case of the differential.

6. Basic Properties of $\widehat{HF}(Y, S; \mathfrak{s})$

6.1. **Examples.**

Example 1: In Figure 2 we examine the homology of a knot in $S^1 \times S^2$ which intersects $[S^2]$ precisely once. Regardless of the knot, K, we may find a diagram as in the figure. The intersection points, after handlesliding, giving generators in the chain complex are precisely $\Theta^{\pm} \times \mathbf{x}$, where $\mathbf{x}$ is a generator for the Knot Floer homology of K in S^3. However, in the complex, only one of the two homotopy classes from Θ^+ to Θ^- does not cross the marked point, z. It is straightforward to verify that $\widehat{\partial}\Theta^+ \times \mathbf{x} = \Theta^- \times \mathbf{x} + \Theta^+ \times \widehat{\partial}_K \mathbf{x}$. In each $Spin^c$ structure, the filtration index collapses; however, the differential as above also produces trivial homology in each $Spin^c$ structure.

Example 2: Suppose we have a connected sum of standard genus 1 diagrams for S^3 and $S^1 \times S^2$. Then the canonical generator for the action of H_1 on the Heegaard-Floer group $\widehat{HF}(Y, \mathfrak{s}_0)$, for the torsion $Spin^c$ structure, is represented by a single, closed intersection point: Θ^+. We choose it as the basepoint for the complete set of paths, and choose a path in each component of the connected sum to θ^-. We can use these to connect Θ^+ to any other intersection point. As there are only 2 discs in each component, which we assume do not cross w and upon which the action of $\mathcal{A}$ takes one into the other, these each will evaluate to the same quantity on the $\overline{j}$ terms. However, since they evaluate the same way on $\overline{j}$ we have seen that $[\Theta^+, 0, \overline{0}]$ and all other Θ's are closed in the complex CF^+. For the complex $\widehat{CF}$ with the additional marked points we will need to make further assumptions.

6.2. **Subtracting a Strand.** Suppose we remove a component strand of $S \subset (Y - B^3)$ to obtain a new string link, S'. We may use the complex and differential defined from a Heegaard diagram for S by ignoring z_k. Without altering the complete set of paths or the point $\mathbf{x_0}$, the diagram without z_k is a Heegaard diagram subordinate to S', and the differential incorporates the same holomorphic discs. When L_k does not algebraically intersect any homology class in Y, we can view the last coordinate, j_k, as a filtration on the complex $\widehat{CF}(Y, S; \mathfrak{s})$ and use the associated spectral sequence with E^1 term $\oplus_r \widehat{HF}(Y, S; \mathfrak{s}, [j_1, \ldots, j_{k-1}], r)$ to calculate $\widehat{HF}(Y, S'; \mathfrak{s}, [j_1, \ldots, j_{k-1}])$. It collapses in finitely many steps.

Adding or subtracting an unknotted, unlinked, null-homologous component corresponds to adding or subtracting an index which behaves like i. The Heegaard diagram corresponds

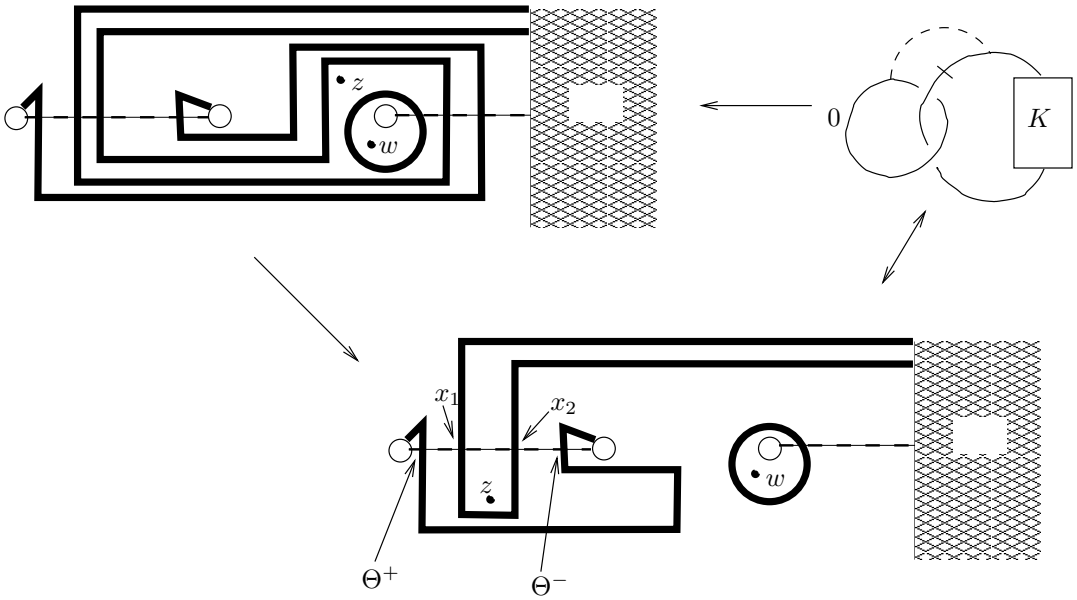

FIGURE 2. 0-surgery on an unknot linked with K. The d-base follows the dashed ard without twisting. The hatched part of the diagram includes the effect of K on the α (heavy) and β (dashed) curves. The portion shown in detail describes the linking and the surgery. Note that placing a meridian instead of the framing curve gives a diagram for K. The intersection points never use x_1 or x_2, hence come from intersection points for the knot diagram. Destabilizing the meridian for K produces a diagram where the only holomorphic discs are those from the complex for K and for $S^1 \times S^2$

to stabilizing in the region containing w and placing a new point z_{k+1} across the new α, but in the same domain as w

6.3. **Mirror String Links.** Let $S \subset Y - B^3$ be a string link in standard form, lying in the plane which defined the projection of our framed link diagram except in neighborhoods of the crossings. Let $\mathfrak{s}$ denote a $Spin^c$ structure on this manifold. Let S' be the string link found through reflection in this plane, reflecting the framed components as well and switching the sign of their framing. Then S' is the string link induced by S in $-Y$ under orientation reversal. Drawing the standard Heegaard diagram for (Y, S), we may fix the β-curves, and change the α-curves for each crossing and framing to obtain a diagram for $(-Y, S')$. The meridians stay in their respective places;however, the marked points for each are reflected to the "other side" of the strand to give marked points: z_i'. The intersection points in $\mathbb{T}_\alpha \cap \mathbb{T}_\beta$ from the original diagram are in bijection with those of the new diagram. Each homotopy class ϕ is carried to a new homotopy class ϕ', but to join the same intersection points it must map in with reversed multiplicities. All this implies that we may calculate $\widehat{HF}_*(-Y, S'; \mathfrak{s}')$ by looking at the intersection points for (Y, S) and the differential for the complex using $-\Sigma$. As in Heegaard-Floer homology, this new complex calculates the

co-homology $\widehat{CF}^*(Y,S;\mathfrak{s})$; there is thus an isomorphism $\widehat{HF}_*(Y,S;\mathfrak{s}) \to \widehat{HF}^*(-Y,S';\mathfrak{s}')$. (This isomorphism maps absolute degrees as $d \to -d$ if $\mathfrak{s}$ is torsion). Using the same marked points, but the image of the basepoint and paths in the complete set of paths we find that $-\overline{\mathcal{F}}$ will be a filtration index for S' when $\overline{\mathcal{F}}$ is for S ($\Lambda_{(-Y,S')} = -\Lambda_{(Y,S)} = \Lambda_{(Y,S)}$). In particular, since each intersection point has fixed image on each meridian, the boundary of a class ϕ must contain whole multiples of the meridian and so $n_{z_i}(\phi) = -n_{z'_i}(\phi')$ since the multiplicities reversed, but $n_{z'_i}(\phi') = n_{z_i}(\phi')$. In summary, there is an isomorphism (including the absolute grading when present):

$$\widehat{HF}_*^{(-d)}(Y,S;\mathfrak{s},[\overline{j}]) \to \widehat{HF}^*_{(d)}(-Y,S';\mathfrak{s}',[-\overline{j}])$$

When $Y = S^3$ and S is a normal string link, then S' is the mirror image of S found by switching all the crossings. The change in indices corresponds to the alteration $t_i \to t_i^{-1}$ in the Alexander polynomial (see section 7).

6.4. **Three Operations on String Links.** Given two string links, S_0 and S_1, in Y_0 and Y_1, there are three simple operations we can perform with two seperate string links, see Figure 3. We always assume that the strands are oriented downwards. We will analyze the effects these operations have on the Floer homology.

6.4.1. $S_1 + S_2$. We assume, for the first, that we have (Y_0,Γ_0) and (Y_1,Γ_1) presented as string links in framed surgery diagrams in $D^2 \times I$. We assume that these have been put in standard form. This means we arrange that all the meridians, at the bottom of each diagram, intersect at most two β's. However, there is only one choice possible for every g-tuple of intersection points due to the presence of U. Amalgamating the second string link does not affect this property for the meridians. Alternately, we can wind in the complement of the star in $D^2 \times \{0\}$ and the amalgamation region as their union is contractible in Σ.

Topologically, the amalgamation is a connect sum of Y_0 and Y_1 where the sums occur for balls removed outside the region depicted as $D^2 \times I$. Thus for two $Spin^c$ structures, $\mathfrak{s}_0$ and $\mathfrak{s}_1$, there is a unique $\mathfrak{s} = \mathfrak{s}_0 \# \mathfrak{s}_1$ on the amalgamated picture. Furthermore, $H_2 \cong H_2(Y_0;\mathbb{Z}) \oplus H_2(Y_1;\mathbb{Z})$. If the first string link has k_0 strands and the second k_1 strands, the amalgamation has filtration index taking values in $\mathbb{Z}^{k_0}/\Lambda_{Y_0} \oplus \mathbb{Z}^{k_1}/\Lambda_{Y_1}$.

Counting α's and β's from the portion if Y coming from Y_0 demonstrates that for an intersection point we must have an α from Y_0 pairing with a β from Y_0 and likewise for Y_1. Even if some β's extend from the Y_0 region to the Y_1 region (which we can avoid if we like), this remains true. In particular, the diagrams drawn from projections in $D^2 \times I$ will have one such β. Therefore, the generators for the new chain group are the product of generators for the two previous groups: as groups $\widehat{CF}(Y,S_0+S_1;\mathfrak{s}) \cong \widehat{CF}(Y_0,S_0;\mathfrak{s}_0) \otimes \widehat{CF}(Y_1,S_1;\mathfrak{s}_1)$. We may choose filtration indices for both links, choosing basepoints and complete sets of paths. The amalgamation will have $(\overline{\mathcal{F}}_0,\overline{\mathcal{F}}_1)$ as a filtration index for the complete set of paths found by using the product of the two basepoints and the paths from complete sets for Y_0 and Y_1. That the domain containing w corresponds to the outer boundary of $D^2 \times I - (S_0 + S_1)$, and that the same is true for each string link individually, ensures that the paths in each complete set need not be alterred. Furthermore, this region separates the domains for classes, ϕ, used in the differentials in the two complexes; thus $\widehat{\partial}_{S_0+S_1} = \left(\widehat{\partial}_{S_0} \otimes I\right) \oplus \left(I \otimes \widehat{\partial}_{S_1}\right)$. We have verified that

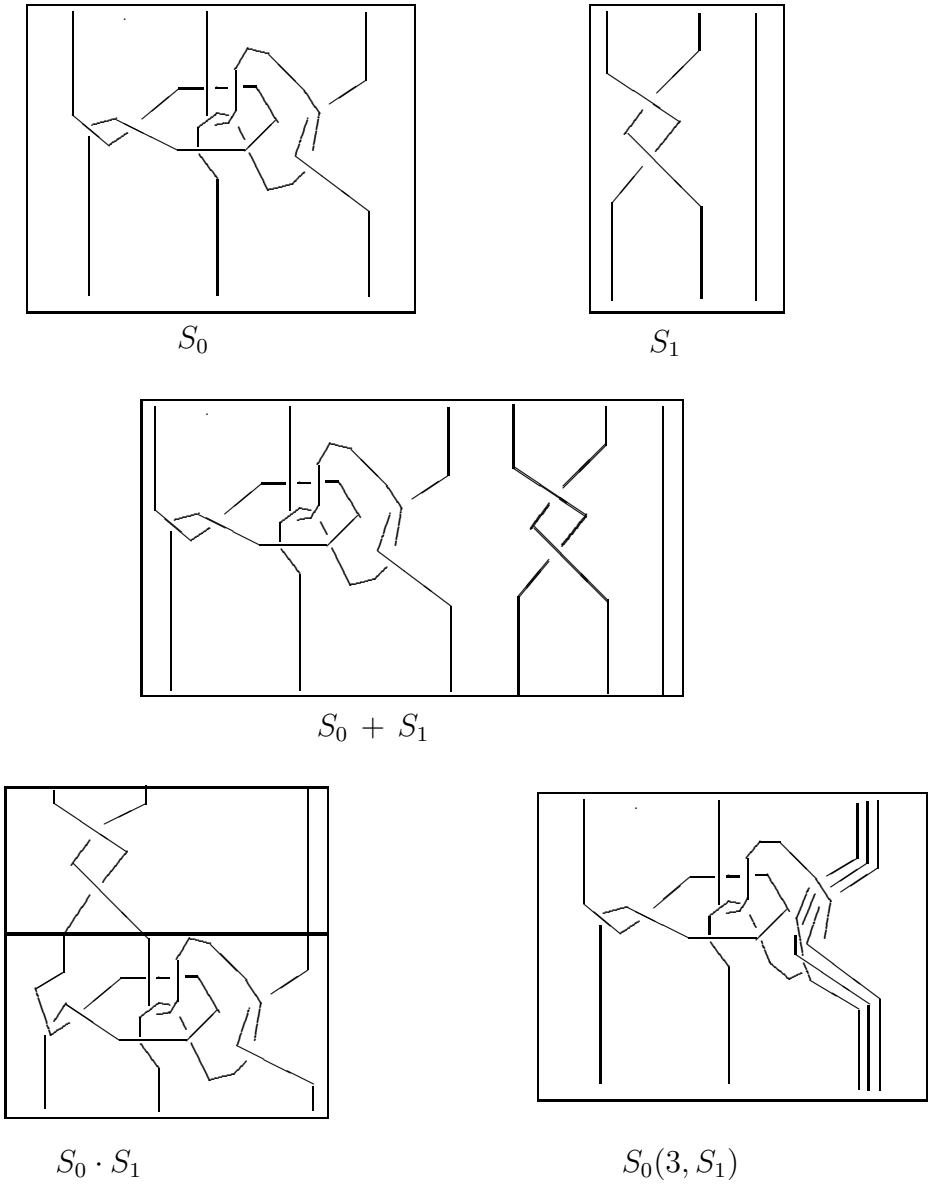

FIGURE 3. Three Simple Operations on String Links

$$\widehat{HF}(Y, S_1 + S_2; \mathfrak{s}, [\bar{j}_0] \oplus [\bar{j}_1]) \cong H_*(\widehat{CF}(Y_0, S_0; \mathfrak{s}_0, [\bar{j}_0]) \otimes \widehat{CF}(Y_1, S_1; \mathfrak{s}_1, [\bar{j}_2]))$$

up to gradings. The grading calculation follows as for connected sums [14]. In particular, for two torsion $Spin^c$ structures on Y_0 and Y_1, the absolute grading satisfies $gr(\mathbf{x} \otimes \mathbf{y}) = gr_{S_0}(\mathbf{x}) + gr_{S_1}(\mathbf{y})$, which is all we require for string links in S^3. We may also establish this relation by using the Maslov index calculation for Y_0 or Y_1, presented as surgery on a link in S^3, found in the absolute gradings section of [16]. Our assumptions include such

presentations for Y_0 and Y_1 and the connect sum provides one for Y. We may use triangles with $n_w = 0$ for Y_0 and Y_1. This allows use to use a product triangle in the calculation for Y. The first Chern class for the associated $Spin^c$ structure will be the sum of those for Y_0 and Y_1. Since the intersection form splits and the Euler characteristics and signatures of the cobordisms add, we see that the gradings for the complexes for Y_0 and Y_1 add to give that for the complex on Y.

6.4.2. $S_1 \cdot S_2$. The second operation is the composition of pure string links, the analog of composition for braids. The torsion of the composite is the product of the torsions of the two factors, [8]. We may prove the analogous result the homologies of the string links. For $n = 1$ stranded string links composition corresponds to the connect sum of knots.

Again we will work with (Y_0, S_0) and (Y_1, S_1) with the assumption that S_0 and S_1 have the same number, n, of strands going from top to bottom. In addition, we require each component of the string links to have one boundary on the top and one boundary on the bottom of the $D^2 \times I$ region in their respective manifolds. No closed component is formed by the stacking operation.

We prove that

$$\widehat{HF}(Y, S_0 \cdot S_1; \mathfrak{s}, [\overline{k}]) = \bigoplus_{[\overline{k}_0]+[\overline{k}_1]=[\overline{k}] \bmod \Lambda} H_*(\widehat{CF}(Y_0, S_0; \mathfrak{s}_0, [\overline{k}_0]) \otimes \widehat{CF}(Y_1, S_1; \mathfrak{s}_1, [\overline{k}_2]))$$

Let $\Sigma_{\alpha_0\beta_0}$ be a weakly admissible Heegaard diagram for (Y_0, S_0) with marked points $w, z_1, \ldots, z_n$ and $\Sigma_{\alpha_1\beta_1}$ be a weakly admissible Heegaard diagram for (Y_0, S_0) with marked points $w', z_1', \ldots, z_n'$. In each case, we use a diagram in standard form. Thus, the region containing w (or w') includes all of $\partial(D^2 \times I)$ minus the strands. The diagram $\alpha_0\alpha_1, \beta_0\beta_1$ is formed as in Figure 4, by joining Σ_0 and Σ_1 with a tube. The end of the tube in S_1 should occur close to w. We have depicted the "star" for S_1 by the thin lines emanating from the tube. As the two w's now occur in the same domain, we will consider only one w point. We let α_i' be the small Hamiltonian isotopes of the α_i curves, except at the meridians. At the meridians we choose curves which traverse the tubeand loop around the i^{th} strand in each diagram, as depicted for the thick curve in Figure 4.

We will analyze the cobordism generated by the triple $\alpha_0\alpha_1$, $\beta_0\beta_1$, and $\alpha_0\alpha_1'$, where the occurrence of repeated sets of curves in a diagram indicates using Hamiltonian isotopes in the standard way. We show a closeup of the meridians in Figure 5. The thick curves should follow the "star" except that the domain containing z_i' must also abut Θ^-.

Each of the ends of this cobordism has $2\,n$ marked points, so we will have filtration indices taking values in $\mathbb{Z}^{2n}$, modulo some lattice. First, we describe the various boundary components.

Boundary I: $\alpha_0\alpha_1, \beta_0\beta_1$

Topologically, this is a connect sum for Y_0 and Y_1 whose Heegaard diagram is drawn in the standard way. Each $Spin^c$ structure is therfore of the form $\mathfrak{s}_0$, $\mathfrak{s}_1$. Inclusion of the marked points puts us into the previous construction: amalgamation. Thus, the generators of the complex for $\mathfrak{s}$ are products of generators from $\mathfrak{s}_0$ and $\mathfrak{s}_1$, which we denote $\mathbf{x} \otimes \mathbf{y}$. We

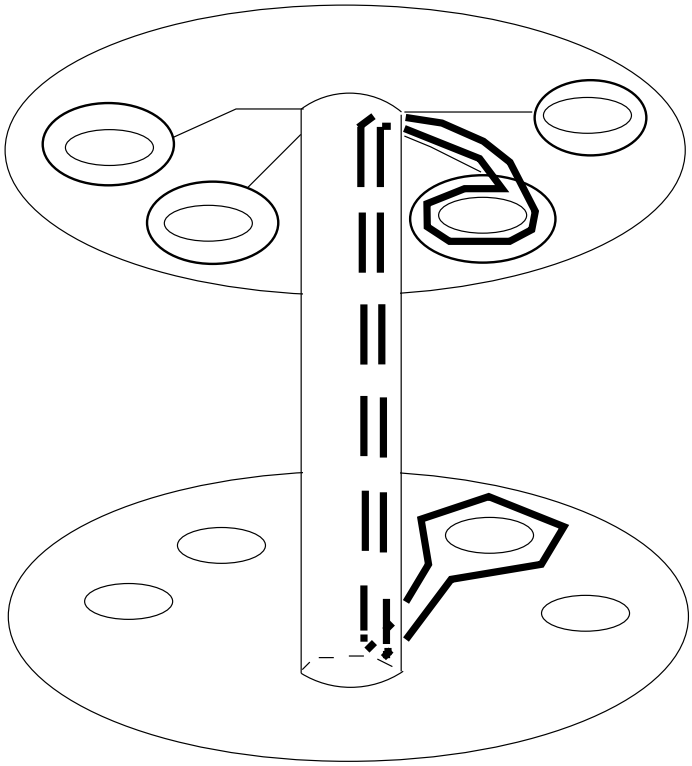

FIGURE 4. Heegaard Diagram for the Composite of String Links

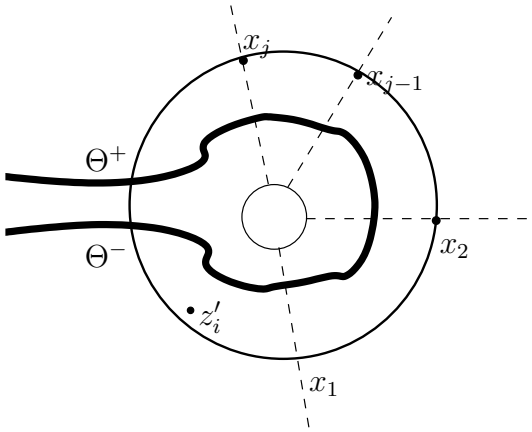

FIGURE 5. The region near the i^{th} meridian in the top diagram. The dashed curves are β's and the thickest curve is the γ curve which replaces the circular meridian

may take the products of our basepoints to be the basepoint for a complete set of paths formed by the product of paths on the two separate diagrams (since w excludes the tube joining the two). As in the amalgamation case, we find that $\Lambda_I \equiv \Lambda_{(Y_0,S_0)} \oplus \Lambda_{(Y_1,S_1)}$ with filtration index $(\overline{\mathcal{F}}_0, \overline{\mathcal{F}}_1)$. We use the previous result to identify

$$\widehat{CF}(Y_0 \# Y_1, S_0 + S_1; \mathfrak{s}, [\overline{j}_0] \oplus [\overline{j}_1]) \cong \widehat{CF}(Y_0, S_0; \mathfrak{s}_0, [\overline{j}_0]) \otimes \widehat{CF}(Y_1, S_1; \mathfrak{s}_1, [\overline{j}_1])$$

Boundary II: $\alpha_0\alpha_1, \alpha_0\alpha_1'$

Topologically, this boundary is a $g_0 + g_1$ fold connect sums of $S^1 \times S^2$'s, which may be seen by isotoping the new α_1' components down the strands of S_0, across the meridians found there, and back up the strands. However, with the additional marked points, it is unclear if the candidate for Θ^+_{std} is closed in this diagram. We can choose Θ^+_{std} as our basepoint, and use products of topological discs in Σ from each connect sum component as our complete set of paths. If we denote by e_i, the i^{th} basis vector in $\mathbb{Z}^{2n}$, the lattice for this component will be $\Lambda_{II} \equiv \mathrm{S}pan\{e_i - e_{n+i}\}$. We now argue that Θ^+_{std} is indeed closed for the differential missing *all* marked points.

There are precisely $2^{g_0+g_1}$ intersection possible for this diagram. We may use our complete set of topological discs to see that Θ^+_{std} has maximal grading. By the Heegaard-Floer homology theory, we must have that the *generator* Θ^+_{std} is closed for the differential only missing w. In particular, a holomorphic disc contributing to this differential cancels with some other holomorphic disc. Suppose we have two such homotopy classes of discs, ϕ and ϕ'. Splicing the inverse of one to the other, $\phi^{-1} * \phi'$ must produce a periodic domain. This periodic domain must evaluate to an element of Λ_{II} under the application of $n_{\overline{z}}$. However, $\sum n_{z_i}(\mathcal{P}) = 0$ for every periodic domain. Since classes with holomorphic representatives must have non-negative multiplicities, it must be the case that when $n_{\overline{z}}(\phi) = 0$ so too $n_{\overline{z}}(\phi') = 0$. As the differential missing all marked points arises from a subset of the moduli spaces in the Heegaard-Floer differential and adding the extra marked points does not eliminate one disk in a cancelling pair without eliminating the other, so Θ^+_{std} is still closed

Boundary III: $\alpha_0\alpha_1', \beta_0\beta_1$

This diagram represents the result of composition. Topologically, each of the new α' curves may be slid down a component of S_0 until it reaches a meridian. After sliding across the meridian, and back up the diagram, we have the connect sum of the diagrams for Y_0 and Y_1. Again, each $Spin^c$ structure on Y is the sum of structures, $\mathfrak{s}_i$, from Y_0 and Y_1. Additionally, $H_2(Y;\mathbb{Z}) \cong H_2(Y_0;\mathbb{Z}) \oplus H_2(Y_1;\mathbb{Z})$. However, the lattices now combine as $\Lambda_{III} \equiv \left(\Lambda_{Y_0} + \Lambda_{Y_1}\right) \oplus \overline{0}$, the span of the two original lattices, and z_i' is in the same domain as w. We required that our original diagrams be weakly admissible for our $Spin^c$ structures. We will see below how to extend periodic domains so that they continue to have positive and negative multiplicities in the diagram for Y. Thus, the new diagram will be weakly admissible.

In the diagram for S_0 there are g_0 α curves and g_0 β curves. As we have not changed these, all the β curves that intersect an alterred α' in the "lower" diagram must pair with an α curve from the lower diagram when describing a generator. Hence, the new α's must

pair with β's from the upper diagram. These intersections have precisely the same form as intersections with the meridians in the original diagram for Y_1. This allows us to establish a one-to-one correspondence between the product of generators for Y_0 and Y_1 and those of Y. The chain complex, as an abelian group, is the product of the original chain complexes. These generators we denote $\mathbf{x}\,\mathbf{y}$.

If we have basepoints for a complete set of paths on Y_0 and Y_1 for our $Spin^c$ structures, we may choose as our basepoint on Y, the generator corresponding to the product of these basepoints. To specify the complete set of paths, consider a class ϕ with $n_w(\phi) = 0$ in either of the original diagrams. If ϕ is in the lower diagram, we may use ϕ in the diagram for Y as the condition on n_w implies that the domain of the disc does not extend into the upper diagram: a small region at the top of each strand lies in the domain containing w in the diagram for Y_0. In ϕ occurs in the upper diagram, its domain may cross $n_{z'_i}$ and include copies of the meridians in its boundary. In the diagram for Y, we may extend this disc by following the strand down to the meridian from S_0. At crossings, the disc gains a boundary component and an intersection point, or a copy of a framed component. However, it will not cross w, and it crosses z_i the same number of times as ϕ crossed z'_i. Periodic domains will continue to have the same multiplicities in the regions coming from their respective diagrams.

The class $\phi^0_{\mathbf{x}}$ may be used to join $\mathbf{x}_0\,\mathbf{y}$ to $\mathbf{x}\,\mathbf{y}$ for any $\mathbf{y}$ coming from the diagram for Y_1. Likewise, $\phi^1_{\mathbf{y}}$, when extended, may be used to join $\mathbf{x}\,\mathbf{y}_0$ to $\mathbf{x}\,\mathbf{y}$. We use these for the complete set of paths, and extend to get $\phi_{\mathbf{x}\,\mathbf{y}}$ by composing $\phi^1_{\mathbf{y}} * \phi^0_{\mathbf{x}}$. In particular, the filtration value for $\mathbf{x}_0\,\mathbf{y}$ is $-n_{\overline{z'}}(\phi^1_{\mathbf{y}})$, and the difference in filtration values between $\mathbf{x}\,\mathbf{y}$ and $\mathbf{x}_0\,\mathbf{y}$ is, $\operatorname{mod}\Lambda$, $-n_{\overline{z}}(\phi^0_{\mathbf{x}})$. Thus, given filtration indices on the two diagrams, we can construct a filtration index on the composite which agrees with the vector sum: $\overline{\mathcal{F}}_0 + \overline{\mathcal{F}}_1$. As we are only concerned with the "hatted" theory we need only identify the coset.

We now return to the triple $\alpha_0\alpha_1$, $\beta_0\beta_1$, and $\alpha_0\alpha'_1$. We call the induced four manifold X. We choose on X the $Spin^c$ structure $\mathfrak{u}$ that is $\mathfrak{s} \times I$ and restricts to the torsion $Spin^c$ structure on the $\alpha_0\alpha_1, \alpha_0\alpha'_1$- boundary. We then have $\Lambda_X \equiv \Lambda_0 \oplus \Lambda_1 + \Lambda_{II}$. We use a homotopy class of triangles to join $\mathbf{x}_0 \otimes \mathbf{y}_0$, Θ^+_{std}, and $\mathbf{x}_0\,\mathbf{y}_0$; a choice made more specific below as the unique local holomorphic class. As we assign Θ^+_{std} filtration index $\overline{0}$ and this local class has $n_w(\psi) = n_{\overline{z}}(\psi) = 0$, we have the following relation for the filtration indices on generators and for some $\lambda \in \Lambda_X$:

$$\overline{\mathcal{F}}(\mathbf{x}\,\mathbf{y}) = \overline{\mathcal{F}}_0(\mathbf{x}) \oplus \overline{0} + \overline{0} \oplus \overline{\mathcal{F}}_1(\mathbf{y}) + \lambda_X$$

Topologically, the cobordism, once we fill in the second boundary, is $Y_0 \# Y_1 \times I$. If we take the quotient $\operatorname{mod}\Lambda_X$, we recover the filtration index on Y as $\mathbb{Z}^{2n}/\Lambda_X \cong \mathbb{Z}^n/\Lambda_{III}$ and the filtrations will add correctly. Since z'_i is in the same domain as w in the diagram for Y, there is a chain isomorphism preserving filtrations which drops their entries in the filtration index. Thus, we recover $\widehat{CF}(Y, S_0 \cdot S_1)$ as a relatively indexed complex (and not, as initially could happen, a quotient of its index group).

The Heegaard triple will be weakly admissible for the doubly periodic domains, so we may choose an area form on Σ assigning the periodic domains signed are equal to zero.

As it stands, this may assign large portions of the diagram small areas because the periodic domains abutting the old meridians from S_1 in the $\alpha_0\alpha_1, \alpha_0\alpha_1'$-boundary are quite substantial. We may address this difficulty by handlesliding the portion of the new α''s down the diagram for S_0 until they are close to the meridians for S_0. By doing this, we will have introduced new intersections between individual α and β curves; however, none of these may occur in a generator. Were we to use one of them, there would be too few α's remaining in the upper region of the diagram to pair with the β's found there, and no means to ameliorate this deficiency with β's from the bottom region. Furthermore, nothing in the previous analysis will be changed by this alteration.

In this new diagram, there are obvious holomorphic triangles abutting each intersection point $\mathbf{x}\otimes\mathbf{y}$ and Θ^+_{std}. These consist of g_0+g_1 disjoint topological triangles embedded in Σ whose domains are contained in the support of the periodic regions from the $\alpha_0\alpha_1, \alpha_0\alpha_1'$-boundary. The triangles near the meridians for S_1 are shown in Figure 5. None of these triangles intersect a marked point We may make those periodic domains arbitrarily small in unsigned area, forcing our local triangles to have area smaller than ϵ. Without the adjustment in the previous paragraph, we would not be able to ensure that only the triangles identified above give rise to ϵ-"small" homotopy classes. Using the induced area filtrations, the chain map decomposes into a "small" portion, which is an isomorphism, and a "large" portion (see Appendix **??** for more details about this technique):

$$F((\mathbf{x}\otimes\mathbf{y})\otimes\Theta^+_{std}) = \pm\mathbf{x}\,\mathbf{y} + \text{lower order}$$

We see then that the chain map found by counting triangles not crossing any marked points induces an injection of $\widehat{CF}(Y_0\#Y_1, S_0+S_1; \mathfrak{s}, [\overline{j}_0]\oplus[\overline{j}_1])$ into $\widehat{CF}(Y, S_0\cdot S_1; \mathfrak{s}, [\overline{j}_0+\overline{j}_1])$ and that the map is a chain isomorphism on $\oplus\widehat{CF}(Y_0\#Y_1, S_0+S_1; \mathfrak{s}, [\overline{j}_0']\oplus[\overline{j}_1'])$ where $[\overline{j}_0+\overline{j}_1] = [\overline{j}_0'+\overline{j}_1]$ mod Λ_{III}. Together with our analysis of boundary I, this proves the result.

Finally, as the small triangles used in the argument each have $n_w = 0$ and $\mu = 0$, and the cobordism induces the torsion $Spin^c$, the absolute grading for the image will be the sum of the absolute gradings for the original intersection points, when $\mathfrak{s}_i$ are torsion. Since there are handleslides in the $\alpha_0\alpha_1', \beta_0\beta_1$ diagram taking the curves replacing meridians in α_1' back to the meridians, and the "small" triangles in each handleslide map link the corresponding generators, the absolute grading for the generators in this diagram are the same as for Y_0 shifted by that of Θ^+.

Note: Θ^+ has grading $\frac{g_i}{2}$. But the cobordism has H_2 free, with dimension g_1+g_2 and signature equal to zero, so the grading shift formula provides the result.

6.4.3. $S_1(i, S_2)$. The third operation is a form of string satellite to a string link. This can be formulated using the Heegaard diagram shown in Figure 6

Once again, for string links in S^3, there is only one way to pair meridians with β curves to achieve an intersection point. Indeed, if we draw α's as vertices of a graph and β's as edges, the meridians and the β's that intersect them form a tree with one edge not possessing a vertex on one end. There is only one way to pair edges to end points in such a graph. The remaining β's in the diagram can only intersect α's according to the intersections in the original diagrams. However, the construction still applies to string links in more general

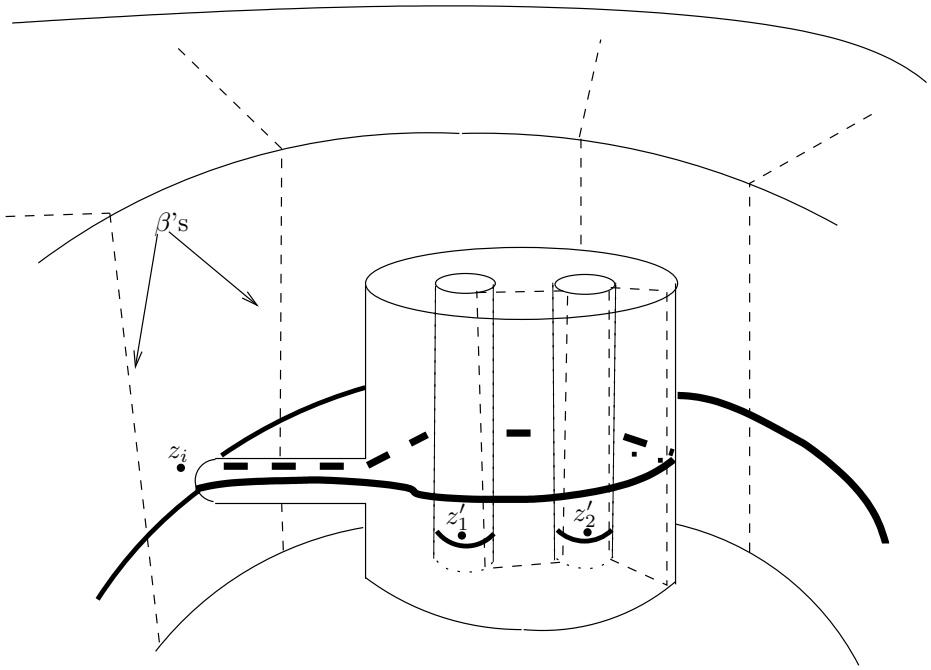

FIGURE 6. The Heegaard Diagram for a String Satellite. This is a cutaway view of a diagram for $S_0(i, S_1)$ with the cut through the i^{th} strand of S_0.

manifolds, presented as surgery on framed links in $D^2 \times I$. A count of α's and β's, shows that generators for this new diagram occur as products of generators from the old diagrams, even when we have wound to achieve some admissibility and possibly increased the number of intersections at each meridian. Alternately, we may use the standard form to obtain diagrams to which the argument from S^3 still applies. Once again, the construction is a connect sum of two three manifolds, and once again the $Spin^c$ structures, etc. transfer as expected.

Thus the chain complex is the product of the chain complexes for the constituent string links. The filtration indices, however, differ from before. To ease the argument, we note that we may think of such a string link as the multiplication of one strand in (Y_0, S_0) n_1 times, followed by a composition with (Y_1, S_1) amalgamated with a trivial string link on n_0 strands. We already know the result of composition, hence we need only understand the string satellite where the inner constituent is an n_1 stranded trivial string link in S^3. This has only one intersection point, hence the chain complex, as a group, is the same as that for (Y_0, S_0) for each $Spin^c$ structure.

Any class ϕ joining two generators, with $n_w(\phi) = 0$ can be extended to the new string link. It includes the new α and thus goes up the inner string link to the top and back down to the new meridians. For each time ϕ crosses z_i, each of the new meridians, $m'_1, \ldots, m'_{n_2}$ will be in the boundary of the new disc. In the trivial string link picture there is one generator: $u_1 \times \cdot \times u_{n_1}$ with one intersection on each meridian. In particular, the new Λ in

$\mathbb{Z}^{n_0+n_1-1}$ is spanned by vectors

$$v' = (\lambda_1, \dots, \lambda_i, \lambda_i, \dots, \lambda_i, \dots, \lambda_{n_1})$$

where λ_i is repeated n_1 times and $(\lambda_1, \dots, \lambda_{n_0})$ is a vector in Λ_{S_0}. We choose the extension of $\phi_{\mathbf{x}}$ to $\phi_{\mathbf{x}\times u_1\times\cdots\times u_{n_1}}$ to give our complete set of paths. The filtration index is now measured by

$$(\mathcal{F}_1, \dots, \mathcal{F}_{i-1}, \mathcal{F}_i, \dots, \mathcal{F}_i, \mathcal{F}_{i+1}, \dots, \mathcal{F}_{n_1})$$

with n_2 copies of $\mathcal{F}_i$.

As a consequence, discs with $n_{z_i}(\phi) = 0$ in the original diagram extend as themselves to the new diagram. In addition, any disc with $n_{z'_i}(\phi') = 0$, $i = 1, \dots, n_2$ corresponds to a disc in the original diagram with $n_{z_i} = 0$. The differentials $\widehat{\partial}$ and $\widehat{\partial}'$ must be the same, and count only classes of discs which do not need to be extended.

Putting all this together, if we denote the string satellite found by substituting S_1 in the i^{th} strand of S_0 by $S_0(i, S_1)$ then

$$\widehat{HF}(Y, S_0(i, S_1); \mathfrak{s}, [(l_1, \dots, l_{n_1+n_2-1})] \cong$$

$$\bigoplus_{[\overline{j}']+[\overline{k}']=[\overline{l}] \bmod \Lambda'} H_*(\widehat{CF}(Y_0, S_0; \mathfrak{s}_0, [\overline{j}]) \otimes \widehat{CF}(Y_1, S_1; \mathfrak{s}_1, [\overline{k}]))$$

where $\overline{j}' = (j_1, \dots, j_{i-1}, j_i, \dots, j_i, j_{i+1}, \dots, j_{n_1})$ and $\overline{k}' = (0, \dots, 0, k_1, \dots, k_{n_2}, 0, \dots, 0)$ and $\Lambda' = \Lambda + \overline{0} \oplus \Lambda_1 \oplus \overline{0}$.

We need also to calculate the absolute grading, when appropriate. When we have inserted the trivial string link into S_0 and a torsion $Spin^c$ structure on Y_0 we may handleslide the new α across the new meridians to arrive at a picture for a standard connect sum. At each handleslide, there is a small $\mu = 0$ homotopy class of triangles with $n_w = 0$ and admitting holomorphic representative joining each intersection point to the corresponding point in the new diagram (the product decomposition of generators is unchanged). In the connect sum picture, the gradings add – the grading of the product generator is the same as the grading of the generator from S_0. In the cobordism induced by the handleslides, the grading does not change: $gr(\mathbf{x} \times u_1 \times \cdot \times u_{n_1}) = gr_{Y_0}(\mathbf{x})$

7. Alexander Invariants for String Links in $D^2 \times I$

Let S be a string link in $D^2 \times I$. In this section we relate the Euler characteristic of $\widehat{CF}(S; \overline{v}) \otimes \mathbb{Q}$ to classical Alexander invariants built from coverings of $D^2 \times I - S$.

7.1. **Alexander Invariants for String Links.** Let $S \subset D^2 \times I$ be a string link; denote a complement of its tubular neighborhood by $X = D^2 \times I - \text{int}N(S)$ and $X \cap D^2 \times \{i\}$ by E_i for $i = 0,\ 1$. By the Meyer-Vietoris sequence we have that $H_1(X; \mathbb{Z}) \cong \mathbb{Z}^k$ and is generated by the meridians of the strands on $D^2 \times \{0\}$. As string links are specialized θ_{k+1}-graphs, to construct an Alexander invariant for the string link we replicate the approach of R. Litherland,

[11], for the Alexander invariants of θ_{k+1}-graphs (cf. [8]). Let $\mathfrak{H}$ be the ring $\mathbb{Z}[t_1^{\pm 1}, \ldots, t_k^{\pm 1}]$; we will consider the torsion properties of the $\mathfrak{H}$-module $H_1(\widetilde{X}, \widetilde{E}_1; \mathbb{Z})$ where $\widetilde{X}$ is the universal Abelian cover of X (determined by the Hurewicz map $\pi_1(X, x_0) \to H_1(X, \mathbb{Z})$ and $\widetilde{E}_1$ is the pre-image of E_1 under the covering map.

Note: Taking the lifts to the universal Abelian cover, we consider the long exact sequence for the pair $(\widetilde{X}, \widetilde{E}_1)$:

$$\longrightarrow H_1(\widetilde{E}_1) \longrightarrow H_1(\widetilde{X}) \longrightarrow H_1(\widetilde{X}, \widetilde{E}_1) \longrightarrow H_0(\widetilde{E}_1) \longrightarrow H_0(\widetilde{X})$$

Now, $H_0(\widetilde{E}_1) \cong \mathbb{Z}$, and it maps isomorphically onto the next term. However, $H_1(\widetilde{E}_1)$ is not generally 0; thus, the invariant derived from $H_1(\widetilde{X}, \widetilde{E}_1)$ is not an invariant of the complement of S alone. (However, for marked knots, i.e. one stranded string links, $\widetilde{N}$ is an infinite strip, and $H_1(\widetilde{X}; \mathbb{Z}) \cong H_1(\widetilde{X}, \widetilde{N}; \mathbb{Z})$ as $\mathfrak{H}$-modules.)

We may construct a relative cell decomposition for (X, E_1). We think of E_1, a punctured disc, as the portion of the boundary $\partial X - X \cap \mathrm{int} D^2 \times \{0\}$. Start by constructing a relative cell complex for (E_0, ∂) which consists of k one-cells joining the internal punctures in a chain to the outer boundary, along the bottom of the projection of S. Then add a two-cell to construct the disc. This may be extended to the entirety of X by attaching one-cells at each of the crossings in the projection along the axis of the projection and two-cells for each face in the projection with the exception of the leftmost one, called U. The two-cells, $R_1, \ldots, R_k$, arising from faces that intersect the 0^{th} level in I must intersect $D^2 \times \{0\}$ in one of the one-cells in its decomposition. Otherwise, the two-cells glue to the one-cells at the crossings with the remainder of their boundaries glued into ∂X according to the projection. Finally, the complement of this complex is the interior of a three-cell, which we glue in to complete X.

We may collapse the two-cell in E_0 into the union of E_1 and the other two-cells by contracting the three-cell. Likewise we may collapse the one-cells in E_0 into the union of E_1 and the other one-cells by contracting $R_1, \ldots, R_k$ respectively. This leaves a relative cell complex with an equal number of 1- and 2- cells. We call this cell complex Y. The homotopy and homology properties of the pair (X, E_1) are encompassed in this complex.

However, the chain complex for $\widetilde{Y}$ as a relative complex becomes

$$0 \longrightarrow C_2(\widetilde{Y}) \xrightarrow{\widetilde{\partial}} C_1(\widetilde{Y}) \longrightarrow 0$$

Thus, $H_1(\widetilde{X}, \widetilde{E}_1) \cong \mathit{coker}\ \widetilde{\partial}$, and the matrix, P, for $\widetilde{\partial}$ as a presentation of the $\mathfrak{H}$-module $H_1(\widetilde{X}, \widetilde{E}_1)$ is square. By taking the homomorphism $\epsilon : \mathfrak{H} \to \mathbb{Z}$, defined by substituting 1 for each variable, we see that $\epsilon(P)$ is the boundary map for the relative chain complex,Y. Since $H_1(X, E_1; \mathbb{Z}) \cong 0$, as E_1 contains meridians of all types, P has non-zero determinant, which we take to be an Alexander polynomial of the string link.

7.2. **Fox Calculus.** A standard approach to calculating the homology of covering spaces is by applying the Fox calculus to the fundamental group of the underlying space. I provide a quick review, used in the next sub-section, followed by some additional comments about the case for string links. For a other accounts see [6] or [21] or Fox's original articles.

Let X be a finite, connected CW-complex with a single 0-cell, p, with no cells of dimension 3 or greater. Below, we will choose this to be the complement of some embedded 1-complex in the three sphere. Let $G = \pi_1(X, p)$, be the fundamental group based at p, and presented as $< s_1, \ldots, s_n \,|\, R_1, \ldots, R_m >$. Let $\phi : G \to H_1(X; \mathbb{Z})$ be the Hurewicz homomorphism. We consider the cover $\widetilde{X}$ determined by this map, and let $\widetilde{X}_0$ be the pre-image of p under the covering map. We choose a specific lift of p, called $\tilde{p}$.

For a path w in the one skeleton of X, there is a lift $\tilde{w}$ to the one skeleton of $\widetilde{X}$, starting at $\tilde{p}$ and defining an element of $Z_1(\widetilde{X}, \widetilde{X}_0)$. If we choose such lifts of the generating paths, s_i, and denote them by $\tilde{s}_i$, we may write the lift of any other path as

$$\tilde{w} = \sum_i \xi_i \tilde{s}_i$$

with $\xi_i \in \mathfrak{H}$ where $\mathfrak{H}$ is the integral group ring for the first homology group of X. We also denote the coefficients in such an expansion by $\frac{\partial w}{\partial s_i}$. These maps may be extended linearly to the group ring of the fundamental group and satisfy a property similar to that of derivations. In particular, in the group ring, $\partial m = 0$ for $m \in \mathbb{Z}$ and $\partial\, g^{-1} = -g^{-1}\, \partial\, g$.

If we choose representative paths for the relations R_j, we may form the matrix $\left(\frac{\partial R_j}{\partial s_i}\right)$. This matrix is a presentation matrix for $H_1(\widetilde{X}, \widetilde{X}_0)$ as an $\mathfrak{H}$-module. More specifically, we should consider the R_j as elements of the free group generated by the s_i, and apply the maps $\frac{\partial}{\partial s_i}$ appplied to the free group. Take the resulting matrix and apply to each entry the quotient maps from the free group to G and from G to the first homology group.

One way to present the fundamental group of the complement $X = D^2 \times I - S$ is to choose a point in $D^2 \times I - S$ and loops through faces of the projection as generators. Using the crossings to provide the relations, we obtain a presentation, similar to the Dehn presentation for a knot group, with k more generators than relations. For this presentation the Fox calculus produces a presentation matrix with k more columns than rows. These correspond to the faces $R_1, \ldots, R_k$ and collapsing these faces to obtain the cell complex Y corresponds to eliminating the columns in the presentation matrices for Alexander polynomials of knots and links.

Furthermore, were we to consider the Heegaard diagrams associated with the string link, we would have k meridians along $D^2 \times \{0\}$. There would only be one choice of intersection between these meridians and the attaching curves derived from the faces, $R_1, \ldots, R_k$, that could be extended to an intersection of $\mathbb{T}_\alpha \cap \mathbb{T}_\beta$. The collapsing of these faces corresponds to this unique choice and to the use of $H_1(\widetilde{X}, \widetilde{E}_1)$ as the appropriate classical analog for the Floer homology.

This suggests using other presentations of the fundamental group to calculate the Alexander invariant. In [8], P. Kirk, C. Livingston, and Z. Wang calculate the invariant using the analog of the Wirtinger presentation. There is a projection of a string link (with kinks at the top of each strand, for example) where the Wirtinger presentation is generated by

$$m_1, \ldots, m_k, u_1, \ldots, u_s, m_1', \ldots, m_k'$$

where m_i is the meridian of the i^{th} component in $D^2 \times \{1\}$ and m_i' is the meridian in $D^2 \times \{0\}$. The kinks ensure that $m_i \neq m_i'$. Applying the Fox calculus to the relations arising from

the crossings we obtain a matrix $(A\ B\ C)$, with entries in $\mathfrak{H}$, where the blocks reflect the division in the generators. It is shown in [8] that $(A\ B)$ is invertible over $F = \mathbb{Q}(h_1, \ldots, h_k)$, the quotient field of $\mathfrak{H}$. They name the determinant, $\det(A\ B)$, the *torsion*, $\tau(L)$, of the string link and relate it to the Reidemeister torsion of the based, acyclic co-chain complex $C^*(X, E_0; F)$ with coefficients twisted by the map $\pi_1 \to \mathbb{Z}^k$. While the particulars: co-homology vs. homology, twisted coefficients vs. coverings, and E_0 vs E_1; are different their torsion, up to these choices, is the Alexander invariant defined for S.

7.3. **Heegaard Splittings and Fox Calculus.** Here we relate the computation of Alexander polynomials to our Heegaard diagrams. The upshot will be to identify the Euler characteristic of $\widehat{CF}(S) \otimes \mathbb{Q}$ with the previously defined Alexander invariant of $H_1(\widetilde{X}, \widetilde{E}_1)$. In particular,

$$\sum_{\overline{v} \in \mathbb{Z}^k} \chi(\widehat{HF}(S, \overline{v}; \mathbb{Q}) t_1^{v_1} \cdots t_k^{v_k}$$

is a generator for the order ideal of this module. Various other authors have used much the same argument in different settings; J. Rasmussen provides a very similar argument for Heegaard diagrams for three manifolds in [19].

Let S be a string link in $D^2 \times I$. We consider the standard Heegaard decomposition induced from a projection described in section 1. Let H_α be the handlebody determined by $\{\alpha_i\}_{i=1}^g$, and H_β be the handlebody determined by $\{\beta_i\}_{i=1}^g$. We assume that our meridians lie in $D^2 \times \{0\}$. Take as our basepoint, p_0 for $\pi_1(X)$ the 0-cell in H_β. For each of the faces, we choose a path f_i, the gradient flow line oriented from the basepoint to the critical point corresponding to β_i which links the core positively in S^3. The other gradient line oriented *from the index 1 critical point to* 0*-cell* will be called $\overline{f}_i$. The loops $b_i = \overline{f}_i \circ f_i$ generate $\pi_1(X, p_0)$.

The α's, not including the meridians, induce the relations for a presentation of π_1 corresponding to the Dehn presentation of the fundamental group, [6]. We choose an intersection point $\mathbf{u} \in \mathbb{T}_\alpha \cap \mathbb{T}_\beta$ which corresponds to points $u_i \in \alpha_{\sigma(i)} \cap \beta_i$ in Σ for some permutation $\sigma \in S_g$. Note that the choice along the meridians is prescribed for each such intersection point: there are k meridians and $k+1$ faces intersecting them, but we cast one aside. This arrangement implies that our only choices occur on non-meridional α's. For a non-meridional α, let $[\alpha_{\sigma(i)}]$ be the path from the basepoint, along f_i, through the attaching disc for β_i to u_i, and around $\alpha_{\sigma(i)}$ with the its orientation, and then back the same way to the basepoint. Each time $[\alpha_j]$ crosses β_i positively, we append a b_i to the relation; each time it intersects negatively we append a b_i^{-1}. The word so obtained is called a_i. We derive this principle by looking at the segments α_j^s into which the β's cut α_i and flowing them forwards along the gradient flow. The interior of each segment flows to the basepoint, while the endpoints flow to critical points in the attaching discs for the β's. Thus, the path from one endpoint of the segment, to the critical point corresponding to that β_s, then along some f_s^{-1} or $\overline{f}_s$, and back along one of f_t or $\overline{f}_t^{-1}$, then to the other end of the segment, and back along the segment, is null homotopic. This allows us to break the α up into the various β's it crosses.

Then $\left(\frac{\partial a_j}{\partial b_i}\right)$, ignoring the columns corresponding to the faces abutting $D^2 \times \{0\}$, is a presentation matrix for the $\mathfrak{H}$-module $H_1(\tilde{X}, \tilde{E}_1)$, and hence its determinant will provide the Alexander invariant.

If we consider the free derivative of a_j with respect to a b_i we find terms which correspond to each intersection point of α_j with β_i. The term possesses a minus sign when the two intersect negatively, otherwise it possesses a positive sign. The terms correspond to paths from the basepoint through $f_{\sigma^{-1}(j)}$ to $\beta_{\sigma^{-1}(j)}$, through the attaching disc to $u_{\sigma^{-1}(j)}$, along α_j to the intersection point with β_i and then back along f_i^{-1}. This can be rewritten as a word in the b_i's. Summing over all intersection points with β_i equals $\partial_{b_i}(a_j)$.

Let μ be is the Hurewicz map from the fundamental group to the first homology group. According to the Fox calculus, the matrix $[\mu(\partial_{b_i} a_j)]$, is a presentation matrix for the homology of the cover as an $\mathfrak{H}$-module. Again, we ignore the b_j's corresponding to the faces abutting $D^2 \times \{0\}$. We calculate the Alexander invariant by computing the determinant of this matrix. Each term in this determinant has the form $sgn(\sigma)(-1)^{\#} h_1^{\rho_1} \cdots h_k^{\rho_k}$, where ρ_i is the sum of the powers of h_i over the terms in the determinant multiplying to this monomial; we do not allowing any cancellation of terms. This monomial corresponds to a specific intersection point in $\mathbb{T}_\alpha \cap \mathbb{T}_\beta$ found from the pairing of rows and columns in the matrix. Likewise $\#$ is the number of negative intersections $\alpha_{\sigma(i)} \cap \beta_i$ in the g-tuple corresponding to this term.

Let $\mathbf{x}$ and $\mathbf{y}$ be two intersection points. We will consider the differences

$$\#_{\mathbf{y}} - \#_{\mathbf{x}} \qquad\qquad \rho_i(\mathbf{y}) - \rho_i(\mathbf{x})$$

Since we are considering points in $\mathbb{T}_\alpha \cap \mathbb{T}_\beta$ for a diagram of S^3, there is a homotopy class of discs $\phi \in \pi_2(\mathbf{x}, \mathbf{y})$.

We place marked points into the diagram corresponding to the strands and according to the method in section 1. We may measure how many times a 2-chain in X, representing a homotopy class of discs, ϕ, intersects the link components by evaluating $(n_w - n_{z_i})(\phi)$. We wish to show that

$$\rho_i(\mathbf{y}) - \rho_i(\mathbf{x}) = (n_w - n_{z_i})(\phi)$$

The right hand side counts the number of times that that the boundary of $\mathcal{D}(\phi)$ winds around the i^{th} meridian. We need only show that the same is true of the left, or, equivalently, that μ_i, the i^{th}-coordinate of the boundary, equals the left hand side.

In the boundary of the disc we have the α's oriented from the points in $\mathbf{x}$ to those in $\mathbf{y}$. We can take segments starting at u_i and travelling along $\alpha_{\sigma(i)}$ to x_i and y_i so that their difference is the oriented segment of the boundary of ϕ in α_i. We join this to the basepoint by using paths in the attaching discs for the β's and the preferred paths f_j or f_j^{-1} at each endpoint. Breaking this up as before, we can convert this path into a word of b_i's and their inverses. If we look at one of the β_i boundary segments in ϕ, we see that the concatentation

of the words for the α segments corresponding to the intersection points with β_i homotopes into the α boundary and the β boundary of ϕ.

Thus μ_i of the concatenation equals μ_i of the boundary of $\mathcal{D}(\phi)$. Furthermore, μ_i applied to each word of the concatenation tells us how many more times the segment in one α corresponding to $\mathbf{y}$, converted into a word of generators, wraps around the i^{th} meridian than does the segment corresponding to $\mathbf{x}$. Taking μ_i of the concatenation gives the sum of these differences, or $\rho_i(\mathbf{y}) - \rho_i(\mathbf{x})$.

We now consider the difference in # between the two intersection points. The intersection point determines a permutation $\sigma_{\mathbf{x}}$ where $x_i \in \alpha_{\sigma(i)} \cap \beta_i$. We orient $\mathbb{T}_\alpha$ by the projection $\alpha_1 \times \cdots \times \alpha_g \to \mathbb{T}_\alpha$, and likewise for $\mathbb{T}_\beta$. The orientation of $Sym^g(\Sigma)$ is given by the orientation of $T_{x_1}\Sigma \oplus \cdot \oplus T_{x_g}\Sigma$. Then $\mathbb{T}_\alpha \cap_{\mathbf{x}} \mathbb{T}_\beta$ has local sign

$$sgn(\sigma_{\mathbf{x}})(-1)^{\frac{g(g-1)}{2}} \cdot (\alpha_{\sigma(1)} \cap_{x_1} \beta_1) \times \cdots \times (\alpha_{\sigma(g)} \cap_{x_g} \beta_g)$$

or

$$sgn(\sigma_{\mathbf{x}})(-1)^{\frac{g(g-1)}{2}}(-1)^{\#(\mathbf{x})}$$

The difference in sign between $\mathbf{y}$ and $\mathbf{x}$ is then multiplication by $sgn(\sigma_{\mathbf{y}})sgn(\sigma_{\mathbf{x}})\cdot(-1)^{\#_{\mathbf{y}}-\#_{\mathbf{x}}}$. This is also the difference in sign between terms in the determinant, and corresponds to the $\mathbb{Z}/2\mathbb{Z}$ grading in section 10.4 of [14].

Thus, if we consider those intersection points with $\rho(\mathbf{x}) = \overline{v}$, for a given vector $\overline{v}$, we recover the intersection points for a given filtration index since ρ satisfies the index relation. In addition, these each correspond to the term $h_1^{v_1} \cdots h_k^{v_k}$ and occur with sign given by the $\mathbb{Z}/2\mathbb{Z}$ grading of the Heegaard-Floer homology, which is also the sign of the corresponding term in the determinant. For rational coefficients, the sum of these generators with sign is the Euler characteristic of the homology group corresponding to $\overline{v}$ for this filtration index.

8. State Summation for Alexander Invariants of String Links in S^3

We consider a generic projection of a string link S in $D^2 \times I$ onto the plane. As in [12], [5], we can use this projection to draw an ancillary rooted, planar graph. The intersection points of $\mathbb{T}_\alpha \cap \mathbb{T}_\beta$ will correspond to a subset of the maximal spanning forests of this graph, subject to certain constraints imposed by the meridians. From these graphs we will prescribe a recipe for computing functions, $\mathcal{F}_i$ and G, on the intersection points which satisfy the same relations relative to homotopy classes ϕ as the exponents and signs of the Alexander invariants. The $\mathcal{F}_i$ will form a filtration index, and G will be the grading of our chain complexes.

Once we have adapted the spanning tree construction to apply to string links, the argument is the precise analog of the argument in [12]. We do not need the results of Heegaard-Floer homology for the filtration calculation, but the discussion of grading will presume some familiarity with them.

8.1. **Planar Graph Preliminaries.** We consider planar graphs in the unit square, I^2. Choose a number, k, and place $\frac{k}{2}$ vertices, marked by $*$, along the bottom edge when k is even ($\frac{k+1}{2}$ when k is odd). Place additional vertices, labelled by $\bullet$, along the top edge until there are k vertices total. Let Γ be a *connected*, planar graph in I^2 which includes these vertices, but whose other vertices and all its edges are in the interior of the square. We let F be a maximal spanning forest for Γ, with a tree component for each $*$ on the boundary, rooted at $*$, and oriented away from its root.

We may define a dual for Γ by taking its planar dual inside I^2, Γ^*, and placing the vertices that correspond to faces of $I^2 - \Gamma$ touching ∂I^2 on ∂I^2. Since Γ is connected, this choice of arc on the boundary is unambiguous. There is one vertex which corresponds to the left side of the square. We replace it with an $*$ and continue counter-clockwise, changing boundary vertices to $*$'s until we have alterred $\frac{k}{2}+1$ (or $\frac{k+1}{2}$, k odd). This graph must also be connected.

We say that F admits a dual forest if the edges in Γ^* corresponding to edges of $\Gamma - F$ form a maximal spanning forest, F^*, with each component rooted at a single $*$. In that case, we orient the forest away from its roots. Not every F admits a dual forest: a component of F^* may contain two $*$'s. We consider the set $\overline{\mathcal{F}}$ of forests in Γ that are part of a dual pair (F, F^*). We will encode F^* in the diagram for Γ by inscribing the edges in $\Gamma - F$ with a transverse arrow which concurs with the orientation of F^*.

Now consider a string link, S in $D^2 \times I$ and a generic projection of S into I^2. We decompose $S = S_1 \cup \cdots \cup S_l$, where each S_j consists of a maximal string link with connected projection, i.e. one whose projection into I^2 forms a connected graph.

Lemma 7. *For the Heegaard decomposition of S^3 defined by the connected projection of a string link, S, there is a one-to-one correspondence between the generators of $\widehat{CF}(S)$ and the set of dual pairs, $\overline{\mathcal{F}}$, for a planar graph $\Gamma \subset I^2$ as above.*

Proof: The regions in $I^2 - p(S)$ can be colored with 2 colors as the projected graph is 4-valent. We label the leftmost region with the letter "U" and color it white. We then alternate between black and white across the edges of the projection. By using vertices corresponding to the black regions and edges corresponding to crossings where two (not necessarily distinct) black regions abut, we may form an second planar graph. For those regions touching the border of I^2, the vertex should be place on the boundary.

We replace the vertex of each black region abutting the bottom edge of I^2 with an $*$. Thus, we have a graph embedded in D^2 with k vertices on the boundary, $\frac{k+1}{2}$ of which are $*$'s when k is odd and $\frac{k}{2}$ when k is even. An example is given in Figure 7. In particular, Γ is connected: starting at a vertex of Γ inside a black region of $p(S)$ we can take a path to $p(S)$ and follow $p(S)$ to a point in the boundary of any other black region. Since any edge of $p(S)$ touches a black region, we may then perturb the path into the black regions and find a corresponding path in the graph of black regions. If we place U's in all the white regions abutting the bottom edge of I^2, then the graph of white regions is connected and, replacing U's with $*$'s is the dual graph, Γ^*, from above.

Note: The dual of Γ is always connected, but it is not always the graph of white regions. When both Γ and the graph of white regions are connected, however, the correspondence is complete. By embedding Γ in the closure of the black regions, we can assign to each white

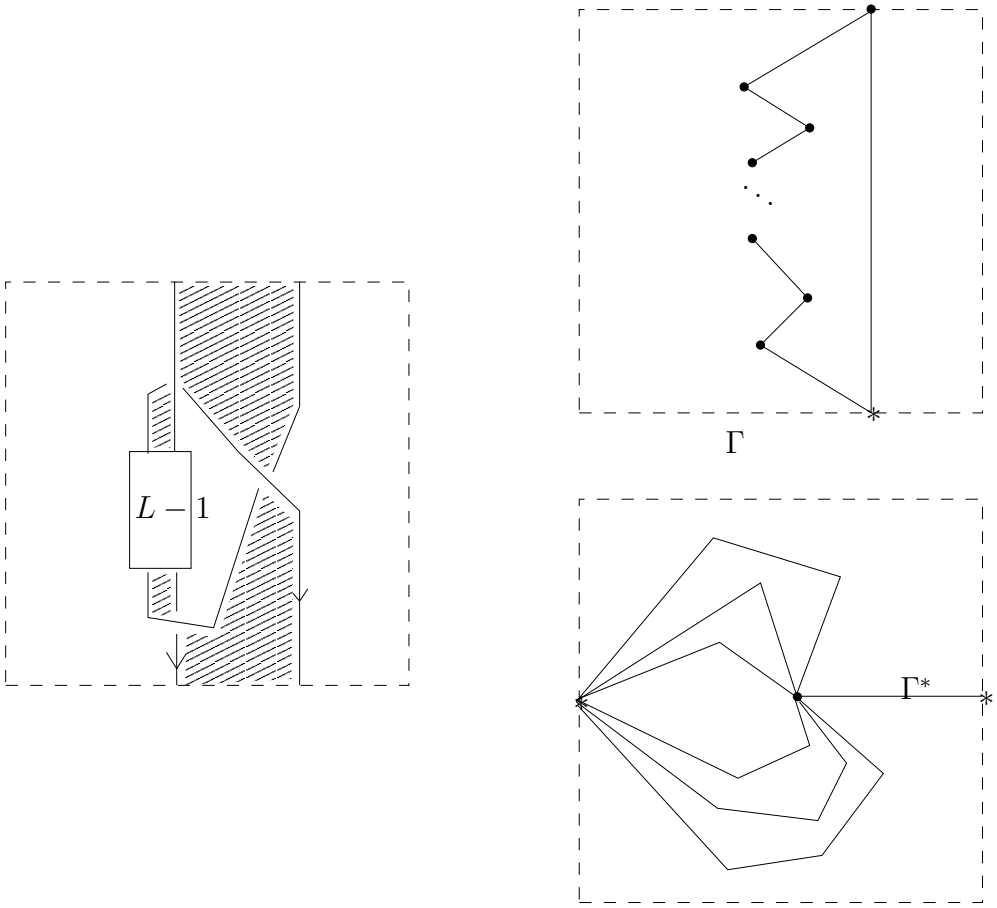

FIGURE 7. An example of the ancillary graph for a simple string link.

region a vertex in Γ^*. If two distinct white regions go to the same vertex, there must be a path in the closure of the black regions from ∂I^2 to ∂I^2 separating the two white regions, but not intersecting a vertex of $p(S)$ (or else the white regions would not map to the same vertex of Γ^*). Such a path disconnects the graph of white regions.

Suppose we use the Heegaard decomposition of S^3 arising from the diagram for S. Following [12], we describe an intersection point in $\mathbb{T}_\alpha \cap \mathbb{T}_\beta$ by local data at the vertices of $p(S)$. For each non-meridional α there are four intersection points with $\{\beta_i\}_{i=1}^g$, corresponding to the four regions in the projection abutting the crossing defined by α. For each meridian there are one or two intersection points depending upon whether it intersects the region U. However, there can be only one choice along all the meridians which assigns each meridian to a distinct β. We will place a $\bullet$ in the quadrant corresponding to the intersection point at each vertex.

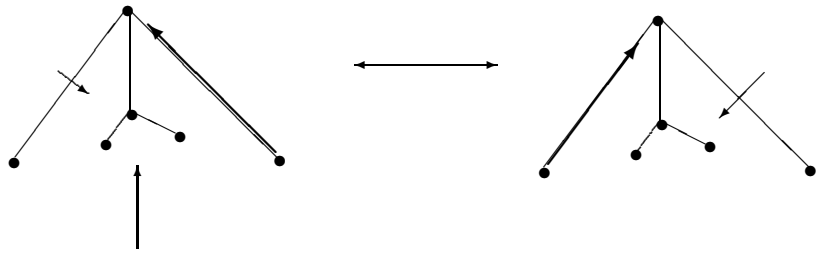

FIGURE 8. The clock $\rightarrow$ and counter-clock $\leftarrow$ moves on maximal forests.

Every intersection point corresponds to a pair of dual maximal spanning forests in the black and white graphs of the projection. The unique choice along the meridians corresponds to the rooting of the forests. We then choose the edges in the black graph which join two regions through a quadrant marked with a $\bullet$. As each black region contains a $\bullet$, this produces a subgraph, F, containing all the vertices of Γ. We can perform the same operation in the white graph to obtain a second sub-graph.

Furthermore, all the components of these sub-graphs are trees. A cycle in F would bound a disc in S^2 not containing a region labelled U. Rounding the crossings of $p(S)$ along the cycle, we find a 4-valent planar graph with B_{in} crossings and $B_{in}+1$ faces not touching the cycle. The original intersection point must form a $1-1$ correspondence between these faces and crossings as all the surrounding faces were consumed by the cycle. There can be no such identification and thus no cycle in the black graph. Similarly, if the intersection point does not produce a forest in the white graph there is a contradiction. Thus we have two maximal spanning forests.

Every component must contain precisely one $*$. It cannot contain more as there is a $\bullet$ for each edge in the tree and for each root. In order for the number of edges plus roots (the α's) to equal the number of β's there must be precisely one root. Thus the two sub-graphs are a dual pair of maximal spanning forests for the graphs of black and white regions

Conversely, the arrows on the edges of Γ found from a dual pair (F, F^*) tell us how to complete the assignment of α's to β's from the unique assignment along the meridians: for each non-meridional α_i we choose the intersection point in $\alpha_i \cap \beta_{\sigma(i)}$ pointed towards by the arrow on the edge corresponding to the crossing defined by α_i. The existence of F^* ensures that no arrow contradicts the assignment along the meridians by pointing into a region labelled with U.

8.2. **A Variant of the Clock Theorem.** We will now examine the structure of the set of dual maximal spanning forests. As in [2] we consider two moves performed on the decorations a dual pair inscribes on Γ: the clock and counter-clock moves. These are moves interchange the two pictures in Figure 8. There should be a face – not labelled with a U – of $I^2-\Gamma$ abutting these two edges at their common vertex. This allows a portion of Γ to be wholly contained in the interior of the face.

A clock move performed on F in Γ corresponds to a clock move performed on F^* in Γ^*. These moves take dual maximal forest pairs into dual maximal forest pairs. If the edge with the transverse arrow joins two distinct components of F, then the new oriented sub-graph,

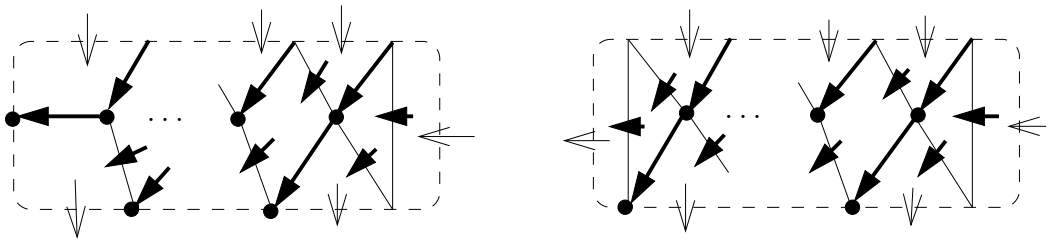

FIGURE 9. Graphs in I^2 admitting a unique pair of maximal spanning forests. In particular, no counter-clock moves can be performed in them. Furthermore, embedded appropriately in a planar graph with a maximal tree inscribing the same decorations, no counter-clock move in the planar graph can alter the decorations in this region. We use the one on the left when k is even, the one on the right when k is odd.

F', of Γ after the clock move is still a forest. The portion of the component through the vertex beyond the vertex is a tree not containing the other vertex of the transverse edge. The move merely prunes this section of one component and glues it to another component. If the edge with transverse arrow joins vertices in the same component of F, it is conceivable that a cycle could form. However, this can only happen if the arrow on the transverse edge points out of the disc bounded by this cycle, and thus a root of the dual graph must be contained in the cycle. Since those roots lie on ∂I^2, this cannot happen.

For a connected, finite planar graph, Γ with only one root, the structure of maximal spanning trees is already understood, [2]. We require that the root be in the boundary of U, the unbounded component of $\mathbb{R}^2 - \Gamma$. Pick one of the trees, T . Each additional edge in Γ, when adjoined to the tree, divides the plane into a bounded and an unbounded component. Draw an arrow pointing into the bounded component on each of these edges. This is the decoration inscribed by the dual tree as before.

In [2], Gilmer and Litherland prove Kauffman's clock theorem:

Theorem 8.1. The Clock Theorem *The set $\mathcal{T}$ of maximal, spanning trees is a graded, distributive lattice under the partial order defined by $T \geq T'$ if we can move from T to T' solely by using clock-moves.*

We will only need that any $T \in \mathcal{T}$ can be obtained from any other T' by making clock and counter-clock moves. It is shown in [2] that only a finite number of clock (or counter-clock) moves can be made successively before we reach a tree not admitting another. Furthermore, this tree is unique for the type of move. We can go from any tree to any other by continually making clockwise moves until we reach the unique un-clocked tree and then make counter-clock moves to get to the other tree.

8.2.1. *The Clock Theorem for Forests.* The vertices on the boundary of I^2 divide the boundary into arcs. We draw an arrow into the the regions labelled by U, across the corresponding arcs. Place arrows pointing out along the other edges. A dual pair (F, F^*) for the string link S extends these arrows in the sense that each face has exactly one arrow pointing into it.

We use the arrows on ∂I^2 to extend Γ to a planar graph with a single root, so that each dual pair (F, F^*) corresponds to a unique maximal spanning *tree* in the resulting graph. To do this we consider a new square with the reverse of the decorations on the boundary of the old square, with the exception that the one on the right edge and the first root from right to left remain the same. We can then extend these decorations by a graph, Γ', and the dual pair as in Figure 9. By inspection, these are the unique decorations providing a dual pair of forests in this graph and extending the boundary conditions. (No two arrows may point into the same white region, if the dual is to be a forest).

We can glue this decorated graph to the one from S to obtain a planar graph where there is only one U, corresponding to the leftmost edge of S, one $*$, and the pair (F, F^*) becomes the decorations from a maximal spanning *tree* as in the clock theorem. Furthermore, a maximal spanning tree in the glued graph inscribing the decorations on the Γ'-portion as in Figure **??** corresponds to a maximal pair (F, F^*) in the graph of black regions for S.

Now we perform counter-clock moves until we reach the maximally clocked tree. At no time do these moves disrupt the decorations in the Γ'-portion. No such move can occur on a face in Γ' as there is no vertex with the requisite arrangement of tree edge and transverse arrow. Furthermore, the Γ' region can be disrupted from outside only when a counter-clock move occurs on a face abutting Γ. Noting that the arrows point out of the vertices on the bottom, and into the vertices on the top, inspection shows that no counter-clock move can occur on such a face at a vertex from Γ'. This is *not* true for clock moves, which can occur on the top left of Γ'. Finally, since the transverse arrows point into the faces that were formerly labelled by U, and these arrows are never altered, no counter-clock move ever involves a face formerly labelled with U. However, as any forest pair for S may be extended to a tree for the new graph and counter-clocked to the maximal clocked tree, there is always a sequence of counter-clock and clock moves, not involving Γ', which connect any two pairs for S.

In short,

Lemma 8. *The dual pairs (F, F^*) for the graph of black regions, Γ, found for a connected projection of a string link may be converted, one into another, by clock and counter-clock moves performed on the decorations coming from the rooting of the string link.*

8.3. **State Summation.** Following [12], we will prescribe weights at the crossings of the string link as in Figure 10, and extend those weights to apply to more than one component. For each intersection point in $\mathbb{T}_\alpha \cap \mathbb{T}_\beta$, we consider the associated dual pair (F, F^*) and locally place $\bullet$'s in the regions abutting each intersection point or merdian according to the direction of the trees. We sum the weights from the marked region at each crossing and meridian. This prescribes $\mathcal{F}_i$ for the i^{th} strand if it is the thick strand. Crossings not involving the thick strand contribute nothing to the weight. When we change from the intersection point obtained from one tree to that obtained from another tree differing by a clock or counter-clock move, the change in exponent is given by $(n_w - n_{z_i})(\phi)$ for any ϕ in $\pi_2(\mathbf{x}, \mathbf{y})$ that joins these intersection points. We verify that this equals the change in the weights. As the Heegaard diagram describes S^3, an integer homology sphere, such a class ϕ must exist. Since the dual pair (F, F^*) coming from an intersection point can be obtained from the dual pair for any other intersection point by clock and counter-clock moves, we

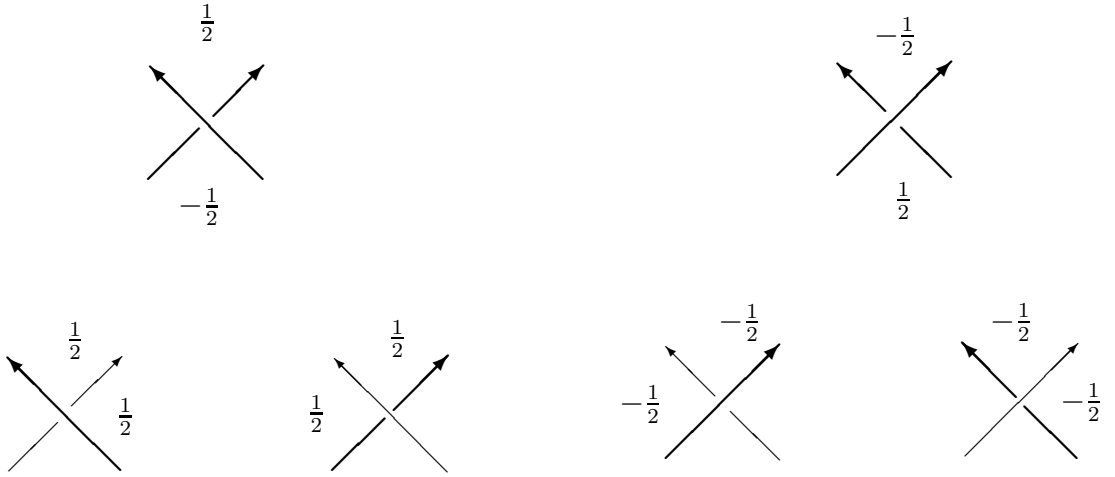

FIGURE 10. Filtration Weights Depicted for the Thick Strand and the i^{th} Filtration Value. The meridians do not contribute to the weights.

FIGURE 11. Weights for the Absolute Grading

may compute the difference in exponents for any two intersection points by looking at the difference in the overall weights.

Likewise, there are weights to calculate the grading for each intersection point. See Figure 11. For each intersection point we add the weights over all the crossings without considering which strands appear. The meridians do not contribute to the grading.

We now prove that the difference in grading and filtration values between one maximal forest and the forest that results after a clock or counter-clock move equals the difference in the weights defined for each tree above. We denote the local contribution to each intersection point by placing a $\bullet$ or $\circ$ at each crossing. We will assume that $\bullet$ and $\circ$ are identical for crossings that are not depicted. Following the definitions of maximal trees and clock and counter-clock moves given above, we can verify that the moves from $\circ$ to $\bullet$ fulfill our

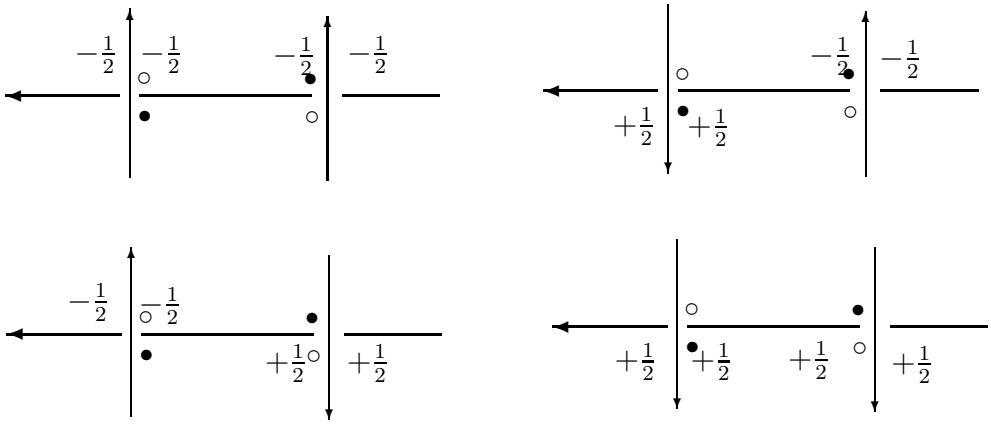

FIGURE 12. Case I: Weights, depicted for the horizontal strand, do not change under the alteration from $\circ$ to $\bullet$. The thin strands do not need to come from the same component. The thin component on the left receives weight 0 from these configurations. The thin strand on the right receives the same weight from $\circ$ and $\bullet$. The grading change occurs along the middle strand, as inspection of the crossings shows.

requirements and exhaust all possible moves. We break the argument up into cases:

Case I: Figure 12 shows the cases where a counter-clock move joins intersection points at two crossings (not meridians). These correspond to unique discs, namely squares, "atop" the Heegaard surface. As the squares do not cross any of the multi-points, there will be no change in exponents corresponding to any of the three strands. This equals the change in the weights. On the other hand. squares always have a one dimensional space of holomorphic representatives, so the intersection point $\circ$ has grading 1 greater than $\bullet$ in Heegaard-Floer homology. This equals the change in the grading weights.

Case II: Figure 13 shows the same alteration but with a different configuration of under and over-crossings. The homotopy class we choose is now a "square" with punctures and handles added to it. In particular, the disc travels off the end of the figure in the direction of the knot picking up punctures at crossings and joins punctures into handles if it happens to go through the same crossing twice. It terminates on the meridian corresponding to the horizontal strand. Thus, the filtrations remain unchanged except in the i^{th} component. But the "disc" passes over z_i once, so $\mathcal{F}_i(\bullet) - \mathcal{F}_i(\circ) = (n_w - n_{z_i})(\phi) = -1$. In [12], P. Ozsváth and Z. Szabó show that $\mu(\phi) = 1$ for such a class, so the grading change equals the change in grading weights.

Case III: For the other cases with three distinct strands, the strand on the right should go under the horizontal strand. However, if we rotate the figures in cases (1) and (2) 180° using the horizontal strand as an axis, we get precisely those cases. The disc also rotates and occurs "beneath" the Heegaard diagram. This disc represents a counter- clock move;

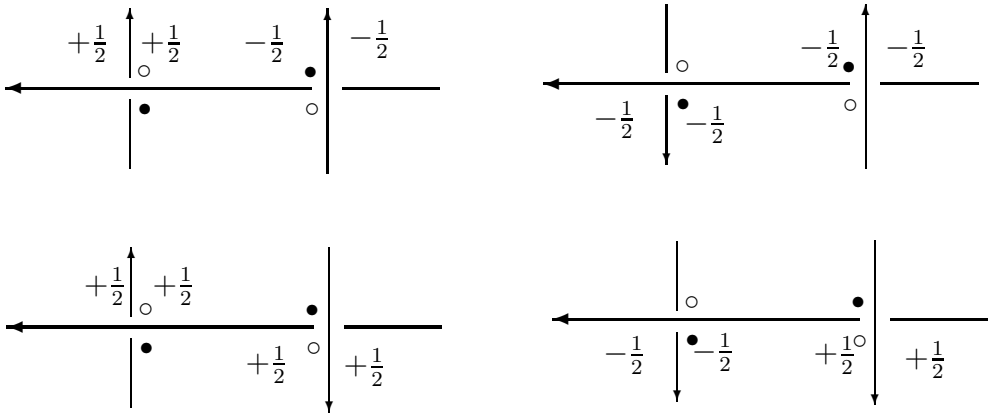

FIGURE 13. Case II: Weights, depicted for the horizontal strand, reduce by 1 under the alteration from ∘ to •. The same comments as in the caption for case I apply to the thin strands and the grading.

However, we will still calculate the difference for a clock move from ∘ to •. For this we use ϕ^{-1} with $\mathcal{D}(\phi^{-1}) = -\mathcal{D}(\phi)$. The weights on the horizontal strands reflect across the horizontal strand as do the weights for the grading. The weights for the thin strands remain the same. Thus $\mathcal{F}_i^{III}(\bullet) = \mathcal{F}_i^{II}(\circ)$ and $\mathcal{F}_i^{III}(\bullet) - \mathcal{F}_i^{III}(\circ) = -\big(\mathcal{F}_i^{II}(\bullet) - \mathcal{F}_i^{II}(\circ)\big) = +1$ for those configurations in case II. But $(n_w - n_{z_i})(\phi_{III}^{-1}) = -(n_w - n_{z_i})(\phi_{III}) = -(n_w - n_{z_i})(\phi_{II}) = +1$ as ϕ_{II} and ϕ_{III} include the i^{th} meridian the same number of times.

Case IV: In the cases where two or more of the above strands are the in the same component, we employ the following observations: 1) if the two thin strands belong to the same link component, then nothing changes, and 2) if the horizontal strand corresponds to the same component as one of the thin strands (or both), the sum of the weights in each quadrant differs by the same amount from that quadrant's weight as a self-crossing. Thus the difference between intersection points of the sum is the same as the difference of the self-intersection weights. The grading computations don't change. Inspecting the values in Figures 12 and 13, we see that the filtration difference still equals the difference in the weights for the horizontal strand.

Finally, we have implicitly assumed that the horizontal strand between the two intersections is locally unknotted. Local knotting alters the topology of the domain $\mathcal{D}(\phi)$ above. Take the square in case I. If we knot the horizontal strand, there is still a class ϕ joining the two intersection points, but it is a punctured disc with the same four points on its outer boundary, and one point that is both • and ∘ on each of its other boundaries. These new boundaries come from the faces in the projection of the local knot, and consist entirely of β curves. The α curve at each intersection point on such a boundary joins that boundary to another boundary β, possibly from the square. Together these form a forest with vertices being β curves, and edges being the α's that join them. In the Appendix we show that these still have $\mu(\phi) = 1$,which is all we need in the proof.

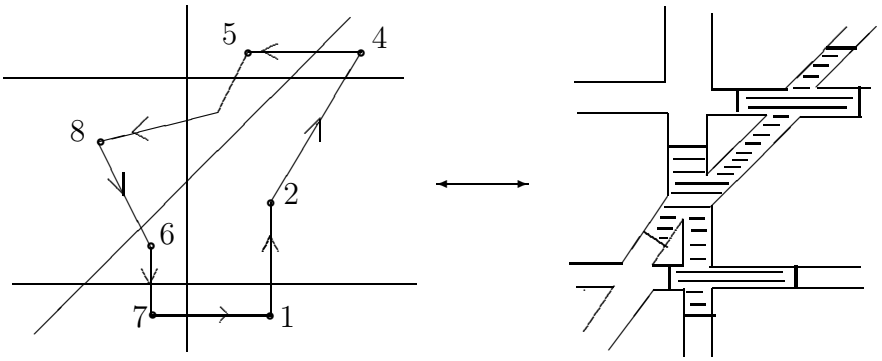

FIGURE 14. The Contradiction in Lemma 9 Arising from a Cycle.

8.4. **Heegaard-Floer Gradings and Grading Weights.** In the remainder of this section we connect the gradings from Heegaard-Floer homology and those from the weights. It should come as no surprise that they are equal and that the argument in [12] adapts readily. For the grading, we know that $\mathbf{gr}(\mathbf{y}) - \mathbf{gr}(\mathbf{x})$ is the same as the difference in weights. However, we will show that there is an intersection point for which the sum of the weights above is the absolute grading obtained from the Heegaard-Floer theory. Thus the sum of the grading weights will equal the grading for every intersection point since the difference between these is equal for distinct intersection points. We will need a lemma before we proceed.

Lemma 9. *Let $G \subset \mathbb{R}^2$ be a finite graph and let H_α be the handlebody that is its regular neighborhood in S^3. Then $S^3 - H_\alpha$ is a handlebody with the co-cores of its one-handles corresponding to the bounded faces of $\mathbb{R}^2 - G$. We choose these co-cores to be the $\{\beta_i\}_{i=1}^g$ of a Heegaard diagram for S^3. Suppose that $\{\alpha_i\}_{i=1}^g$ contains α's which intersect at most 2 β's, each geometrically once. Furthermore, assume that each α links exactly one edge of G. Then there is only one point in $\mathbb{T}_\alpha \cap \mathbb{T}_\beta$.*

Proof: Supppose $\mathbf{x}$ and $\mathbf{y}$ are points in $\mathbb{T}_\alpha \cap \mathbb{T}_\beta$ and $\mathbf{x} \neq \mathbf{y}$. Then $\mathbf{x} = \{x_1, \ldots, x_g\}$ and $\mathbf{y} = \{y_1, \ldots, y_g\}$ where $x_i \in a_{\sigma(i)} \cap \beta_i$ and $y_i \in a_{\psi(i)} \cap \beta_i$ with $\sigma, \psi \in S_n$. If $\mathbf{x} \neq \mathbf{y}$ then $\psi^{-1} \circ \sigma$ is not the identity. It must therefore have a decomposition into cycles with at least one of length greater than or equal to 2. In the planar graph formed by placing a vertex in each bounded face of Γ, and an edge between each pair of faces abutted by an α curve, each non-trivial cycle in the cycle decomposition corresponds to a cycle in the graph. Each cycle in the graph implies the existence of a collection of α's that are null-homologous in Σ, contradicting the Heegaard assumption (see Figure **??**). Thus at most one intersection point exits. Since $\widehat{HF}(S^3) \simeq \mathbb{Z}_{(0)}$, there is at least one intersection point, $\mathbf{x}_0$.

Starting with a string link in S^3, we use handleslides to construct a Heegaard diagram as in the lemma. The intersection point in this Heegaard diagram will correspond to one in the diagram for the string link. We will ensure that the handleslides do not alter the

absolute grading. The intersection point for the string link must then have absolute grading equal to 0. This will also be the value of $G(\mathbf{x})$ for that intersection point. Since we know that $G(\mathbf{y}) - G(\mathbf{x}) = gr(\mathbf{y}) - gr(\mathbf{y})$, the weights above will give the absolute grading of each intersection point.

To obtain an acceptable diagram, it suffices that the new α link an edge entering the crossing defined by the old α before the handlesliding as the weights for the grading only occur in the quadrant between the two edges exiting a crossing. The unique intersection point will then correspond to an old intersection point with $G(\mathbf{x}) = 0$. We ignore the points $\{z_1, \ldots, z_k\}$ to find a pointed diagram for S^3.

We order the crossings in the string link projection by the following conditions. Each crossing of L_k is larger than any crossing of strands L_i and L_j with $i, j < k$. For any k, the crossings with L_i for $i \leq k$ are enumerated from largest to smallest by the first time they are encountered while travelling backwards along L_k from the meridian. We adjust each crossing in increasing order by starting at that crossing (either for L_j with itself or between L_i and L_j with $i \leq j$) and isotoping and handelsliding the α-curve in the direction of L_j, going over all the α's along that route. At self-crossings we choose to follow the edge which exits the crossing and arrives at a meridian without returning to the crossing. When we arrive at the meridian we handleslide across it, and then repeat the procedure in reverse. This produces an α linking the penultimate edge through the original crossing. Furthermore, for each crossing the ordering implies that there is a path to the meridian along the orientation of one or other strand, along which the crossing does not recur, and such that none of the α's encountered have been previously alterred.

The handleslides do not take the α's across w. By inspecting the standard handleslide diagram, [13], we can see that the new intersection point is the in the image of one of the original intersection points, the one with marking in the same quadrant at each crossing, under the composition of the handleslide maps. The cobordism induced by the handleslides is $S^3 \times I$, so the formula calculating the change in absolute grading imples that the grading does not change. Moreover, since the triangle does not cross w we know that the image is $[\mathbf{x_0}, 0]$ which has absolute grading zero. This equals the absolute grading assigned by the weights.

Note: For a single knot in S^3, a string link consists solely in the choice of a point on the knot. This gives a preferred position for the meridian and the two points w, z used in [15] to calculate the knot Floer homology. The weights above agree with those of [12].

8.5. **Example.** In the graph of black regions for Figure 7 we may form dual forests in two ways, see Figure 15. First, we may have arrows pointing up the segments on the left side of the graph of black regions. Second, we may have some arrows pointing up that side, then a transverse arrow, then arrows pointing down the remainder of the segments on the left side. To join the vertices at top and bottom we have an arrow up the single segment on the right side.

When all the arrows go up the left side, they place the local intersection points on the opposite side of L_2 from that pointed to by the orientation of L_1. Looking at the weights

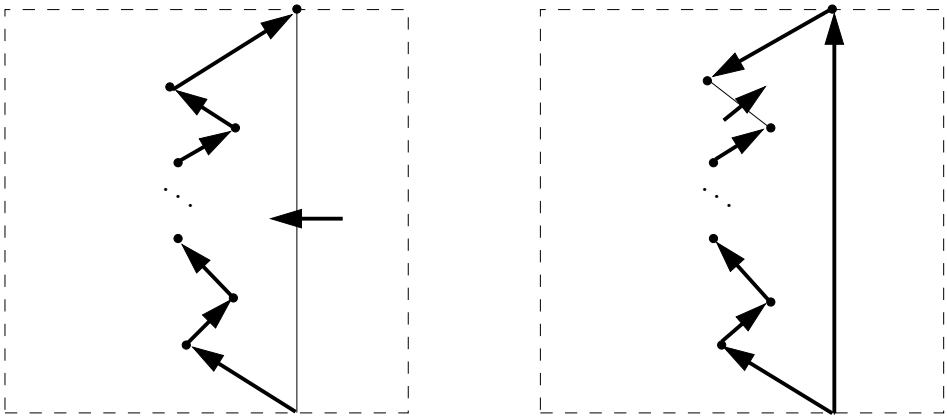

FIGURE 15. Examples of dual maximal forests for the graph Γ from Figure 7

indicates that, regardless of the crossing type, such a tree contibutes 0 to the filtration index for L_2 and 0 to the grading weight. On the other hand, when the crossings are positive all the segments on the left are assigned $-\frac{1}{2}$ for the weight on L_1. The transverse arrow on the right will contribute nothing to either sum. A similar analysis for negative linking implies that this forest contributes $h_1^{-lk(L_1,L_2)}$ to the Euler characteristic.

For the second type of forest, let m be the number of arrows pointing up on the left side. Then m can vary between $m = 0$ and $m = 2\,lk(L_1, L_2) - 1 = 2\,L - 1$ when the linking number is positive. The monomial for this state is $h_1^{-s}h_2^{-L+s}$ when $m = 2\,s$ and $-h_1^{-s-1}h_2^{-L+s}$ when $m = 2\,s + 1$. The minus sign in the latter comes from the generator having grading -1. Together these imply a polynomial of the form

$$\left(h_1^{-L} + h_1^{-L+1}h_2 + \cdots + h_2^{-L}\right) - \left(h_1^{-L}h_2^{-1} + \cdots h_1^{-1}h_2^{-L}\right)$$

Since the string link is alternating, and the minus signs occur from grading -1, we can determine the homology for the string link from the above polynomial (see the next section). It is $(v_1, v_2 \leq 0)$

$$\widehat{HF}(S, (v_1, v_2)) \cong \mathbb{Z}_{(0)} \quad v_1 + v_2 = -lk(L_1, L_2)$$

$$\widehat{HF}(S, (v_1, v_2)) \cong \mathbb{Z}_{(-1)} \quad v_1 + v_2 = -lk(L_1, L_2) - 1$$

8.6. **Braids and Alternating String Links.**

8.6.1. *Triviality for Braids.* In section 7, we saw that the Euler characteristic of the chain groups for a string link in S^3 produces the torsion of the string link $\tau(S_L)$ defined in [8]. The torsion is known to be trivial if the string link is a pure braid. Analogously, we may prove:

Lemma 10. *$\widehat{HF}(S_L) \cong \mathbb{Z}_0$ when S_L is a pure braid. Using the weights from the previous section, the homology is non-trivial only for the index* $(0, \ldots, 0, 0)$

Proof: There are two ways to prove this statement. The first analyzes the combinatorics of Kauffman states in the diagram. There is only one state: The meridians consume the first row of β-curves. Each crossing then has three regions already claimed, so it must use the fourth. This consumes the second set, and we proceed up the diagram. However, a more conceptual explanation may also be given. We know that the invariant we have defined does not depend upon how the strands move about on $D^2 \times \{1\}$. We may simply undo the braid to obtain the trivial string link.

The statement about filtration indices follows from the weights defined in the previous section and the observation that the unique state assigns its local contributions to the quadrant between two edges pointing into the crossing as the strands are oriented down the page.

8.6.2. *Vanishing Differential for Alternating String Links.* We call a string link, S, *alternating* if there is a projection of S where proceeding along any strand in S from $D^2 \times \{0\}$ to $D^2 \times \{1\}$ encounters alternating over and under-crossings. In a projection, we may place a small kink (formed using the first Reidemeister move) in any strand which does not initially participate in any crossing (self or otherwise) without changing whether the projection is alternating.

We call the i^{th} strand, s_i when counting from left to right on $D^2 \times \{0\}$ and s^i when counting on $D^2 \times \{1\}$. If we follow the s_i from $D^2 \times \{0\}$ to $D^2 \times \{1\}$ find that it is $s^{\sigma(i)}$ for some permutation $\sigma \in S_k$.

At each end of $D^2 \times I$ we may label the strands as u or o for whether the strand is the over or under strand in the crossing immediately preceding (following) the end of the strand on $D^2 \times \{1\}$ ($D^2 \times \{0\}$). This assigns a k-tuple called the *trace* of the string link at that end. We denote the trace at $D^2 \times \{i\}$ by $T_i(S)$. There is an inversion on such k-tuples found by interchanging u's and o's, which we denote $v \to \overline{v}$. To compose alternating string links to have an alternating result requires $T_1(S_1) = \overline{T_0(S_2)}$.

Our goal is to show

Theorem 5. *Let S be a string link with alternating projection. Then the chain complex, $\widehat{CF}(S, \overline{j})$, arising from the projection Heegaard splitting has trivial differential for every index $\overline{j}$. In fact, all the generators have the same grading.*

This generalizes the result in [12] for alternating knots. We will need the knot case for the general result. The result in [12] is somewhat stronger (by identifying the grading).

Note: We call Morse critical points of index 1 for the projection of s_i to the I factor a "cap". Critical points of index 0 are called "cups".

Lemma 11. *We may draw an alternating projection for S so that 1) Every crossing occurs with both strands oriented up, 2) No two crossings, caps, or cups occur in the same level in the I factor.*

Proof: Rotate every crossing without the correct orientations so that both strands go up. This can be done in a small neighborhood of the crossing at the expense of introducing cups and caps. The second condition is achieved by a small perturbation of the diagram.

Given a diagram in this form, we proceed with a few combinatorial lemmas. These are devoted to showing that an alternating string link may be closed up to give an alternating knot with certain additional properties. At each time t in the parametrization of the i^{th} strand, let $f_i(t)$ be the number of strands strictly to the left of that point on s_i.

Lemma 12. *Let t be a time when $s_i(t)$ is in a level (in I) not containing any caps or cups, and not at a crossing. The total number of crossings encountered along the strand s_i by the time t is $\equiv |f_i(t) - i + 1| \mathrm{mod}\ 2$ when s_i is oriented up and $\equiv |f_i(t) - i| mod\ 2$ when s_i is oriented down.*

Proof: The number of caps plus the number of cups encountered in the i^{th} strand, by time t, is even when the strand is oriented up, and odd when the strand is oriented down. $f_{i(t)}$ changes value by 1 as $s_i(t)$ goes through a cap, cup or crossing. It changes value by 2 at levels where a cap or cup occurs to the left of $s_i(t)$. By reducing modulo 2 we eliminate the latter variation. Since there are $f_i(t)$ strands to the left, having started with $i-1$ strands to the left, the number of cups, caps and crossings must be congruent to $|f_i(t) - i + 1|$ modulo 2. Removing the parity of the number of caps and cups gives the result.

Corollary 2. *The total number of crossings encountered by the i^{th} strand is congruent modulo 2 to $|\sigma(i) - i|$.*

This lemma has the following consequence:

Lemma 13. *Suppose s_i and s_j cross somewhere in S. If $T_0(s_i) = T_0(s_j)$ then $i \equiv j$ mod 2. If $T_0(s_i) \neq T_0(s_j)$ then $i \equiv j + 1$ mod 2*

Proof: Consider the first time that they cross in the ordering on s_i. Suppose that $i < j$, and that there are k strands to the left of the point in s_i just before the crossing. Then there must be $k \pm 1$ strands to the left of s_j. We label each point on the strands, except at crossings, by a u or an o depending upon whether an over, or under, crossing must occur next. The labels of the points on the two strands just before the crossing of s_i and s_j must be different. If s_i has encountered an even number of crossings prior to this point, it will have label $T_0(s_i)$, otherwise it has label $\overline{T_0(s_i)}$. The same will be true of s_j. We have assumed that both strands are oriented up just before the crossing. Thus, the parity of the number of crossings involving s_i is that of $|f_i(t_i) - i + 1| = |k - i + 1|$ and the same parity for s_j is $|f_j(t_j) - j + 1| \equiv |k - j|$. If $T_0(s_i) = T_0(s_j)$, then one strand must have experienced an even number of crossings, while the other experienced an odd number. This happens when $i \equiv j$. Otherwise, both strands must enounter the same parity of crossings and $i \equiv j + 1$.

We decompose $S = S_1 \cup \cdots \cup S_l$, where S_j consists of a maximal string link with connected projection. We apply the following lemma to each S_j.

Lemma 14. *For a connected, alternating string link $T_0(S)$ must be either $(u, o, u, \ldots)$ with alternating entries, or $(o, u, o, \ldots)$*

Proof: For s_i and s_j there is a sequence $s_{i_0}, \ldots, s_{i_r}$ with $s_{i_0} = s_i$ and $s_{i_r} = s_j$ and where consecutive entries cross one another. The result follows from induction using the conclusion of the previous lemma, which also proves the base case.

Since any strand in S_j divides the projection into two parts, we see that each S_j must consist of consecutive strands in the diagram (along both ends). Furthermore, we have shown

Lemma 15. *For an alternating projection of S, $T_0(S) = \overline{T_1(S)}$.*

This lemma guarantees that the usual closure of the string link (join s^i to s_i for all i) is alternating.

Proof: We divide $S = S_1 \cup \cdots \cup S_l$ and apply the corollary above to each maximal substring link. By the preceding lemma, we have an alternating trace for the end $D^2 \times \{0\}$. By the corollary, the other end of s_i has the same label when $\sigma(i) - i$ is even, and different labels when $\sigma(i) - i$ is odd. The result follows directly.

In fact, a repetition of u or o in $T_0(S)$ implies that $S = S_1 \cup S_2$ for an alternating string link. S_1 consists of those strands including and to the left of the first u, and S_2 consists of those strands including and to the right of the second.

Note: Recall that we add kinks by the first Reidemeister move to strands who don't cross any other strand (including themselves). This is how they get labelled.

The chain complex of a string link S which decomposes as $S_1 \cup \cdots \cup S_l$ for the index $(\overline{j}_1, \cdots, \overline{j}_l)$ is $\widehat{CF}(S_1, \overline{j}_1) \otimes \cdots \otimes \widehat{CF}(S_2, \overline{j}_l)$ with the standard tensor product differential. Thus, proving the theorem for connected, alternating string links will prove the general result. Our strategy is to compare the chain group from out projection to the chain group of an alternating knot.

We make a few observations about braids. First, their projection Heegaard diagrams possess only one generator. Second, given the projection of a braid, forgetting over and under crossings, there is precisely one set of crossing data with $T_0(B) = (u, o, u, o, \ldots)$. Write the braid as a product of generators or their inverses. The traces picks out which (generator or inverse) must occur. Pushing up the diagram, the traces $(u, o, u, o, \ldots)$ repeats as $T_0(B')$ for the remainder of the braid.
We choose a braid representing a permutation τ such that $\tau \circ \sigma$ is a cyclic permutation taking 1 to k. As we have just seen, we may use $T_0(B) = \overline{T_1(S)}$ to choose a braid so that $S\#B$ is still an alternating string link. We complete the construction by closing the new string link as in one of the diagrams in Figure 16. The trace at the bottom of $S\#B$ determines which to use. Due to our assumption about τ, the result is a knot, K.

By construction, the knot is alternating. We draw a Heegaard diagram for this knot by using m_1 from the string link diagram to give a meridian for the knot. This meridian intersects only one β. It is a basing for the knot in the Kauffman state picture of [12]. We analyze the generators of this knot. In particular, we have seen that a generator $\mathbf{x}$ of $\widehat{CF}(S, \overline{j})$ extends uniquely to a generator $\mathbf{x}'$ for $S\#B$. We would like to extend $\mathbf{x}'$ to a generator of $\widehat{CF}(K)$. However, when we forget the states on the other meridians, we have

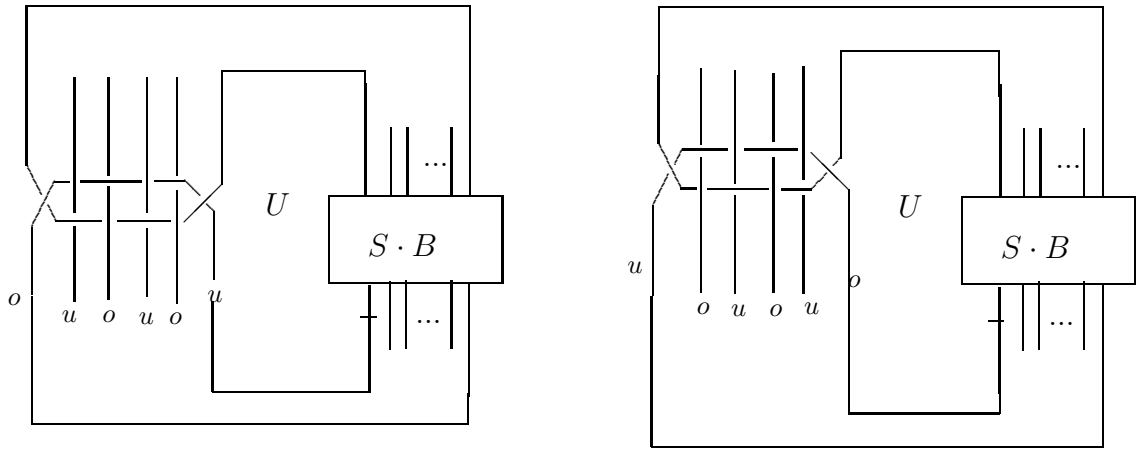

FIGURE 16. The closures to construct an alternating knot from an alternating string link. The case for an odd number of strands is similar. The basing (meridian) for the new knot is shown as a small line across the knot and intersecting U. Of course, the strands should meet at top and bottom as for the closure of a braid.

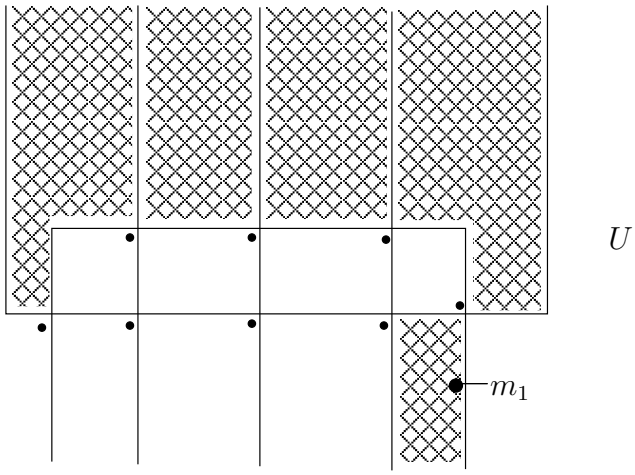

FIGURE 17. The Unique Extension of Generators. The shaded regions have already been assigned to a crossing by the generator in $S\#B$. This corresponds to the extension of dual pairs used to extend the clock theorem to string links.

that the shaded regions of Figure 17 receive an assignment, but the others do not. There is a unique way to complete the figure to a generator $\mathbf{x}''$ in the knot complex, and this corresponds to a Kauffman state.

Suppose that there is a $\phi \in \pi_2(\mathbf{x}, \mathbf{y})$ with $\widehat{\mathcal{M}}(\phi) \neq \emptyset$ and with $n_w(\phi) = n_{z_i}(\phi) = 0$ in the Heegard diagram for S. The condition at the marked points, and that for a string link there is only one choice of assignment along the meridians, implies that the homotopy class ϕ gives a homotopy class $\phi'' \in \pi_2(\mathbf{x}'', \mathbf{y}'')$ in the diagram for K. That there is no variation on the meridians allows us to alter the generators as in the extension. The marked point conditions ensure that $\mathcal{D}(\phi)$ is wholly insulated from the additional braid and the closure construction. Furthermore, a nighborhood of each meridian is eliminated by the condition that $n_{z_i}(\phi) = 0$ as ϕ must contain whole multiples of the meridians in its boundary. There must then exist two intersection points $\mathbf{x}''$ and $\mathbf{y}''$ in the *same filtration index* for the knot (since ϕ doesn't cross the marked points) but which *differ in grading* by 1. This contradicts the statement in [12] that, for an alternating knot, the grading of every Kauffman state representing the same filtration index is the same (determined by the signature of the knot!). Hence, all moduli spaces contributin to the differential must be trivial, $\widehat{\partial}_S \equiv 0$. The same argument holds for ϕ as above with $\mu(\phi) \neq 0$, thus all the generators of the chain complex in a given filtration index in fact lie in the same grading.

8.7. **Euler Characteristic Calculations.** Let G and $\mathcal{F}_i$ be the sums if weights giving the grading and the filtration indices. To each intersection point in $\mathbb{T}_\alpha \cap \mathbb{T}_\beta$ assign the monomial $(-1)^{G(\mathbf{x})} h_1^{\mathcal{F}_1(\mathbf{x})} \cdots h_k^{\mathcal{F}_k(\mathbf{x})}$ in $\mathbb{Z}[h_1^{\pm 1}, \ldots, h_k^{\pm 1}]$. From the description of Alexander invariants for string links, the Laurent polynomial,

$$\nabla_S(h_1, \ldots, h_k) = \Sigma_{\mathbf{x}} (-1)^{G(\mathbf{x})} h_1^{\mathcal{F}_1(\mathbf{x})} \cdots h_k^{\mathcal{F}_k(\mathbf{x})}$$

is the torsion of the string link. Furthermore, it satisfies the Alexander-Conway skein relation in h_i at self-crossings of L_i. The proof is a comparison of the weights assigned to forests in the projections for the positive, negative, and resolved crossings. In fact, the three Reidemeister moves also preserve this summation, when we fix the ends of the string link.

We may ask how this sum, when restricted to a certain strand, L_i relates to the Alexander-Conway polynomial of the knot, $\widehat{L}_i$ formed by closing the strand. It is shown in [12] that for 1-stranded string links (marked knots) they are identical. In this section we prove the following lemma, relating the above multi-variable Laurent polynomial to its single variable specifications:

Lemma 16. *The polynomial $\nabla_S(h_1, \ldots, h_k)$ evaluates to $\Delta_{\widehat{L}_i}$, the Alexander-Conway polynomial of $\widehat{L}_i$, upon setting $h_j = 1$ for $j \neq i$.*

In [12] the proof of the statement for knots follows from two observations: I) from Kauffman, that the polynomial formed by the weights at crossings is the Alexander-Conway polynomial, and II) that the polynomial formed by using the first Chern class as the filtration index is symmetric due to the symmetries of *Spin*^{c} structures on the three manifold found from 0-surgery on the knot. Since both schemes assign values to intersection points that satisfy the filtration relation, and both produce symmetric polynomials under $h \to h^{-1}$, they must be equal. We do not have at hand an analog of the first observation, and thus will resort to model calculations.

To prove the lemma, we first observe that

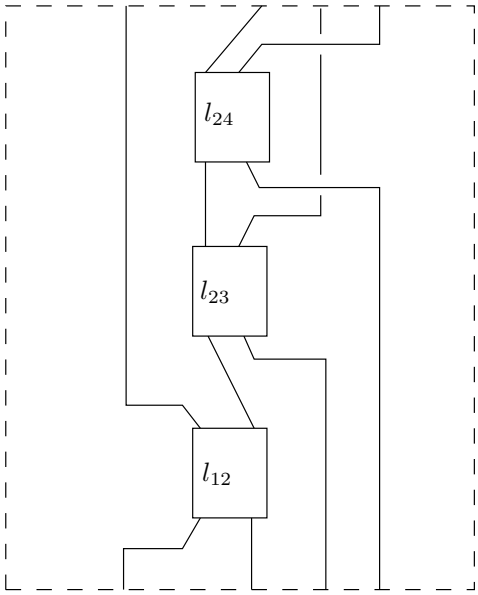

FIGURE 18. Reduced Form for a String Link when $i = 2$. The numbered boxes indicate the number of full twists between the two strands. Notice that this is actually a braid.

Lemma 17. *Suppose we may interchange*

(1) *Crossings of L_i with itself*
(2) *Crossings of L_j with L_k when $j, k \neq i$*

Then the string link S may be put in the form of a braid as found in Figure **??**.

Proof: By interchanging self-crossings of L_i we may arrange for this strand to be unknotted. We may then isotope so that it is a vertical strand. Consider $D^2 \times I$ to be $I^2 \times I$ with the i^{th} strand given as $(\frac{1}{2}, \frac{3}{4}) \times I$. By isotoping the other strands vertically, switching crossings where necessary, we can ensure that each is contained in a narrow band $I^2 \times (a_j - \epsilon, a_j + \epsilon)$ except when coming from or going to the boundary, when we assume that they are vertical. If we look in the band $I^2 \times (a_j - \epsilon, a_j + \epsilon)$ for the j^{th} strand, we see that all the other strands are vertical segments and the j^{th} strand is some strand in a string link. We may isotope L_j past all the vertical segments except that for L_i. By effecting self-crossing changes in L_j we can make it unknotted. It can then be isotoped so that it reaches the level $I^2 \times a_j$ from the bottom, winds around L_i in that plane exactly $lk(L_i, L_j)$ times, and then proceeds vertically to the top. We un-spool this winding veritcally so that the result is a braid, where all the clasps are once again in $I^2 \times (a_j - \epsilon, a_j + \epsilon)$. Doing this to each of the strands produces a string link with projection as in Figure 18 when we choose $a_j < a_k$ if $j < k$ for $j, k \neq i$.

Consider the closure, $\widehat{L}_i$ formed by taking the i^{th} strand and joining the two ends in S^3 by a simple, unknotted arc. The intersection points in the Heegaard diagram give rise to $Spin^c$ structures on the three manifold formed by taking 0-surgery on this knot, [15]. Let $\mathcal{P}_i$ be

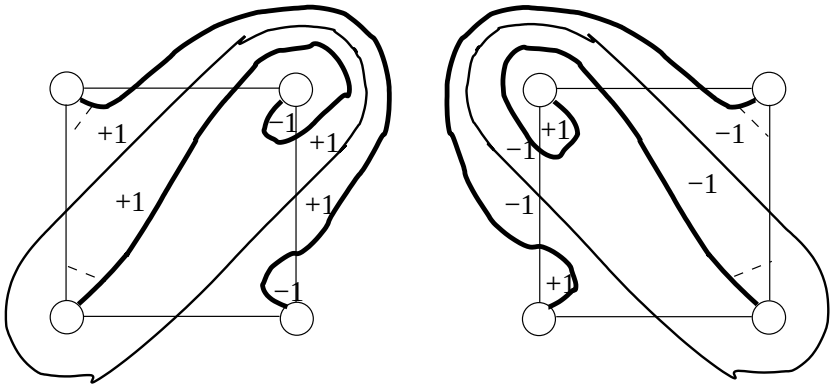

FIGURE 19. Local Heegaard diagrams for self-crossings of L_i. The thick curves are the α-curves. The thickest is the longitude, used as a surgery curve; while the middle thickness depicts the crossing. There is a positive crossing on the left, and a negative crossing on the right. The multiplicities are for the band added at the crossing according to Seifert's algorithm.

the periodic domain corresponding to the Seifert surface in the Heegaard diagram for the 0-surgery manifold. We already know that the sum of the filtration weights assigned to $\mathbf{x}$ by L_i differs from $\frac{1}{2} < c_1(\mathfrak{s}(\mathbf{x}), \mathcal{P}_i >$ by a constant, independent of $\mathbf{x}$, but which may depend upon S. Each of these quantities satisfies the same difference relation for a class ϕ joining two distinct intersection points. The crossings of L_j with L_k do not contribute to either calculation as the periodic domain $\mathcal{P}$ does not change topology or multiplicities when we interchange such crossings. It consists of puctured cylinders arising from the linking of L_i with L_j or L_k and terminating on the meridian for that strand. However, the punctures and multiplicities remain the same regardless of the type of crossing between L_j and L_k. Since only the topology and multiplicities contribute to the calculation of the first Chern class for the intersection points, and the intersection points correspond under crossing changes, the value of the first Chern class does not change. Nor do the weights change as such crossings are assigned a weight of 0. As a result, interchanging crossings of L_i and L_j does not affect the value of the constant.

It requires more effort to see that interchanging self-crossings of L_i will not alter the constant. But presuming that, we see that the polynomial $\nabla_S(h_1, 1, \ldots, 1)$ must be $h_i^{C_i(S)}\nabla_{L_i}$, since by [12] the polynomial determined by the first Chern class is the Alexander-Conway polynomial of the knot. Furthermore, we may calculate $C_i(S)$ by finding the polynomial assigned to the reduced form above, since it does not change under the moves of Lemma 17. The i^{th} strand is then the unknot, with Alexander-Conway polynomial equal to 1, and the value of $C_i(S)$ is 0 from our calculation for braids in the previous section.

That $C_i(S)$ does not change when interchanging self-crossings of L_i follows by seeing that the first Chern class calculation changes in the same way as the filtration weights. Notice that we may do the calculation for the multiplicities shown in Figure 19

By adding multiples of $[\Sigma]$ and $\mathcal{P}$ we may realize a periodic region with the multiplicities for the crossing as shown in the figure. We fix the intersection point to be considered. On the left we have a local contribution to $n_{\mathbf{x}}$ of $+2$ on top, $+1$ on left and right, and 0 on bottom. We may always pick and intersection point where the longitude pairs with a β intersecting the meridian, and thus does not incur an additional contribution from any crossing. On the right, the contribution is -2, -1, and 0, respectively. All other local contributions are equal as is the value of n_w on the periodic region. The only other variation that can occur will be in the Euler measure, $\hat{\chi}(\mathcal{P})$. Outside of the depicted region, $\mathcal{P}$ does not change. Indeed, if we divide $\mathcal{P}$ by cutting the corners of the large $+1$ or -1 region along the dashed lines, we have a disc of multiplicity ± 1 and the remainder,R, of $\mathcal{P}$, which is the same in both diagrams. Then on the left $\hat{\chi}(\mathcal{P}) = \hat{\chi}(R) + 1 - 2$ while on the right $\hat{\chi}(\mathcal{P}') = \hat{\chi}(R) - 1 + 2$. The sign changes occur because of the Euler measure; in the first we add a $+1$ disc joined along two segments to a $+1$ region and at two points to a -1 region, which contributes nothing. In the second case the multiplicities are reversed, and the Euler measure must be calculated differently. Taking the difference of these, and adding the difference of the contribution from each quadrant gives $+2-(-2)+(-1-1) = 2$ on top, $+1-(-1)+(-1-1) = 0$ on left and right, and $0-0+(-1-1) = -2$ on bottom. This is -2 times the difference in the weights for these quadrants, but that is precisely the factor we divide into the first Chern class to get a filtration index. Hence, the weights for any intersection point before and after a crossing change differ from the first Chern class calculation for the corresponding intersection point by the same amount. In particular, $C_i(S)$ does not change.

Implicit in this discussion is the following corollary:

Corollary 3. *For the filtration indices, $\mathcal{F}_i$, calculated from the weights*

$$< c_1(\mathfrak{s}(\mathbf{x}), \mathcal{P}_i >= 2\,\mathcal{F}_i(\mathbf{x})$$

8.8. **Tangles.** Recall the definition of a tangle:

Definition 8.2. *A* tangle*, τ, in $D^2 \times I$ is an oriented smooth 1-sub-manifold whose boundary lies in $D^2 \times \{0,1\}$. Two tangles are isotopic if there exists a self-diffeomorphism of $D^2 \times I$, isotopic to the identity, fixing the ends $D^2 \times \{0,1\}$, and carrying one tangle into the other while preserving the orientations of the components.*

Suppose we have a tangle with n-components. We will call it m-colored if there is a function, c, from the components of the tangle, τ_j, to $\{1,\dots,m\}$. We require our isotopies to preserve the value of c. We restrict to those tangles for which exactly one component in $c^{-1}(i)$ is open for each $i \in \{1,\dots,m\}$, and this component is oreiented from $D^2 \times \{1\}$ to $D^2 \times \{0\}$. The collection of open components will then form a string link.

To construct a Heegaard diagram we convert the tangle, τ, to an associated string link, $S(\tau)$ in another three manifold. First, connect the components with the same color by paths in the complement of the tangle so that, with the paths as edges and the components as vertices, we have a tree rooted at the open component for that color. These paths may be used to band sum the components together, using any number of half twists in the band which will match the orientations on components correctly. We then perform 0-surgery on an unknot linking the band once. The resulting manifold, Y, is a connect sum of s copies of

$S^1 \times S^2$'s where s is the number of closed components. The image of τ after perfoming the band sums is a multi-component "string link", $S(\tau)$, in the complement of a ball. We have a color map c on this string link which we use to index the components. The homology group for index $\overline{j}$ for the colored tangle, τ, is defined to be $\widehat{HF}(Y, S(\tau); \mathfrak{s}_0, \overline{j})$ where $\mathfrak{s}_0$ is the torsion $Spin^c$ structure. Underlying this construction is the following lemma:

Lemma 18. *The isotopy class of $S(\tau)$ is determined by that of τ*

Proof: This follows as for Proposition 2.1 of [15]. It suffices to show that the choices made in performing the band sums do not affect the isotopy class of $S(\tau)$. Once we add the 0-framed handles, the choice of the bands no longer matters. In each band, we may remove full twists by using the belt trick to replace them with a self-crossing of the band. We may then isotope the 0-framed circle to the self-crossing and slide *one* of the strands in the band across the handle. Done appropriately this will undo a full twist in the band. Furthermore, by sliding across the 0-framed handles, we may move the bands past each other or any component in the string link. By using the trick from [15] illlustrated in Figure 20, we may arrange that all the closed components of the same color are linked in a chain to a single open component. In addition, we may interchange any two components along the chain. The combination of these moves provides Heegaard equivalences, not involving the meridians, between any two ways of joining the closed components in a color to that with boundary, regardless of the paths for the band sums, or twists in the bands.

8.8.1. *Long Exact Sequences.*
The tangle formulation where there is one open component for each color permits the introduction of the skein long exact sequence found in [15] where we may resolve crossings of components with the same color, but not crossings involving different colors. We should think of the resolved crossing, arising from 0-surgery on an unknot in the long exact surgery sequence, in the context of tangles. We let L^c_- be a tangle with a negative self-crossing in color c, L^c_+ be the tangle with a positive self-crossing instead, and L^c_0 be the tangle resulting from resolving the crossing. As in [15] there are two sequences. If the crossing is a self-crossing of a component then

$$\to \widehat{HF}(L^c_-, \overline{j}) \to \widehat{HF}(L^c_0, \overline{j}) \to \widehat{HF}(L^c_+, \overline{j}) \to$$

whereas if the crossing occurs between different components of the same colot we have

$$\to \widehat{HF}(L^c_-) \to \widehat{HF}(L^c_0) \otimes V \to \widehat{HF}(L^c_+) \to$$

where $V = V_{-1} \oplus V_0 \oplus V_{+1}$ and V_{-1} consists of a $\mathbb{Z}$ in filtration index -1 for the color c and 0 for all others, V_0 consists of $\mathbb{Z}^2$ with filtration index 0 for all colors, and V_{+1} consists of a $\mathbb{Z}$ in color c filtration index $+1$. The maps preserve the filtration indices with the tensor product index defined as the sum of those on the two factors. The proof is identical to that in [15].

Note: Since the theory for tangles arises from thinking of them as string links in an another manifold, the result for composition of string links extends to composition of this sub-class of tangles. The sub-class condition disallows the formation of new closed components when composing.

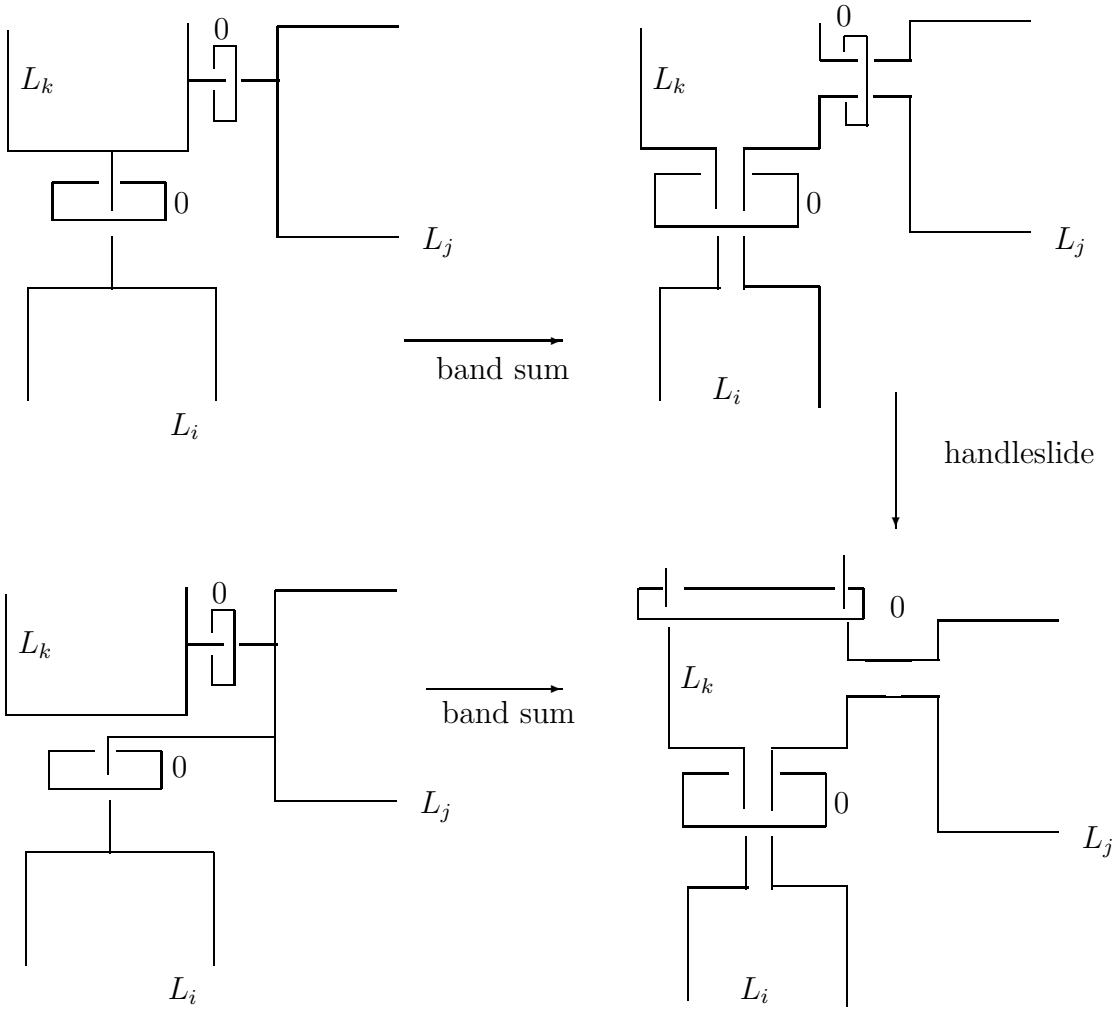

FIGURE 20. Kirby Calculus Interchange of Connecting Paths for a Tangle

APPENDIX A. MASLOV INDEX CALCULATION

Let $\phi \in \pi_2(\mathbf{x}, \mathbf{y})$ be a class with a multiplicity 1 domain, $\mathcal{D}(\phi)$. Then the new class $\phi' \in \pi_2(\mathbf{x} \times c, \mathbf{y} \times c)$ in $\Sigma \# T^2$ found as in Figure 21 has the same maslov index as ϕ.

First, notice that the intermediary ϕ'' in the stabilization, found from the domain $\mathcal{D}(\phi) \# T^2$ has the same Maslov index as ϕ. This follows from the observation that $[\Sigma] - \phi$ and $[\Sigma \# T^2] - \phi''$ have the same domain. Splicing this to ϕ and ϕ'' give the class $[S]$ in each diagram, and this always has Maslov index 2.

We prove this by considering the Heegaard triple represented in Figure **??**, where all the γ's are small Hamiltonian isotopes of a α except that γ_1 is found from the result of sliding α_1 over α_{g+1}. There are small triangles at each intersection between α and β curves in this triple, joining them to Θ^+ and a unique intersection point in $\mathbb{T}_\gamma \cap \mathbb{T}_\beta$. These form

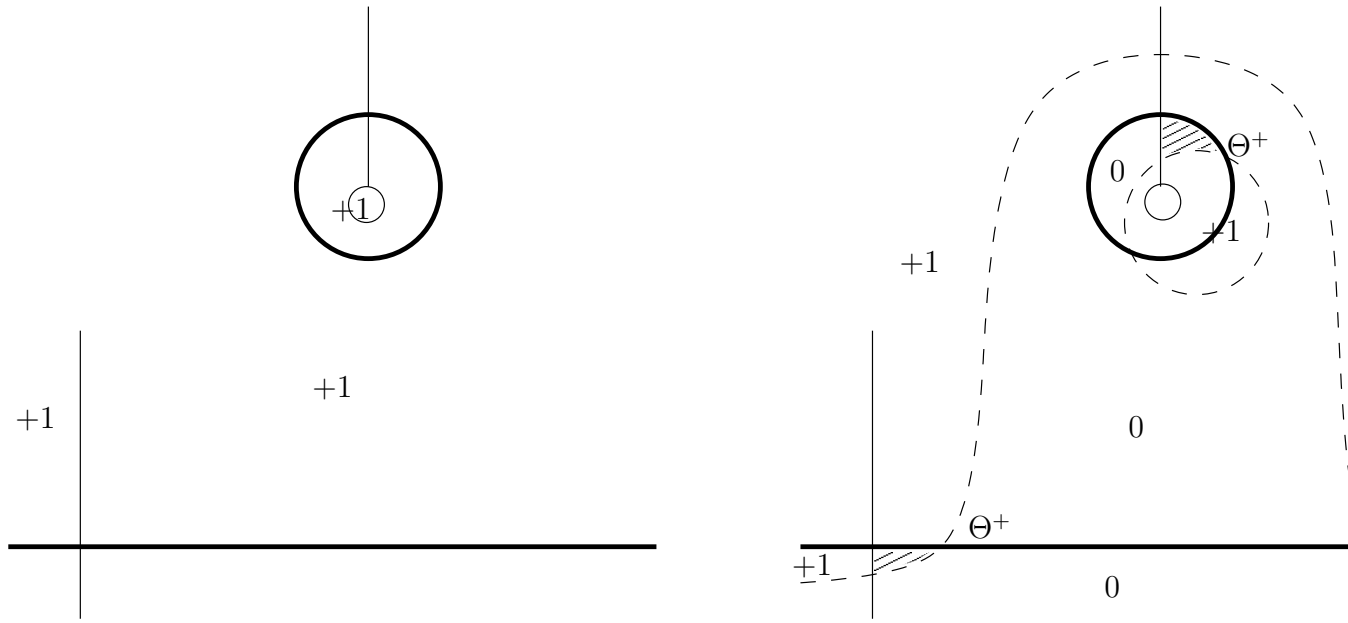

FIGURE 21. The diagram on the left shows the original domain in the stabilization and its multiplicities. The diagram on the right shows the stabilization and the result after the handlslides (dashed curve). The multiplicities on the right show are for the new class ϕ'. Notice that within the region of the handleslide there is a part of a periodic domain. The other portions of the Heegaard triple need to be chaecked as well, but the same observations apply.

homotopy classes of triangles which we denote $\triangle_{\mathbf{x}}$ and $\triangle_{\mathbf{y}}$ for the two intersection points. Examining multiplicities in the diagram shows that there is some doubly periodic domain $\mathcal{P}_{\gamma\alpha}$ such that

$$\phi' * \triangle_{\mathbf{x}} = \triangle_{\mathbf{y}} * \phi + \mathcal{P}_{\gamma\alpha}$$

However, the homotopy classes of triangles have Maslov index 0, as their domains consist of $g+1$ disjoint triangles, cf. [13], and these have a unique holomorphic representative. Likewise, the Maslov index of $\mathcal{P} \in \pi_2(\Theta^+, \Theta^+)$ is 0 since the value of the first Chern class of the torsion $Spin^c$ structure evaluated on $[\mathcal{P}]$ is 0. Since the Maslov index is additive we must have $\mu(\phi) = \mu(\phi')$.

This provides enough for the application in the main body of the test. There we start with a ϕ whose domain is a square with $\mu = 1$, since it has holomorphic representatives. The domain we are interested in is found by repeatedly stabilizing, and then isotoping the new handles so that their β's joined by the α's form a tree joined to the boundary of the square. Repeated application of the above argument, working up the tree, shows that $\mu(\phi') = 1$

References

[1] K. Fukaya, *Morse Homotopy and its Quantization*, Geometry and Topology (W. Kazez, ed.), International Press, 1997, pp. 409 - 440.

[2] P. M. Gilmer & R. A. Litherland, *The Duality Conjecture in Formal Knot Theory*, Osaka J. Math. 23 (1986), 229 - 247.

[3] R. E. Gompf & Andras I. Stipsicz, 4-Manifolds and Kirby Calculus. Graduate Studies in Mathematics v. 20. AMS. Providence, Rhode Island, 1999.

[4] N. Habegger & X. S. Lin. *The Classification of Links up to Link Homotopy.* J. of AMS, v. 3 no. 2 (1990) 389 - 419.

[5] L. H. Kauffman, Formal Knot Theory. Mathematical Notes, Vol. 30, Princeton University Press, 1983.

[6] L. H. Kauffman, On Knots. Annals of Mathematical Studies, Vol. 115. Princeton University Press, Princeton, New Jersey, 1987.

[7] L. H. Kauffmann, *Invariants of Graphs in Three-Space* Trans. AMS, 1989. Vol. 311

[8] P. Kirk, C. Livingston & Z. Wang. *The Gassner Representation for String Links*. Commun. Contemp. Math. v. 3 (2001), no. 1, 87 - 136.

[9] J. Levine. *The $\overline{\mu}$-invariants of Based Links*, Differential Topology, Proceedings Siegen 1987 (ed. U. Koschorke), Lecture Notes No. 1350, Springer-Verlag, New York, p. 87 -103.

[10] J. Levine. *A Factorization of the Conway Polynomial*Comment. Math. Helveticii 74 (1999), 1-27.

[11] R. Litherland, *The Alexander Module of a Kotted Theta-Curve*. Math. Proc. Camb. Phil. Soc. 1989. v. 106, 95 - 106

[12] P. Ozsváth & Z. Szabó, *Heegaard-Floer Homology and Alternating Knots*. Geom. Topo. 7 (2003) 225-254.

[13] P. Ozsváth & Z. Szabó, *Holomorphic Disks and Topological Invariants for Closed Three Manifolds*. math.SG/101206. To appear in *Ann. Math.*.

[14] P. Ozsváth & Z. Szabó, *Holomorphic Disks and Three Manifold Invariants: Properties and Applications*. math.SG/0105202. To appear in *Ann. Math.*.

[15] P. Ozsváth & Z. Szabó, *Holomorphic Disks and Knot Invariants. Adv. Math.*, 186(1): 58-116, 2004.

[16] P. Ozsváth & Z. Szabó, *Holomorphic Triangles and Invariants of Smooth Four Manifolds*. math.SG/0110169.

[17] P. Ozsváth & Z. Szabó, *Absolute Grading Floer Homologies and Intersection Forms for Four-Manifolds with Boundary*. Advances in Mathematics, 173 (2): 179-261, 2003.

[18] P. Ozsváth & Z. Szabó, *Holomorphic Disks and Genus Bounds. Geom. Topol.* 8: 311-334, 2004.

[19] J. Rasmussen *Floer Homology and Knot Complements*. PhD thesis, Harvard University, 2003.

[20] V. Turaev, Torsions Invariants of *Spin^c* Structures on 3-Manifolds, Math. Res. Letters 4, 679-695 (1997).

[21] Zeischang & Burde, Knots. 2nd Rev. Ed. De Gruyter Studies in Mathematics, 5. De Gruyter. Berlin, 2002.